Structural and functional neural correlates of impulsivity:

Brain imaging studies of psychopathic criminals, non-criminals, and mindfulness practitioners

by

Cole Korponay

A dissertation submitted in partial fulfillment of

the requirements for the degree of

Doctor of Philosophy

(Neuroscience)

at the

UNIVERSITY OF WISCONSIN-MADISON

2017

Date of final oral examination: 8/30/2017

The dissertation is approved by the following members of the Final Oral Committee:

Michael Koenigs, Associate Professor, Psychiatry
Richard Davidson, Professor, Psychology
Craig Berridge, Professor, Psychology
Brian Baldo, Associate Professor, Psychiatry
Josh Cisler, Assistant Professor, Psychiatry

Acknowledgements

An enormous thank you to:

- Mike Koenigs and my labmates in the Koenigs Lab: Maia Pujara, Phil Deming, Carissa Philippi, Rick Wolf, Monika Dargis, and Jaryd Hiser

- Richie Davidson and my labmates and advisors in the Davidson Lab: Robin Goldman, Martina Ly, Tammi Kral, Daniela Dentico, Matt Hirshberg, Ceci Westbrook, Joe Wielgosz, Sasha Sommerfeldt, Kaley Ellis, Leandro Chernicoff, Ted Imhoff-Smith, and Lawrence Tello

- Collaborators Nagesh Alduru, Kent Kiehl, Dave Kosson, Jean Decety, Ayla Kruis, and Antoine Lutz

- Committee members Craig Berridge, Brian Baldo and Josh Cisler

- Neuroscience & Public Policy Program founder Ron Kalil

- Funding and Support: Neuroscience Training Program

- Mallory Musolf, Tera Holtz, and everyone in the NTP Office

- My Mom, Dad, brothers Tanner and Derrick, Casey, Aunts Carol, Candy and Danni and Uncles Bob, Rick, and Ev, cousin Chelsea, Granny, Pop and Pop Pop

- My fiancée and best friend Lina

Table of Contents

Dissertation Abstract

Given the negative impact that impulsivity has on both individual and societal well-being, it is of interest to elucidate the neurobiological underpinnings of impulsive behavior, with the hope that this knowledge could assist in identifying individuals who are at risk for exhibiting impulsive behavior as well as lead to better treatment options. Toward this end, this dissertation had three aims: 1) to clarify whether the neurobiological underpinnings of clinical impulsivity in psychopathy are distinct from or an extreme manifestation of the neurobiological underpinnings of high levels of impulsivity in the general population; 2) to use machine learning to predict levels of impulsive-antisocial psychopathic traits from voxel-level variation in gray matter volume; and 3) to evaluate the effect of mindfulness meditation on impulsivity and its neurobiological correlates.

We first find that individuals in the general population with the highest levels of impulsivity had the lowest levels of gray matter volume in the right medial orbitofrontal cortex, whereas individuals in the incarcerated sample with the highest levels of impulsive-antisocial traits had the highest levels of gray matter volume in the right medial orbitofrontal cortex. Impulsivity in both samples was associated with elevated resting-state functional connectivity in prefrontal and striatal circuits, but these relationships were observed primarily between local nodes of the basal ganglia-thalamo-cortical loop in the incarcerated sample and in more global circuits of this loop in the healthy sample. Second, a machine learning model was able to predict incarcerated offenders' level of impulsive-antisocial traits based on levels of gray matter volume

throughout the brain with modest accuracy. Lastly, we found evidence that long-term, but not short-term, mindfulness meditation may be effective in reducing some, but not all, dimensions of impulsive behavior in the general population, and that long-term meditators have less gray matter volume in the prefrontal cortex and striatum than non-meditators. Collectively, these studies help clarify the neural underpinnings of impulsive behavior, provide proof of concept of a method to identify impulsive individuals from neural data, and provide a more nuanced understanding of the potential for mindfulness meditation to be used as a treatment for impulsive behavior.

List of Figures

List of Tables

Chapter 1: Introduction

1.1 Overview and Objectives

Impulsive decisions are typically not good decisions. They are made in haste, are often spurred by the prospect of an immediate reward or by impatience, and are usually made without sufficient regard for their long-term consequences. Every human being is liable to making impulsive decisions, and occasionally we all do. But for individuals with a consistent propensity for impulsive decision-making – and especially for individuals with psychiatric conditions featuring clinical levels of impulsivity – everyday functioning can become impaired to the point that quality of life suffers. In the general population, impulsivity has been associated with poorer academic outcomes[1], greater propensity for substance abuse[2] and risky sexual behavior[3], and a myriad of other negative life outcomes. The most severe manifestations of impulsive behavior – such as those present in disorders like psychopathy, substance abuse disorder, and attention-deficit/hyperactivity disorder – are estimated to cost nearly one trillion dollars annually in the U.S. alone from criminal social costs, medical care costs, and losses in economic productivity[4]. Given the negative impact that impulsivity has on both individual and societal well-being, it has therefore been of interest to elucidate the neurobiological underpinnings of impulsive behavior, with the hope that this knowledge could assist in identifying individuals who are at-risk for exhibiting impulsive behavior as well as lead to better treatment options.

Several decades of research have identified a number of brain regions and circuits whose integrity appears to underlie individual differences in impulsivity. However, there

remains a lack of consensus regarding the precise nature of what kind of aberrance in these neural substrates leads to impulsive behavior. For instance, while levels of gray matter volume in the prefrontal cortex have been consistently associated with individual differences in impulsive behavior, it is not clear whether it is too much, too little, or an amount at either extreme that increases the propensity for impulsive behavior. Findings from prior literature suggest that perhaps these relationships may be different in the general population than they are in populations with certain disorders, such as psychopathy. As such, the first objective of my thesis (**Chapters 2-4**) is to clarify whether the neurobiological underpinnings of impulsivity in psychopathy are distinct from or an extreme manifestation of the neurobiological underpinnings of high levels of impulsivity in the general population. The second objective of my thesis (**Chapter 5**) is to then assess whether individuals' levels of impulsive-antisocial psychopathic traits can be ascertained from their neural data – specifically the voxel-level variation in gray matter volume throughout the brain – using machine learning. Finally, the third objective of my thesis (**Chapter 6**) is to examine the efficacy of a potential intervention – mindfulness meditation – to reduce impulsive behavior and alter its neurobiological underpinnings. These three objectives are elaborated upon in greater detail below:

Objective 1: Clarify whether the neurobiological underpinnings of clinical impulsivity in psychopathy are distinct from or an extreme manifestation of the neurobiological underpinnings of high levels of impulsivity in the general population.

The neural circuitry underlying decision-making and reward sensitivity is complex and multifaceted, consisting of multiple gray matter nodes, functional connectivity networks, and neurotransmitter systems. As such, deficient decision-making and reward sensitivity that manifests in impulsive behavior may arise from aberrance in any number of these neural components. Furthermore, conflicting findings across different populations in prior literature suggest that aberrance in a given component may take on more than one form. In this aim, I examine structural and functional neural correlates of impulsivity in two separate populations – healthy adults in the general population, and incarcerated adult male inmates with psychopathic traits –and assess the similarities and differences of these neural correlates.

Objective 2: Use machine learning to predict levels of impulsive-antisocial psychopathic traits from voxel-level variation in gray matter volume.

Presently, psychiatric and personality disorders are diagnosed almost exclusively based upon self-reported and clinician-evaluated behavioral criteria. Although substantial progress has been made in identifying neural abnormalities present in groups of individuals with a range of disorders, not enough is known yet about the neural bases of these disorders for application to clinical diagnosis or prognosis. However, machine learning models that can identify patterns in vast amounts of neural data have shown promise in classifying between healthy brains and brains with one or another disorder, offering the potential for a bottom-up, data-driven approach to diagnosis. Such an approach may be particularly valuable in the legal setting, such as to provide an

objective, neurobiological evaluation of mental health for risk assessments. Here, I design a machine learning algorithm to evaluate psychopathy severity – with a focus on impulsive-antisocial psychopathic traits – on a continuous scale based on voxel-level variation in gray matter volume.

Objective 3: Evaluate the effect of mindfulness meditation on impulsivity and its neurobiological correlates.

Recent interest has grown in using mindfulness meditation to help treat conditions featuring high levels of impulsivity and deficits in behavioral control, such as attention-deficit/hyperactivity disorder and substance use disorder. In this aim, I examine the effect of mindfulness meditation on impulsivity and its neurobiological correlates in healthy adults in two fashions. First, I compare non-meditators to expert, long-term meditators on self-report and task-based measures of impulsivity, as well as on structural and functional neural correlates of impulsivity. Next, I examine the effect of an eight-week mindfulness meditation intervention on these impulsivity and neurobiology measures in individuals with no prior mindfulness meditation experience.

Collectively, completion of these three aims will advance the understanding of the neurobiology underlying impulsivity and leverage the knowledge that is gained for practical application in both identifying individuals at risk for impulsive behavior and evaluating the efficacy of interventions to reduce impulsive behavior.

1.2 Background

Substantial progress has been made over the past few decades in identifying the neural substrates whose integrity appears to mediate individual differences in impulsivity. Across numerous species, and in both clinical and healthy samples, researchers have highlighted a distinct set of brain regions, connections, and neurotransmitter systems that participate in what has come to be known as the brain's reward-processing and decision-making circuitry. This circuitry involves gray matter nodes in the ventral midbrain, basal ganglia, thalamus, motor cortices and prefrontal cortex, the structural and functional connections between these nodes, and the neurotransmitters that innervate these connections – most notably dopamine and norepinephrine. In studies of human subjects, the integrity of this circuitry can be evaluated along a number of neurobiological metrics. These include gray matter volume (GMV), resting-state functional connectivity (RSFC), changes in blood-oxygen-level dependent (BOLD) signal during behavioral tasks or in response to stimuli, neurotransmitter levels, and neurotransmitter receptor availability. Each metric provides complementary but also unique information. GMV roughly indexes the amount of neural cell bodies available to carry out the computational functions of a brain region; RSFC measures the degree to which neural activity in different gray matter nodes is synchronized at rest and, under the Hebbian assumption that "cells that fire together wire together" (i.e. that synchronously activated neurons are likely communicating and are involved with aspects of the same function), provides information about the integrity of the functional connections between these nodes; changes in BOLD signal during behavioral tasks or in response to stimuli provide information about the magnitude and nature of neural activity during functioning; neurotransmitter levels and

receptor availability provide indicators of the molecular-level functioning within the circuitry.

Despite the identification of the network of neural substrates associated with impulsivity, there remains a lack of consensus regarding the precise nature of what kind of aberrance in these neural substrates leads to impulsive behavior. The following sections will provide the necessary background for further investigating this issue. First, the relevant neural substrates and their network of connections will be discussed. Second, the interrelations amongst the above-discussed neurobiological metrics will be detailed. Under the assumption that structure and function are interrelated, as well as the assumption that integrity at local and micro levels of a network are interrelated with the integrity of the global and macro level of the network, an understanding of how the different neurobiological metrics that describe this network (e.g., GMV, RSFC, BOLD signal, and neurotransmitter levels) are interrelated to one another is crucial to the development of an internally consistent framework describing the neurobiological basis of impulsivity. Third, findings on the relationships between each neurobiological metric and impulsivity will be reviewed in both healthy samples and in samples of individuals with psychopathy. Finally, evidence for multiple neurobiological paths to impulsivity will be discussed.

The Reward and Decision-Making Network

The primary brain areas relevant to behavioral control and decision-making in the brain are the prefrontal cortex and basal ganglia. Each of these regions consists of a number of functionally distinct subdomains, through which at least three general categories of information are processed: limbic, cognitive, and motor[5]. In the prefrontal

cortex, areas largely involved in limbic processing (i.e. information about emotion and reward) include the orbitofrontal cortex, ventromedial prefrontal cortex, and the anterior cingulate cortex. The dorsolateral prefrontal cortex deals largely with cognitive processing, such as cognitive control and procedural learning, while more posterior dorsal regions are important for motor processing and control of movement. These three streams of information project topographically from the prefrontal cortex onto the basal ganglia, which consist of the striatum, globus pallidus, subthalamic nucleus, substantia nigra, and ventral tegmental area[6]. The striatum, which consists of the putamen, caudate, and nucleus accumbens, serves as the input structure to the basal ganglia from the prefrontal cortex, from which it receives dense monosynaptic inputs. The limbic stream of information from the orbital and medial prefrontal cortex projects largely to the nucleus accumbens and ventromedial striatum; the cognitive stream from dorsolateral areas projects largely to the central regions of the caudate and putamen; the motor stream from the posterior dorsal areas of prefrontal cortex project largely to the dorsolateral regions of the caudate and putamen[5]. Despite the general topographic organization of these processing streams, the striatum is also thought to consist of "hub" areas where information from across the different processing streams is integrated[5,7]. The striatum's major output structures are the globus pallidus and the dopaminergic neuron-containing substantia nigra pars compacta (SNc). The interior segment of the globus pallidus (GPi) and the SNr both project to the thalamus, which then projects back to the prefrontal cortex. This particular loop through the basal ganglia is referred to as the "direct pathway" back to cortex. Alternatively, the striatal projection to the exterior segment of the globus pallidus (GPe), which projects to the subthalamic nucleus, which in turn

projects to the GPi and then onward to the thalamus and cortex, is referred to as the "indirect" pathway[5]. Overall, this network is often termed the "cortico-basal ganglia-thalamo-cortical loop". The anatomical projections and resulting topographic map described above, which was largely ascertained from early tracing studies in primates, has more recently been corroborated by both diffusion tensor imaging (DTI) studies[8] and fMRI studies[9] of functional connectivity in humans.

The next section will now describe what is currently known about the interrelations amongst the neurobiological metrics in this circuitry.

Interrelations amongst the Neurobiological Metrics in the Reward and Decision-Making Network

Particular interrelations between neurobiological metrics in the brain's reward and decision-making circuitry have been well-studied, while some interrelations have not been reported on at all. The following interrelations will be discussed below: blood-oxygen-level-dependent (BOLD) and dopamine activity, functional connectivity and dopamine activity, and functional connectivity and gray matter volume.

Blood-Oxygen-Level-Dependent (BOLD) signal and Catecholaminergic Activity: Positive Correlation

Studies using PET-fMRI and pharmacological MRI designs have provided an abundance of evidence suggesting that striatal dopamine release is positively correlated with striatal neural activation as measured by blood-oxygen-level-dependent (BOLD) signal (see[10] for review). For instance, Schott and colleagues (2008)[11] found that BOLD signal during reward anticipation in the substantia nigra/ventral tegmental area (SN/VTA) – a primary origin of dopaminergic neurotransmission – positively correlated with

dopamine release in the ventral striatum, a main target of SN/VTA neurons. They also found that BOLD activity in the ventral striatum during reward anticipation positively correlated with dopamine release in this same region. Similar results have been reported in other PET-fMRI studies[12]. Pharmacological MRI studies corroborate these findings by showing that substances known to up-regulate catecholaminergic functioning result in increased BOLD signal in frontostriatal regions. For example, methamphetamine injections - which increase dopamine levels but also serotonin and norepinephrine levels - were found to prompt increased BOLD signal in the nucleus accumbens and mesial prefrontal cortex[13].

Functional Connectivity and Catecholaminergic *Activity: Positive Correlation*

A number of other studies using similar designs have examined the relationship between catecholaminergic neurotransmission and frontostriatal functional connectivity. It is more difficult to generalize about the interrelations between these two metrics because the functional connectivity between any two specific regions is likely to be uniquely related to neurotransmitter activity. Nonetheless, while findings on the relation between neurotransmitter activity and functional connectivity between frontostriatal regions and regions in other networks has been somewhat inconsistent[14,15], a fairly consistent pattern has begun to emerge between these metrics between the striatum and frontal lobe. Specifically, there appears to be a positive correlation between catecholaminergic functioning and frontostriatal functional connectivity. One study found that increasing catecholamine levels with levadopa - a precursor to dopamine, norepinephrine and epinephrine - increased functional connectivity between the right caudate and a right frontoparietal network and between the ventral striatum and a fronto-

insular network[16]. A further study found that levadopa increased functional connectivity between the ventral striatum and ventrolateral prefrontal cortex[17]. Lastly, one study found that frontostriatal functional connectivity was reduced in subjects who underwent dopamine depletion via the acute phenylalanine/tyrosine depletion (APTD) technique, compared to subjects who did not undergo depletion[14]. It should be noted that this technique may also deplete levels of norepinephrine, given that dopamine is a molecular precursor to norepinephrine.

Other Interrelations

Interrelations other than the catecholaminergic activity-BOLD signal and catecholaminergic activity-functional connectivity associations summarized above have received either sparse or no attention. One study has reported on an indirect relationship between frontal lobe gray matter concentration and intra-frontal functional connectivity in psychopathic individuals, finding that both metrics were positively correlated with a measure of impulsivity[18]. Beyond this, there have been little to no data on the relationships between gray matter and functional connectivity in this circuitry. Furthermore, to the best of my knowledge, there have been no reports on the relationship between gray matter and catecholaminergic functioning.

Having set the stage of the relevant neural correlates and the neurobiological metrics that gauge their integrity, the following section will summarize findings relating variability in impulsivity to variability in the integrity of the relevant neural correlates.

Relationships between Neurobiological Metrics and Impulsivity

Healthy Adults

Impulsivity and Gray Matter: Negative Correlation

Several studies have found that self-reported trait measures of impulsivity, such as score on the Barratt Impulsiveness Scale (BIS-11), are negatively correlated with prefrontal gray matter, specifically in the orbitofrontal cortex, anterior cingulate cortex, and dorsolateral prefrontal cortex[19-21] (but see[22,23]). Regarding task-based measures of impulsivity, no study has reported on GMV relationships with performance on motor inhibition tasks such as the go/no-go or stop-signal tasks in healthy adults. Studies of delay discounting tasks in healthy adults have found both negative[22] and positive[23] correlations between prefrontal GMV and magnitude of delay discounting (in the lateral and medial prefrontal cortex, respectively); two studies have found negative correlations between putamen GMV and magnitude of delay discounting[23,24].

Impulsivity and Functional Connectivity: Mixed Findings

A few recent studies in healthy adults have also found evidence for relationships between impulsivity and resting-state functional connectivity (RSFC). These studies have examined associations between RSFC and self-reported impulsivity[25], delay discounting[26], and whether changes in RSFC and impulsivity co-occur in response to pharmacological dopamine challenges[16,27]. In one such study, up-regulation of catecholamine levels via tolcapone resulted in a co-occurrence of decreased RSFC between the ventral putamen and pregenual cingulate cortex and decreased delay-discounting[27]. In another, self-reported "fun-seeking" as measured by the Behavioral Inhibition and Activation Systems (BIS/BAS) Questionnaire was positively correlated

with RSFC between the putamen and middle orbitofrontal cortex[25], though this study also found a negative correlation between self-reported "drive" and RSFC between the caudate and mid-cingulate cortex.

Impulsivity and Catecholaminergic Neurotransmitter Activity: Mixed Findings

The relationship between impulsivity and catecholamine levels has been studied in a variety of ways. Studies that manipulate catecholamine levels via administration of stimulant drugs such as d-amphetamine (which at low levels increase extracellular levels of dopamine and norepinephrine[28]) have shown that upregulation of catecholamine levels is associated with decreased motor impulsivity on the stop-signal and go/no-go tasks as well as decreased delay discounting in healthy adults[29]. Studies have also used positron emission tomography (PET) to study this relationship. For instance, correlations between impulsivity and striatal D_2/D_3 dopamine receptor availability have been observed in a number of PET studies, though reports diverge on the direction of this relationship[30-32]. PET imaging quantifies the availability of receptors for radiotracer binding, and this metric is difficult to interpret because it likely reflects the confluence of a variety of factors, including levels of the endogenous ligand that competes for receptor binding with the radiotracer and the density of receptors themselves[33]. As an example of a correlation with one receptor class in one area of the brain in healthy adults, several studies have found that decreased dopamine receptor availability in the dorsal striatum is associated with better rapid motor response inhibition[30,31]. These findings are consistent with the interpretation that the reduced receptor availability is in part due to increased competition from elevated levels of endogenous dopamine in individuals with better response inhibition capacities. However, in apparent contrast, another PET study found that

decreased striatal dopamine receptor availability was associated with increased levels of trait impulsivity as measured by the BIS-11[32].

Several studies have also attempted to examine the role of dopamine in relation to impulsivity via spontaneous eye blink rate (sEBR), which convergent evidence from several lines of research suggests provides a gross peripheral indication of dopaminergic functioning[34-43] in the basal ganglia, though it should be noted that whether sEBR is singularly dependent on dopamine transmission is unclear. While the precise mechanism through which dopamine influences sEBR is still being worked out (cortical input - possibly originating in the angular gyrus[44] - to the basal ganglia is thought to activate brainstem circuits responsible for sEBR generation via inhibitory inputs to the superior colliculus[45]; as such, dopamine levels in the basal ganglia may modulate the degree to which the brainstem sEBR generator is activated[44]) a number of studies (though not all[46]) have provided evidence of a direct, positive relationship between sEBR and central dopaminergic functioning. For instance, pharmacological studies in both animals and healthy humans have shown that dopamine agonists increase sEBR while dopamine antagonists decrease sEBR[35-38,42] (however, again, the exact mechanism of action is still being worked out - while one study reported that both the full D1R agonist dihydrexidine and selective D2R agonist (+)-PHNO increased sEBR, another study found that while the high-efficacy D1R agonist *R*-(+)-6-Br-APB also increased sEBR and that the D1R antagonist SCH 39166 attenuated this effect, D2R agonist (+)-PHNO was also found to attenuate the effects of *R*-(+)-6-Br-APB). sEBR has been found to be lower in patients with Parkinson's disease, which is characterized by low dopamine levels[34], and has been shown to be upregulated by administration of L-DOPA[47]. A recent PET study in primates

also found that sEBR was correlated with D2-like receptor availability in the caudate and ventral striatum, and that D2-like receptor availability was correlated with D2-like agonist induced sEBR changes[43].

However, despite the generally consistent relationship between sEBR and dopaminergic functioning, the relationship of sEBR to impulsivity has been mixed. One study of sEBR and the stop-signal task found that higher sEBR was associated with slower/worse reaction time on "stop" trials, indicative of poorer inhibitory control[48]. An examination of the relation of sEBR to delay discounting found no main effect, but found that individuals with high self-ratings of disinhibition and low sEBR showed greater delay discounting[49]. A study of trait impulsivity found no relationships between sEBR and the BIS subscales[49].

Overall, structural findings appear to point to a negative relationship between GMV in limbic and cognitive control regions of the prefrontal cortex and impulsivity; fewer studies on the relationship between RSFC and impulsivity have been conducted and the results from these studies are somewhat varied; findings on the relationship between neurotransmitter functioning and impulsivity have been mixed and potentially point to a non-linear relationship.

Psychopathy

Psychopathy is a mental health disorder characterized by callous lack of empathy and impulsive antisocial behavior. Present in roughly one-fourth of adult prison inmates, psychopathy is associated with a disproportionately high incidence of violent crime, substance abuse, and recidivism[50,51]. The detrimental behaviors committed by

psychopathic individuals, estimated to result in $460 billion annual costs in the U.S. alone[4], have been linked to the impulsive-antisocial aspects of the disorder[52,53].

Several studies have found that impulsive-antisocial traits in psychopathy are associated with increased prefrontal GMV[18,54] (but see[55]) – these positive relationships have been found in medial dorsal and lateral frontal cortex[56], mOFC and ACC[57], and the medial, middle, and superior frontal gyri[58]. RSFC in relation to impulsive-antisocial psychopathic traits has not been studied as extensively as GMV, but at least one study has found increased intra-frontal RSFC in psychopaths compared to non-psychopaths[59]. In regards to neurotransmitter functioning, several lines of evidence suggest that impulsivity in psychopathy may be associated with elevated dopamine and other monoamine levels. Two studies of cerebrospinal fluid, from which levels of the dopamine metabolite homovanillic acid (HVA) can be measured, have found a positive correlation between HVA levels and severity of psychopathic traits in criminal offenders[60,61]. In addition, a PET study found that increasing severity of impulsive-antisocial psychopathic traits in a community sample was associated with greater dopamine release in the nucleus accumbens in response to administration of amphetamine. Given that amphetamine elevates dopamine, norepinephrine, and, depending on dose, serotonin, widely in the brain, it is possible that a similar sensitization of multiple monoamines in multiple brain regions could be associated with psychopathic traits [12]. And a study of spontaneous eyeblink rate (sEBR) in criminal inmates (of which individuals with psychopathy comprise a disproportionate percentage of in general[4]) found that higher sEBR – potentially indicative of higher levels of central dopaminergic functioning – was associated with greater impulsivity[62].

Multiple Paths to Impulsivity? Evidence from Studies of Catecholamine Activity

The findings reviewed in the previous section suggest the possibility that the neural substrates of decision-making and behavioral control can take on different forms of aberrance that lead to a similar behavioral phenotype broadly characterized by impulsivity. For example, findings appear to show that impulsivity is associated with decreased prefrontal GMV in the general population but increased prefrontal GMV in psychopathic individuals. However, the relatively modest number of studies specifically examining the relation of impulsivity to metrics like gray matter volume and RSFC in humans, and the challenges of examining causal relationships in these studies, makes it difficult to determine at this point whether inconsistencies across studies truly represent meaningful differences that indicate there are multiple neurobiological "paths" to impulsivity. Nonetheless, non-linear relationships of this kind between neurobiological metrics and behavioral measures of impulsivity[63], reward processing[64], and cognitive control[65] have been well-documented in both animal models and humans (see[65] for review) for the metric of dopaminergic functioning[63-65]. Indeed, a number of researchers have posited the existence of an inverse U-shaped relationship between levels of prefrontal dopaminergic and noradrenergic neurotransmission and adaptive behavioral functioning[66]. This hypothesis suggests that there is a "Goldilocks Zone" of catecholamine activity that facilitates optimal behavioral functioning and that levels of activity either appreciably above or below this level will result in functional deficits. The following section will detail these findings as a way of establishing the potential

legitimacy of this kind of relationship being present for other neurobiological metrics like gray matter volume in their relation to impulsivity.

Evidence for a non-linear or U-shaped relationship between impulsivity and neurotransmitter levels come from several lines of work. First, a number of studies have shown that pharmacological manipulations can have opposite effects on impulsivity - and on other cognitive and behavioral processes such as working memory and attention - depending on their dosage level. For example, Eagle and Robbins (2003) showed that while a small dosage of d-amphetamine recovered performance on a stop-signal reaction-time task in rats with medial striatal damage, a large dosage (which would also be expected to increase serotoninergic activity) resulted in exacerbated performance deficits[67]. Another study in rats showed that small acute dosages of methamphetamine decreased impulsive responding on a delay-discounting task, but that chronic large dosages increased impulsive responding[68]. At least two mechanisms may be responsible for the dose-dependent effects of catecholamines such as dopamine. One is U-shaped action at receptors in the prefrontal cortex (which can increase attention, working memory and planning capacities). Another is the fact that at low, clinically relevant dosages, catecholamine-upregulating agents like methylphenidate elicit their largest increases in DA in the prefrontal cortex, which can help enhance cognitive functioning[69], whereas larger dosages can also activate receptors in the striatum that can increase motor activity and impulsive tendencies.

Second, several studies have shown that identical dosages of catecholamine up-regulating drugs can have opposite effects on impulsivity-related behaviors in different individuals depending on individuals' baseline levels of impulsivity. For example, one

study of performance on a stop-signal task - which measures the ability to stop an action that has already been initiated (motor impulsivity) - found that the stimulant methylphenidate slowed stop-signal reaction time (SSRT) in rats with faster SSRT at baseline but quickened SSRT in rats with slower SSRT at baseline; the stimulant drug modafinil also quickened SSRT in rats with slower SSRT baseline impulsivity but did not affect rats with faster baseline SSRT[70]. In another study, rats raised in an enriched environment were found to have less delay discounting (cognitive impulsivity) at baseline than isolated rats, and it was found that d-amphetamine (though not methylphenidate) increased delay discounting in the environmentally enriched rats and decreased delay discounting in the isolated rats[71]. Similarly, in humans, acute administration of d-amphetamine was found to quicken SSRT on a stop-signal task only in subjects with slower SSRTs at baseline[72]. This kind of response divergence to manipulations of catecholamine activity has also been frequently observed between Parkinson's disease (PD) patients with and without Impulse Control Disorders (ICDs). Studies typically report that up-regulators of catecholaminergic activity increase impulsivity in PD patients with an ICD[73,74] – some evidence suggests that chronic dopaminergic pharmacotherapy, particularly with high dosages of dopamine agonists, may even lead to the development of ICDs in some PD patients[75,76] – while these same agents are typically not reported to affect impulsivity in PD patients without an ICD[73].

Third, findings between different samples often are conflicting. In rats, some studies show that acute administration of stimulants, such as cocaine and d-amphetamine, increases impulsive responding on delay-discounting tasks[77-79], whereas other studies show that monoamine agonists decrease impulsive responding on these tasks, and that

monoamine antagonists increase impulsive responding[80,81]. In humans, one study found that baseline levels of dopaminergic activity – as measured by spontaneous eye-blink rate – were positively correlated with impulsive responding on a stop-signal task (as measured by increased stop-trial reaction times)[48], while another study found that acute administration of d-amphetamine decreased impulsive responding on a stop-signal task and also decreased impulsive responding on a go/no-go task and delay-discounting task[29]. It is possible that these discrepancies in findings are partly attributable to variation between studies in dosage levels of dopaminergic drugs and/or individual differences in baseline dopaminergic metrics. It is also possible that discrepancies are attributable to differences in task structure - the ADHD literature, for instance, has shown that the effects of clinically-relevant doses of methylphenidate on delay discounting are highly dependent on the nature of the delay and reward (e.g. magnitude, experiential vs. hypothetical, etc.)[82].

Overall, an important logical outgrowth of findings in support of a U-shaped relationship between catecholaminergic neurotransmitter levels and impulsivity has gone relatively underappreciated. Given that levels of catecholamines like dopamine appear to be inherently linked to other neurobiological metrics such as functional connectivity, it may be possible that these other metrics have a similar U-shaped relationship with impulsivity. Might such a relationship explain the divergent prefrontal GMV findings in relation to impulsivity in prior studies of healthy samples and psychopathic samples? And is this relationship observed in regard to RSFC?

In order to address these questions, the following three studies (**Chapters 2-4**) examine impulsivity in relation to GMV and RSFC in a sample of inmates with psychopathy and a sample of healthy adults from the general population.

Chapter 2: Impulsive-antisocial dimension of psychopathy linked to enlargement and abnormal functional connectivity of the striatum

Published as: Korponay, C., Pujara, M.S., Deming, P., Philippi, C., Decety, J., Kosson, D.S., Kiehl, K.A., & Koenigs, M. (2017) Impulsive-antisocial dimension of psychopathy linked to enlargement and abnormal functional connectivity of the striatum. *Biological Psychiatry: Cognitive Neuroscience and Neuroimaging*, 2:149-157.

2.1 Introduction

The literature on impulsive-antisocial behavior, in psychopathy as well as in related disorders such as antisocial personality disorder[83] and drug addiction[84-86], has frequently implicated aberrance of the mesolimbic dopamine reward circuitry and striatum[87]. Abnormalities in structure[87] and response to reward[12,88] in the ventral striatum are common findings among these populations. However, the direction of these relationships across studies, particularly with respect to structure, has been mixed. Studies have associated psychopathy with increased ventral striatum volumes[89,90], decreased ventral striatum volumes[91], volume increases[92] and decreases[93] in more dorsal and lateral regions of the striatum, and with no relationship to striatal volume at all[57,94]. The mixed findings may be attributable to differences in analysis methodologies, subject populations (e.g., prison inmates vs. community samples), psychopathy severity, sample sizes, and substance use history. Furthermore, little is known about resting-state functional connectivity (RSFC) of the striatum in psychopathy, particularly as it relates to impulsive-antisocial behavior.

The present study used a unique mobile scanner to collect multimodal magnetic resonance imaging (MRI) from a sample of adult male prison inmates (N=124) with a broad range of psychopathy severity. First, we assessed whether and how volumes of

striatal subnuclei were linked to psychopathy severity, in terms of overall psychopathy and the distinct components of psychopathic traits (Factor 1: affective and interpersonal traits; Factor 2: impulsive, antisocial, and lifestyle traits). Next, we analyzed RSFC data from the same participants to determine whether the observed striatal structural abnormalities were accompanied by alterations in striatal RSFC. Finally, we assessed the relative contributions of striatal volume and RSFC to psychopathy severity. This combination of analyses comprises the most comprehensive study of striatum structure and RSFC in psychopathy to date.

2.2 Methods

Participants

124 participants from a medium-security Wisconsin correctional facility were selected based on the following inclusion criteria: (1) less than 45 years old; (2) IQ greater than 70; (3) no history of psychosis or bipolar disorder; (4) no history of significant head injury or post-concussion symptoms; (5) no current use of psychotropic medications; and (6) completed interview assessments for psychopathy and substance use disorder (see below). Of these 124 subjects, RSFC data were obtained for 115 subjects; 8 of these were excluded due to excessive motion in the scanner, leaving a total of 107 subjects for RSFC analysis. Informed consent was obtained both orally and in writing.

Psychopathy was assessed with the Psychopathy Checklist Revised (PCL-R) by trained research assistants[51]. The PCL-R is a 20-item scale completed based on a semi-structured interview and file review. Each item is scored as 0, 1, or 2 based on the severity of each trait. Total scores ≥30 (n=41) indicate psychopathy; scores >20 and <30 (n=48) are considered intermediate, and scores ≤20 (n=35) are non-psychopathic [51]. Inter-

rater reliability (intraclass correlation) for total PCL-R score was 0.98 based on 10 dual ratings. Total PCL-R, Factor 1 and Factor 2 scores were used for separate regression analyses[95].

Substance use disorder was assessed with the Structured Clinical Interview for DSM-IV Axis I disorders (SCID-IV)[96]. This measure classifies whether a subject meets criteria for lifetime history of substance abuse or dependence, for each of the following substances: alcohol, cannabis, cocaine, opioids, stimulants, sedatives, and hallucinogens. Participant characteristics are summarized in **Table 1**.

Table 1. *Participant characteristics: Incarcerated sample*

	All (*n*=124)		**Non-Psychopathic (*n*=35)**		**Intermediate (*n*=48)**		**Psychopathic (*n*=41)**		
	Mean	***SD***	***Mean***	***SD***	***Mean***	***SD***	***Mean***	***SD***	***p*[a]**
Age	31.6	7.3	31.3	7.9	31.8	6.7	31.5	7.7	0.93
IQ	98.1	11.5	97.3	12.0	95.3	11.6	101.5	10.3	0.19
Total PCL-R score	24.8	7.1	15.3	3.4	25.6	2.3	32.1	1.6	<.001
Factor 1 score	9.2	3.3	5.5	2.1	9.3	2.3	12.3	1.8	<.001
Factor 2 score	13.6	3.9	8.6	2.8	14.3	1.9	17	1.5	<.001
Addiction Severity Index (transformed)	0.59	0.37	0.56	0.29	0.54	0.40	0.66	0.38	.203
	%	***n***	***%***	***n***	***%***	***n***	***%***	***n***	
SUD: abuse	24.2	30	22.9	8	25	12	24.4	10	.88
SUD: dependence	55.6	69	40	14	56	27	68.3	28	.01
Race									
Caucasian	56.6	70	60	21	45.8	22	65.6	27	0.52
African-American	41.1	51	34.3	12	52.1	25	34.1	14	0.52
Hispanic	1.6	2	2.9	1	2.1	1	0	0	N/A
Native American	0.8	1	2.9	1	0	0	0	0	N/A

Participant demographic and neuropsychological information is presented by group for non-psychopathic (PCL-R ≤20), intermediate (PCL-R >20 and <30) and psychopathic (PCL-R ≥30) inmates. [a]p-values are reported for two-sample t-tests (for age, IQ and psychopathy scores), Fisher's Exact Test (for Race) and Pearson Chi-Square test (for substance abuse and dependence) comparing psychopathic and non-psychopathic inmates.

MRI Acquisition

MRI data were acquired using the Mind Research Network's Siemens 1.5T Avanto Mobile MRI System equipped with a 12-element head coil. All participants underwent scanning on correctional facility grounds. A high-resolution T1-weighted structural image was acquired for each subject using a four-echo magnetization-prepared rapid gradient-echo sequence (TR=2530 ms; TE=1.64, 3.5, 5.36 and 7.22 ms; flip angle=7°; FOV=256x256 mm^2 ; matrix=128x128; slice thickness=1.33 mm; no gap; voxel size=1x1x1.33 mm^3;128 interleaved sagittal slices). All four echoes were averaged into a single high-resolution image[97]. Resting-state functional images (T2*-weighted gradient-echo functional echo planar images (EPIs)) were collected while subjects lay still and awake, passively viewing a fixation cross for 5.5 min (158 volumes)[98], and were acquired with the following parameters: flip angle=75°; FOV=24x24 cm; matrix=64x64; slice thickness=4 mm; gap=1 mm; voxel size=3.75x3.75x5 mm; 27 sequential axial oblique slices.

Preprocessing and analyses of structural MRI data were conducted in both Freesurfer 5.3[99] in Linux and Statistical Parametric Mapping software (SPM12; http://www.fil.ion.ucl.ac.uk/spm). RSFC data analysis was performed using AFNI[100] and FSL (http://fsl.fmrib.ox.ac.uk/fsl/fslwiki/).

Structural MRI Preprocessing: Freesurfer

Freesurfer's automated preprocessing procedure includes skull-stripping, registration, intensity normalization, Talairach transformation, tissue segmentation, and surface tessellation [101]. Freesurfer provides volume measurements for eight striatal subregions (left and right putamen, left and right caudate, left and right globus pallidus, and left and right nucleus accumbens).

Structural MRI Preprocessing: SPM

T1 images were manually realigned; segmented into gray matter, white matter, and cerebrospinal fluid; normalized to Montreal Neurological Institute (MNI)-152 space; modulated to preserve volume after normalization; and smoothed with an 8mm full-width at half-maximum (FWHM) Gaussian kernel [102]. Individual Brain Atlases using Statistical Parametric Mapping 71 (IBASPM 71) (http://www.thomaskoenig.ch/Lester/ibaspm.htm) in the Wake Forest University (WFU) Pick Atlas Toolbox was used to create masks of the eight striatal subregion ROIs (**Figure 1**).

Figure 1: *Striatal subnuclei segmentation in FreeSurfer 5.3 (left) and in SPM12 as defined by Individual Brain Atlases using Statistical Parametric Mapping 71 (right)*

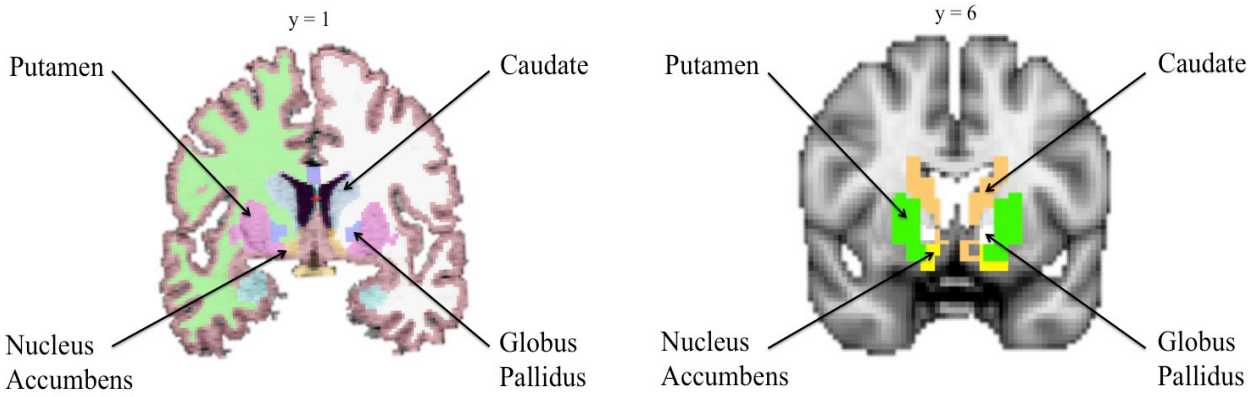

Functional MRI Preprocessing

The following preprocessing steps were performed: (1) EPI volumes were slice time corrected, (2) motion corrected by rigid body alignment, (3) deobliqued, (4) the first three volumes were omitted, (5) data were then motion corrected (3dvolreg in AFNI) and (6) despiked to remove extreme time series outliers and then (7) bandpass filtered ($0.009<f<0.08$) and spatially smoothed with a 6mm FWHM Gaussian kernel [103]. The

skull-stripped anatomical scan for each participant was rigidly coregistered with the EPI and diffeomorphically aligned to MNI-152 space [104]. The transformation matrix from this registration was then used to align the EPI scans to MNI-152 space. Finally, the EPI scans were resampled to 3mm cubic voxels for subsequent functional connectivity analyses.

Because individual differences in subject motion can contribute to resting-state correlations [105-107], we excluded subjects with mean framewise motion displacement (i.e., volume to volume movement across the time series) >2mm and/or total scan time <4 min after censoring all time points with framewise motion displacement >0.2mm and extreme time series displacement (i.e., time points in which 10% of voxels were outliers [105-107]. 8 participants were excluded for excessive motion, leaving a final sample of 107 participants.

Analytic Strategy

Because processing pipelines and region of interest (ROI) parcellations differ between image processing software programs, and because studies have reported that results may vary as a function of program[108], we computed volumes of striatal subnuclei ROIs (nucleus accumbens, putamen, caudate, and globus pallidus) from two separate programs – Freesurfer and SPM – and performed analyses with both sets of values. Significance for the subnuclei ROI analyses was $p < 0.05$. Additionally, SPM was used to perform small volume-corrected voxel-wise analyses within ROIs – both because this type of analysis can detect focal aberrations that may be missed in the regional volume analysis, and because this analysis allows for more specific localization of the areas where volume is most strongly linked to psychopathy severity. Significance for the

voxel-wise analyses was evaluated using the cluster-level family-wise error (FWE) rate at p_{FWE} <0.05.

After performing the volumetric analyses, we then examined whether the identified volume abnormalities were associated with abnormalities in RSFC. To do this, we created 3mm-radius spherical seeds around the peak coordinates of each focal cluster - identified via the within-ROI voxel-wise analysis - where volume was related to psychopathy severity, and subsequently assessed RSFC between these areas and other areas of the brain in relation to psychopathy ratings.

Seeds were evaluated in RSFC regressions only in relation to the specific psychopathy score-type (Total PCL-R, Factor 1, and/or Factor 2) for which the seed had demonstrated a relationship within the volumetric analysis. To correct for multiple comparisons, we used FWE-correction at the cluster level using a whole-brain mask (3dClustSim in AFNI)[109,110] and applied cluster extent thresholding. The cluster extent threshold corresponded to the statistical probability (α=0.05, or 5% chance) of identifying a random noise cluster at a predefined voxel-wise (i.e., whole-brain) threshold of p=0.01 (uncorrected). Using this whole-brain FWE cluster correction, a cluster-corrected size of ≥106 voxels was significant at p_{FWE} <0.05.

Covariates

Total PCL-R scores and Factor 2 scores were significantly correlated with substance use disorder (r=0.34, p<0.001 and r=0.39, p<0.001, respectively). Because gray matter volume has been shown to relate to substance use[111-115], we included presence of substance use disorder (None, Abuse, or Dependence), using the SCID-IV diagnoses, as a covariate in all regression models. Furthermore, we observed a significant group

effect ($p<0.05$) of race (between Caucasian and non-Caucasian subjects) on volume of many of the striatal ROI's, and thus race was also included as a covariate in all regression models. Additionally, we included age and intracranial volume as covariates in all regression models, as these factors correlate with gray matter volume[116,117]. IQ was not related to psychopathy severity or striatal volumes, and so was not included as a covariate. In regressions where the main variable of interest was a factor score, the other factor score was included as a covariate. There was no significant relationship between PCL-R score and intracranial volume as measured by either SPM (p=0.50) or Freesurfer (p=0.34). In addition to regression analyses, we calculated zero-order (bivariate) correlations between PCL-R factor scores and structural volumes.

2.3 Results

Striatal Subnuclei Volumes

Total PCL-R scores were positively related to accumbens volumes in both Freesurfer and SPM (**Figure 2**). Factor 2 scores were positively related to volume in right putamen in both Freesurfer and SPM; in accumbens bilaterally, right globus pallidus, and right caudate in SPM; and in left putamen in Freesurfer. These findings were significant in the full regression model and zero-order correlations. In contrast, Factor 1 scores were negatively related to right putamen volume, though this relationship was not significant as a zero-order correlation and was only present in SPM. See **Tables 2a-c** for complete results**.**

Table 2a. *Total PCL-R regional volume regressions in FreeSurfer and SPM*

Region	Standardized Beta	t-value	p-value	Relationship	Zero-Order Correlation (p-value)
	FreeSurfer				
Accumbens (L)	0.231	2.558	**0.012**	Positive	0.076
Accumbens (R)	0.176	1.919	0.057	Positive	**0.032**
	SPM				
Accumbens (L)	0.180	2.007	**0.047**	Positive	0.077
Accumbens (R)	0.205	2.243	**0.027**	Positive	**0.022**

Table 2b. *Factor 1 (covarying for Factor 2) regional volume regressions in SPM*

Region	Standardized Beta	t-value	p-value	Relationship	Zero-Order Correlation (p-value)
Putamen (R)	-0.207	-2.061	**0.042**	Negative	0.658

Table 2c. *Factor 2 (covarying for Factor 1) regional volume regressions in FreeSurfer and SPM*

Region	Standardized Beta	t-value	p-value	Relationship	Zero-Order Correlation (p-value)
	FreeSurfer				
Putamen (L)	0.234	2.116	**0.036**	Positive	0.176
Putamen (R)	0.234	2.098	**0.038**	Positive	0.192
	SPM				
Putamen (R)	0.368	3.422	**0.001**	Positive	**0.015**
Caudate (R)	0.303	2.617	**0.010**	Positive	**0.035**
Accumbens (L)	0.239	2.095	**0.038**	Positive	**0.044**
Accumbens (R)	0.380	3.351	**0.001**	Positive	**0.002**
Globus Pallidus (R)	0.336	3.090	**0.003**	Positive	**0.049**

Figure 2: *Zero-order correlation plots for significant relationships between PCL-R scores (total, factor 2) and striatal subnuclei. L; PCL-R, Psychopathy Checklist–Revised; R; SPM, Statistical Parametric Mapping*

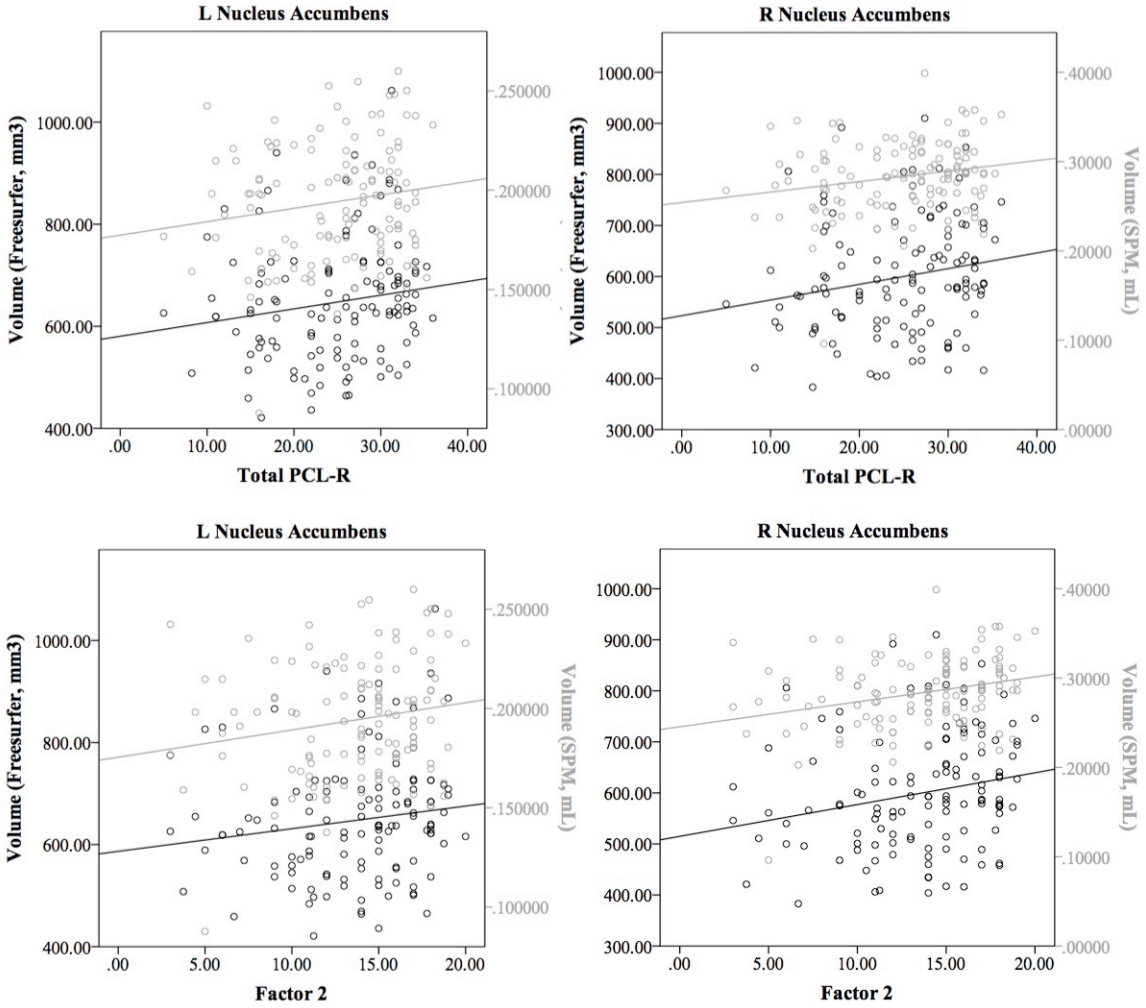

Voxel-Wise Volume Analysis

Voxel-wise regressions within striatal subnuclei revealed a number of focal regions in the striatum where volume increased with increasing psychopathy severity (**Figure 3**). Total PCL-R scores were positively related to focal volume clusters in the accumbens bilaterally, globus pallidus bilaterally, and left putamen; Factor 1 scores were positively related to a focal volume cluster in the right putamen; and Factor 2 scores were positively related to focal volume clusters in the accumbens bilaterally, putamen bilaterally, left caudate, and right globus pallidus. There were no focal volume clusters negatively related to psychopathy scores. See **Tables 3a-c** for full results.

Table 3a. *Total PCL-R focal volume voxel-wise regressions in SPM*

Region	pFWE	MNI Peak Coordinates	Relationship	Cluster Size
Putamen (L)	**0.022**	(-20, 15, 3)	Positive	27
	0.035	(-14, 12, -6)	Positive	7
	0.042	(-16, 15, -4)	Positive	2
Globus Pallidus (R)	**0.017**	(20, -4, 6)	Positive	3
	0.035	(16, -2, 2)	Positive	2
Globus Pallidus (L)	**0.021**	(-12, 8, -6)	Positive	17
Accumbens (R)	**0.021**	(14, 12, -8)	Positive	21
Accumbens (L)	**0.011**	(-12, 8, -8)	Positive	26

Table 3b. *Factor 1 (covarying for Factor 2) voxel-wise regressions in SPM*

Region	pFWE	MNI Peak Coordinates	Relationship	Cluster Size
Putamen (R)	**0.028**	(24, -10, 14)	Positive	3

Table 3c. *Factor 2 (covarying for Factor 1) voxel-wise regressions in SPM*

Region	pFWE	MNI Peak Coordinates	Relationship	Cluster Size
Caudate (L)	**0.006**	(-2, 8, -9)	Positive	20
	0.006	(-18, 18, 3)	Positive	32
	0.030	(-21, 15, 14)	Positive	
Accumbens (L)	**0.018**	(-8, 8, -12)	Positive	44
Accumbens (R)	**0.001**	(6, 10, -10)	Positive	145
	0.001	(16, 14, -12)	Positive	
Globus Pallidus (R)	**0.016**	(16, 10, -4)	Positive	260
	0.016	(26, -10, 2)	Positive	
	0.020	(20, -3, 4)	Positive	
Putamen (L)	**<0.001**	(-20, 18, -2)	Positive	135
	0.001	(-21, 14, 8)	Positive	
Putamen (R)	**0.004**	(18, 14, -10)	Positive	172
	0.028	(21, 10, 3)	Positive	
	0.036	(27, -10, 0)	Positive	34

Figure 3: *Focal areas within striatum (shown in red) where volume has a positive relationship with PCL-R scores (total, factor 1, factor 2). PCL-R, Psychopathy Checklist–Revised.*

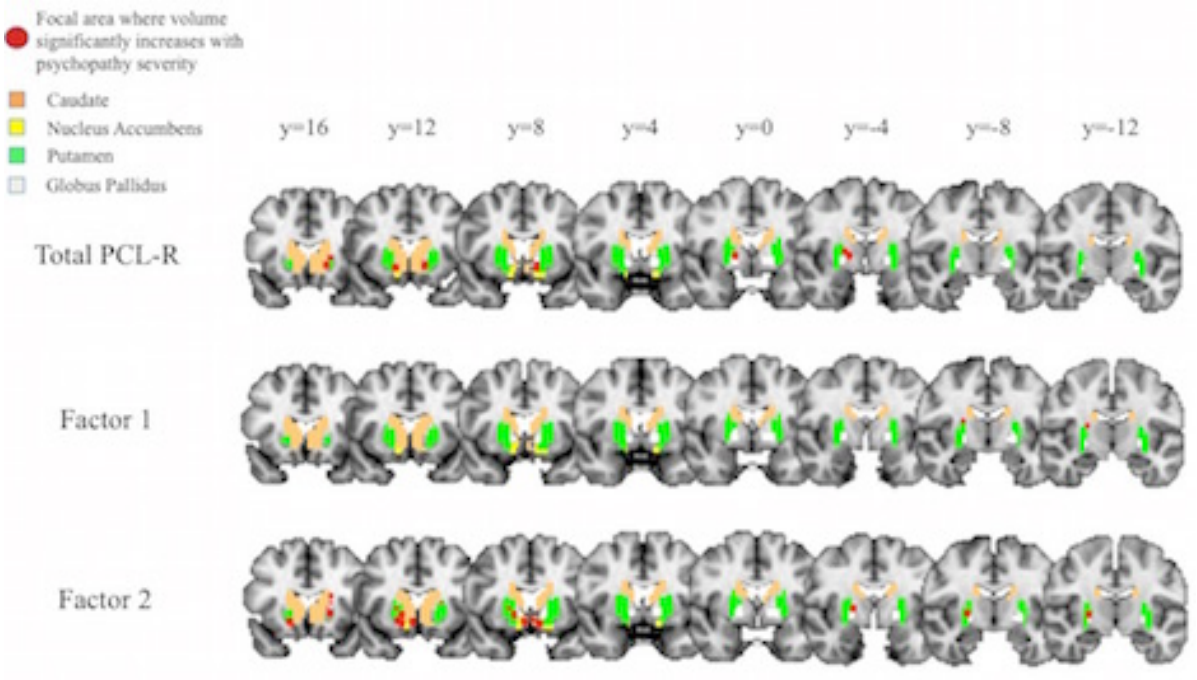

Resting-State Functional Connectivity

Total PCL-R scores were inversely related to RSFC between left putamen and right superior lateral occipital cortex, and also between right globus pallidus and right occipital cortex (**Figure 4**). Factor 1 scores were not related to RSFC for any seeds. Factor 2 scores were positively related to RSFC between striatal seeds and the ventral midbrain, dorsolateral prefrontal cortex, and other areas of the striatum. Factor 2 scores were inversely related to RSFC between striatal seeds and precentral gyrus, postcentral gyrus, and lateral occipital cortex (**Figure 4**). See **Tables 4a-b** for full results.

Table 4a. *Total PCL-R RSFC regressions*

Focal Seed	Seed Origin Coordinates	RSFC Relationship with:	MNI Peak Coordinates	Cluster Size	t-value
Putamen (L)	(-20, 15, 3)	Superior Lateral Occipital Cortex (R)	(-32.5, 59.5, 33.5)	146	-5.18
Globus Pallidus (R)	(16, -2, 2)	Cuneal Cortex (R)	(-5.5, 86.5, 39.5)	366	-5.13

Negative t-value indicates negative relationship.

Table 4b. *Factor 2 RSFC regressions*

Focal Seed	Seed Origin Coordinates	RSFC Relationship with:	MNI Peak Coordinates	Cluster Size	t-value
Caudate (L)	(-18, 18, 3)	Putamen (L)	(18.5, -6.5, 3.5)	124	4.00
Accumbens (R)	(6, 10, -10)	Dorsolateral Prefrontal Cortex (R)	(-38.5, -30.5, 39.5)	188	4.26
	(16, 14, -12)	Postcentral Gyrus (L)	(24.5, 32.5, 54.5)	202	-5.31
Globus Pallidus (R)	(16, 10, -4)	Precentral Gyrus (L)	(12.5, 8.5, 63.5)	561	-4.41
		Postcentral Gyrus (L)	(24.5, 32.5, 54.5)	188	-4.77
Putamen (L)	(-20, 18, -2)	Ventral Midbrain	(3.5, 17.5, -23.5)	149	4.09
		Superior Lateral Occipital Cortex (R)	(-38.5, 83.5, 27.5)	113	-3.79
		Globus Pallidus (L)	(18.5, 11.5, -5.5)	106	3.85
Putamen (R)	(18, 14, -10)	Postcentral Gyrus (L)	(24.5, 32.5, 51.5)	209	-5.67
	(21, 10, 3)	Putamen (L)	(27.5, -6.5, -5.5)	123	4.70

Negative t-value indicates negative relationship.

Figure 4: *Resting-state functional connectivity results for focal volume clusters within the striatum.*

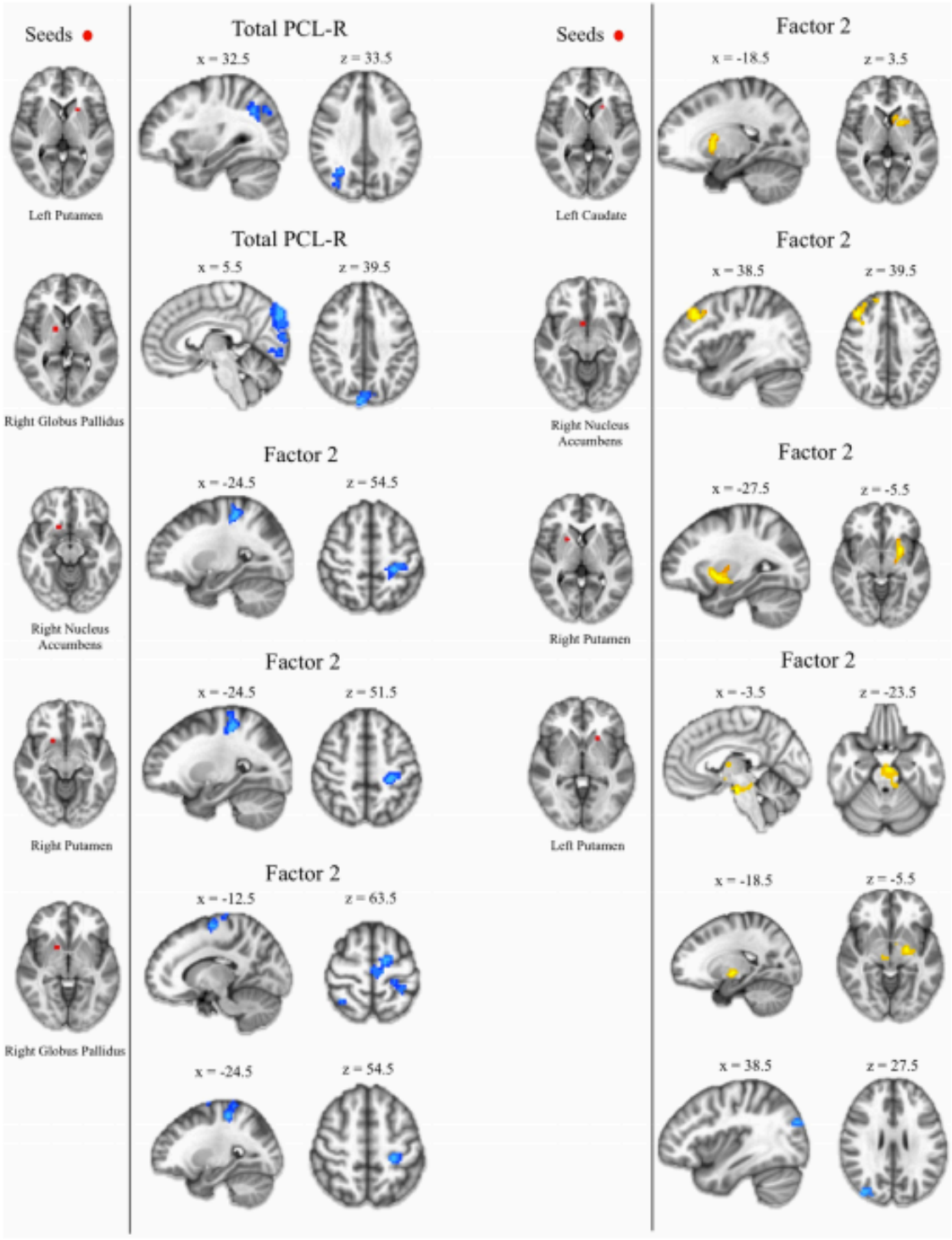

Positive relationships between focal clusters and PCL-R scores (total, factor 1, factor 2) are shown in yellow. Negative relationships are shown in blue. PCL-R, Psychopathy Checklist–Revised.

2.4 Discussion

This study used a multimodal neuroimaging approach to investigate the neural underpinnings of psychopathy in the striatum. First, we investigated how volumes of striatal subnuclei relate to psychopathy severity as measured by total PCL-R, Factor 1, and Factor 2 scores. In general, we found that psychopathy severity was linked to larger striatal subnuclei volumes – most robustly in accumbens and putamen – and that this enlargement was more strongly linked to Factor 2 scores than Factor 1 scores. Next, we performed voxel-wise analyses to identify the focal areas within the striatum where volume was most strongly related to psychopathy severity. These results aligned with those of the regional volume analyses, as volume in focal areas throughout the striatum, including the nucleus accumbens and putamen, were positively associated with psychopathy severity – driven predominantly by Factor 2 scores.

We then performed RSFC analyses to examine whether areas of the striatum for which structural analyses had revealed abnormal volumes associated with psychopathy also displayed functional connectivity abnormalities. Indeed, we found that at many of these striatal areas, psychopathy severity was also associated with abnormal RSFC to other areas of the brain. Psychopathy severity was positively associated with RSFC between striatal areas and other areas of the striatum, dorsolateral prefrontal cortex, and ventral midbrain; conversely, psychopathy severity was inversely related to RSFC between striatal areas and areas within the parietal and occipital lobes. As in the structural analyses, Factor 2 scores predominantly drove the RSFC findings.

Overall, these findings help clarify the structural and functional features of the striatum in psychopathy. Our results are consistent with studies finding volume increases

of the striatum in psychopathy[89,90], provide the first detailed analysis of how these structural abnormalities may correspond to abnormalities in functional connectivity, and provide the first assessment of the relative contributions of striatal volume and functional connectivity to psychopathy severity.

Of particular note is the strong relationship observed here between Factor 2 scores and striatal neurobiology. As the Factor 2 dimension of psychopathy is characterized in part by impulsive behavior[51,95] and excessive need for stimulation, our finding that striatal neurobiology related most strongly to Factor 2 is consistent with a large literature implicating abnormality of the striatum in deficits in reward-processing and impulse control[83,87,118-122]. For instance, we found that Factor 2 severity was positively associated with functional connectivity between the nucleus accumbens and dorsolateral prefrontal cortex. Evidence suggests that individual differences in reward-processing and impulse control are related to the integrity of fronto-striatal circuitry[123]. Relatedly, we observed that Factor 2 severity was positively associated with functional connectivity between the striatum and ventral midbrain. The ventral midbrain is known to communicate with the striatum via dopaminergic transmission as part of the reward processing circuit[124]. Furthermore, we observed three distinct instances of elevated striato-striatal functional connectivity in relation to Factor 2 severity. Collectively, cortico-striato-midbrain circuitry is thought to be central to the brain's reward system[125], and our finding of abnormal fronto-striatal, striato-midbrain, and striato-striatal functional connectivity in relation to Factor 2 severity provides evidence for a neural substrate for the deficits in reward processing observed in psychopathy[126], and may be related to the heightened

mesolimbic dopamine response to reward associated with impulsive-antisocial psychopathic traits[12,126]

Several striatal subregions also showed inverse relationships between psychopathy severity and functional connectivity with areas of the pre- and post-central gyri. Imaging studies in humans have shown cortical thinning in the pre-central gyrus bilaterally in psychopathy[97], as well as thinning in the sensorimotor cortex more generally in a community sample of violent individuals with antisocial personality disorder[127]. Our results suggest that the volumetric abnormalities observed in these areas in relation to psychopathic traits may be related to abnormalities in functional connectivity with the striatum.

Another intriguing observation in this study is the stark difference in the neural correlates of Factor 1 and Factor 2 scores. Whereas Factor 2 scores were uniformly positively associated with both regional and focal volumes in the ventral striatum, Factor 1 scores did not have robust or consistent relationships with striatal subregion volumes. Furthermore, whereas Factor 2 scores were associated with multiple patterns of abnormal striatum functional connectivity, there were no such correlations with Factor 1 scores. These distinct relationships suggest that Factor 1 and Factor 2 traits, despite being highly correlated in terms of PCL-R subscores, are clearly dissociable at the neural level. This conclusion is consistent with recent neuroimaging studies examining white matter microstructure as well as cortical functional connectivity[18,98,128].

One issue that warrants consideration is the substantial rate of substance use disorder in this sample. Multiple studies have linked substance use disorder to structural and functional abnormalities in the striatum[113,129,130]. We included a substance use

disorder variable in our regression models to account for this feature of the study population. Hence, the findings we report here do not appear to be due to individual differences in substance abuse histories. A second issue worth addressing in future studies is the relationship between volumetric and RSFC findings. While our approach allowed us to directly assess whether structural and functional abnormalities were co-localized, this method may be considered liable to statistical non-independence[131], in that the volume and RSFC of striatal subnuclei may be inherently linked. Future studies, in both clinical and non-clinical samples, could establish whether this is indeed the case. Another consideration to address is the relationship between the findings of this study and those of previous imaging studies of psychopathy from our group. Two volumetric studies from Ermer et al.[57,94] – both in samples entirely distinct from the sample of the present study – did not report a relationship between psychopathy and striatal volume in a whole-brain analysis in SPM. However, the striatum was not investigated via an ROI approach, as the focus of these investigations was paralimbic regions. Another volumetric study by Pujara et al.[89] – from which there is an overlap of 12 of the 124 subjects in the present study – used an extreme group design (psychopathic vs. non-psychopathic inmates) with a small sample size (n=41) and did not assess the relationship between psychopathy and striatal volume across the full, continuous range of severity, nor did it examine individual factor scores. Nonetheless, the present results are somewhat consistent with the within-group regressions performed in that study, which show a significant positive relationship between psychopathy severity and ventral striatal volume in the psychopathic (PCL-R≥30) group, but not in the non-psychopathic (PCL-R<20)

group. Furthermore, a prior RSFC study by Philippi et al.[98], which used the same subjects as the present study, only examined cortico-cortical relationships.

In sum, we have analyzed a unique set of multimodal neuroimaging data from a large sample of incarcerated criminal offenders to characterize the relationships between striatal neurobiology and distinct clusters of psychopathic traits. Our findings provide evidence that striatal enlargement and aberrant functional connectivity between the striatum and other brain regions may contribute to the impulsive-antisocial dimension of psychopathy. In **Chapter 3**, an analogous investigation will be conducted for prefrontal volume and RSFC as it relates to impulsive-antisocial psychopathic traits.

Chapter 3: Impulsive-antisocial psychopathic traits linked to increased volume and functional connectivity within prefrontal cortex

Published as: Korponay, C., Pujara, M.S., Deming, P., Philippi, C.L., Decety, J., Kosson, D.S., Kiehl, K.A., and Koenigs, M. (2017) Impulsive-antisocial psychopathic traits linked to increased volume and functional connectivity within prefrontal cortex. *Social Cognitive and Affective Neuroscience,* 12, 169-1178.

3.1 Introduction

In addition to the striatum, another area of the brain that is believed to play a central role in the pathophysiology underlying impulsive-antisocial psychopathic traits is the prefrontal cortex. Subregions of the prefrontal cortex are important for a variety of functions, including self-control and decision-making. For instance, ventromedial prefrontal cortex (vmPFC) and medial orbitofrontal cortex (mOFC) are thought to represent the values of potential decision outcomes and update these values based on ongoing experiences of reward or punishment[132,133]. Dorsolateral prefrontal cortex (dlPFC), which consists of the middle frontal gyrus (MFG) and superior frontal gyrus (SFG), has been implicated in cognitive control[134]. Also, the anterior cingulate cortex (ACC), a limbic structure surrounded by and densely interconnected with prefrontal cortex, has been linked to error detection, performance monitoring, cognitive control, and goal-directed behavior[135,136]. Psychopathic individuals, as well as individuals with acquired damage to the prefrontal cortex, display deficits in many of these functions. Indeed, some of the earliest evidence to suggest involvement of prefrontal cortex dysfunction in psychopathy came from studies of patients who began to display psychopathic-like traits—including poor planning, irresponsibility, and failure to learn from punishment—after acquiring damage to the vmPFC/mOFC[137-140].

While a host of recent studies have demonstrated abnormal structure and function of the prefrontal cortex in psychopathy, the findings have not yet converged to yield a clear relationship between abnormalities in specific subregions of prefrontal cortex and particular psychopathic traits. Studies reporting group differences between psychopathic and non-psychopathic groups have almost exclusively found prefrontal gray matter reductions in psychopathic individuals[56,97,141-143], but correlational findings between PCL-R Total, Factor 1, and Factor 2 scores and prefrontal gray matter have been mixed. For example, medial PFC volume has been inversely correlated with Factor 1 scores[56,57,141], Factor 2 scores[55], and PCL-R Total scores[55,57,141] in a variety of subject populations (adult male and female community psychiatric patients[141], incarcerated adult male offenders[56,144], incarcerated male youth offenders[57] and incarcerated female youth offenders[55]), whereas positive correlations between medial PFC volumes and Factor 1 scores[58] and Factor 2 scores[56-58] have also been observed in these and other samples (a community sample of adult male and female substance abusers[58]). It is notable that two of these studies[56,57] found that medial PFC volume related negatively to Factor 1 scores and positively to Factor 2 scores within the same sample. The mixed findings may be attributable to differences in analysis methodologies (e.g., voxel-based morphometry vs. surface-based morphometry; manual vs. automated tracing methods; measurement of either gray matter volume, density, or thickness; peak height vs. cluster-based statistical thresholds), inclusion/exclusion of moderating variables (e.g., total brain volume, IQ, substance abuse severity), subject populations (e.g., prison inmates vs. community samples; adult vs. youth samples; male vs. female samples), psychopathy severity, and sample sizes.

In addition to structural measures like volume, another important metric of prefrontal cortex integrity is resting-state functional connectivity (RSFC). Studies have found decreased RSFC between the prefrontal cortex and amygdala[145], posterior cingulate cortex[146], insula[97], and limbic and paralimbic regions[56] in psychopathic individuals (but see[147,148]). On the other hand, two studies provide evidence for increased RSFC within prefrontal cortex in psychopathic individuals[56,149], particularly in relation to increasing Factor 2 scores[149]. With regard to the relationship between the structural and functional abnormalities in the prefrontal cortex in psychopathy, only two studies have reported evidence of co-localization of these deficits within the same sample[56,97].

To help resolve some of the inconsistencies and gaps in knowledge reviewed here, we conducted a multimodal neuroimaging investigation of prefrontal cortex structure and function in psychopathy. Using a mobile scanner, we collected magnetic resonance imaging (MRI) from a sample of adult male prison inmates (*N*=124) with a broad range of psychopathy severity. First, we assessed whether the volumes of frontal lobe subregions were correlated with psychopathy severity, in terms of PCL-R Total, Factor 1, and Factor 2 scores. We performed region of interest (ROI)-based analyses in two separate image processing software programs (FreeSurfer and SPM), as well as a voxel-wise analysis in SPM. Next, we analyzed RSFC data from the same participants to determine whether the observed prefrontal structural abnormalities were accompanied by alterations in prefrontal RSFC. This set of analyses comprises the largest study to date to examine both structural and functional features of the prefrontal cortex in psychopathy.

3.2 Methods

Participants

See section **2.2.**

Substance use severity was assessed with the Addiction Severity Index (ASI) [150]. Following the method used previously in adult male inmates [94], years of regular use were summed for each substance (alcohol and drug) that the participant reported using regularly (3 or more times per week for a minimum period of one month); total scores were then divided by age (to control for opportunity to use) and a square root transformation was applied. Participant characteristics are summarized in **Table 1**.

MRI Acquisition

See section **2.2**.

Analytic Strategy

Because processing pipelines and region of interest (ROI) parcellations differ between image processing software programs, and because studies have reported that results may vary as a function of program [108], we computed volumes of the prefrontal cortex ROIs (medial orbitofrontal cortex, lateral orbitofrontal cortex, inferior frontal gyrus, middle frontal gyrus, superior frontal gyrus, and anterior cingulate cortex) from two separate programs (FreeSurfer and SPM) and performed separate analyses with both sets of values. Statistical significance for the ROI analyses was evaluated at a Bonferroni-corrected $p<0.004$ that accounted for the 12 analyses conducted in each program (left and right hemisphere of six ROIs). Additionally, SPM was used to perform small volume-corrected voxel-wise analyses within the prefrontal cortex. This type of analysis can detect smaller, focal aberrations in volume that may not be detected in the subregion volume analysis, and allows for more specific localization of the areas where volume is most strongly linked to psychopathy severity. These analyses were restricted to a mask

encompassing the union of the six bilateral ROIs listed above. Peak height with correction for multiple comparisons using a family-wise error (FWE) rate of $p<0.05$ was used to assess statistical significance for these voxel-wise analyses.

After performing the volumetric analyses, we then examined whether the identified volume abnormalities were associated with abnormalities in RSFC. We chose seeds centered at the peak coordinates of the focal volume clusters identified in the voxel-wise analyses in order to directly assess whether areas where volume correlated with psychopathy severity also had functional connectivity relationships that correlated with psychopathy severity, as the co-localization of these abnormalities may point to a common underlying pathophysiology [59]. We created a 6mm-radius spherical seed around these peak coordinates, and subsequently assessed RSFC between these seeds and other areas of the brain in relation to psychopathy ratings. While creating seeds based on the exact voxel sizes and shapes of each volume cluster would have provided the greatest degree of precision in assessing the overlap between volume and RSFC metrics, 6mm-radius spheres are the standard seed size and shape for cortical resting state analyses based on the literature. Seeds were visually inspected to ensure that they did not include volume outside of the whole-brain mask; seeds that did expand beyond the brain mask were excluded from analysis.

Seeds were evaluated in RSFC regressions only in relation to the specific psychopathy score-type (PCL-R Total, Factor 1, and/or Factor 2) for which the focal area (on which the seed was based) had demonstrated a relationship with in the volumetric analysis. To correct for multiple comparisons, we used FWE-correction at the cluster level using a whole-brain mask (3dClustSim in AFNI, using the version updated

December 2015) [109,110] and applied cluster extent thresholding. We used the autocorrelation function to calculate the full width at half maximum (FWHM) in order to address the non-Gaussian nature of functional MRI data [151]. The cluster extent threshold corresponded to the statistical probability (α=0.05, or 5% chance) of identifying a random noise cluster at a predefined voxel-wise (i.e., whole-brain) threshold of p<0.001 (uncorrected). Using this whole-brain FWE cluster correction, a cluster-corrected size of ≥47 voxels was significant at p_{FWE}<0.05.

Covariates

We found the expected [116] negative correlations between age and the gray matter volume of all ROIs (significant at p<0.05 in ten out of 12 FreeSurfer ROIs and in three out of 12 SPM ROIs). Thus, age was included as a covariate in all models. Also, Factor 2 scores had a trending positive relationship with substance use severity as measured by the ASI (p=0.055). Because gray matter volume has been shown to relate to substance use[111-115], we included substance use severity using the transformed ASI variable as a covariate in all regression models. Furthermore, we observed a significant group effect (p<0.05) of race (between Caucasian and non-Caucasian subjects) on volume of 11 out of 12 ROIs in FreeSurfer and ten out of 12 ROIs in SPM, and thus race was also included as a covariate in all regression models. IQ was not related to psychopathy severity (PCL-R Total: p=0.405; Factor 1: p=0.726; Factor 2: p=0.730) but was significantly positively correlated (p<0.05) with the volumes of three ROIs in FreeSurfer and ten ROIs in SPM. However, when race was added to the model testing the main effect of IQ on volume, the relationship between IQ and volume did not remain significant in any ROI in either program. On the other hand, when IQ was added to the model testing the main effect of

race on volume, race maintained a significant relationship with the volume of 11 of the 12 ROIs in FreeSurfer and nine of the 12 ROIs in SPM. These data suggest that race accounts for much of the variance in IQ in this model. Coupled with the observation that race was highly correlated with IQ ($p<0.001$), we excluded IQ from our main analysis models in order to reduce multicollinearity. Additionally, in order to account for variation in overall brain size, we included brain volume (gray matter + white matter) as a covariate in all structural analyses. There was no significant relationship between PCL-R Total score and brain volume as measured by either SPM ($p=0.65$) or FreeSurfer ($p=0.43$). We also ensured that problematic levels of multicollinearity were not present between brain volume and age; the variance inflation factor was less than 1.4 for both brain volume and age in regression models for all of the ROIs, indicating unproblematic levels of multicollinearity. In regressions where the main variable of interest was a Factor score, the other Factor score was also included as a covariate. In addition to regression analyses, we calculated zero-order (bivariate) correlations between PCL-R scores and structural volumes.

3.3 Results

ROI Volume Analysis

PCL-R Total scores and Factor 2 scores were positively related to specific subregion volumes throughout the prefrontal cortex (all covariates included age, race, substance abuse severity, and brain volume; Factor 1 score was also included as a covariate for Factor 2 analyses). The most robust relationships (surviving a $p<0.004$ Bonferroni correction for multiple comparisons) were observed between Factor 2 scores and volume of the right medial orbitofrontal cortex, left middle frontal gyrus, and left

superior frontal gyrus (**Figure 5**). Zero-order correlations between Factor 2 scores and each of these three subregions were significant (p<0.05) in SPM but were not always significant in FreeSurfer. The directions of findings were consistent for the volume values extracted from both SPM and FreeSurfer, though significance levels differed. See **Tables 5a-c** for regression data. There were no significant relationships between Factor 1 scores and ROI volumes. In addition to these main analyses, we performed the following supplementary analyses with different models to assess the sensitivity of the findings to covariates: factor score analyses without covarying for the other factor, and replacing the continuous ASI substance use severity covariate with the categorical substance use disorder (SUD) covariate (None, Abuse, or Dependence) from the Structured Clinical Interview for DSM-IV Axis I disorders (SCID-IV) [96]. Findings remained essentially the same with the alternate factor score and substance abuse models.

Table 5a. *Total PCL-R regional volume regression results from FreeSurfer and SPM*

Region	Standardized Beta	t-value	p-value	Zero-Order Correlation R-value (p-value)
	FreeSurfer			
Middle Frontal Gyrus (L)	0.127	1.815	0.072	0.165 (0.067)
	SPM			
Lateral Orbitofrontal Cortex (L)	0.141	2.025	0.045	0.162 (0.074)
Middle Frontal Gyrus (L)	0.186	2.629	0.010	0.219 (0.015)
Inferior Frontal Gyrus (L)	0.173	2.108	0.037	0.206 (0.022)
Lateral Orbitofrontal Cortex (R)	0.166	2.358	0.020	0.181 (0.045)
Medial Orbitofrontal Cortex (R)	0.184	3.382	**0.001**	0.224 (0.013)
Middle Frontal Gyrus (R)	0.161	2.550	0.012	0.196 (0.029)

Displaying relationships with p<0.10. Relationships with p<0.004 (surviving Bonferroni correction) are bolded.

Table 5b. *Factor 1 (covarying for Factor 2) regional volume regression results from FreeSurfer and SPM*

Region	Standardized Beta	t-value	p-value	Zero-Order Correlation R-value (p-value)
	SPM			
Superior Frontal Gyrus (L)	-0.215	-2.293	0.024	-0.011 (0.901)

Displaying relationships with $p<0.10$. Relationships with $p<0.004$ (surviving Bonferroni correction) are bolded.

Table 5c. *Factor 2 (covarying for Factor 1) regional volume regression results from FreeSurfer and SPM*

Region	Standardized Beta	t-value	p-value	Zero-Order Correlation R-value (p-value)
	FreeSurfer			
Medial Orbitofrontal Cortex (R)	0.175	1.952	0.053	0.202 (0.025)
	SPM			
Superior Frontal Gyrus (L)	0.329	3.499	**0.001**	0.244 (0.007)
Middle Frontal Gyrus (L)	0.293	3.238	**0.002**	0.298 **(0.001)**
Superior Frontal Gyrus (R)	0.179	2.156	0.033	0.153 (0.092)
Middle Frontal Gyrus (R)	0.200	2.459	0.015	0.245 (0.006)
Medial Orbitofrontal Cortex (R)	0.216	3.068	**0.003**	0.263 **(0.003)**

Displaying relationships with $p<0.10$. Relationships with $p<0.004$ (surviving Bonferroni correction) are bolded.

Figure 5: *Zero-order correlation plots for significant relationships (P < 0.004) between Factor 2 scores and volume of prefrontal cortex subregions.*

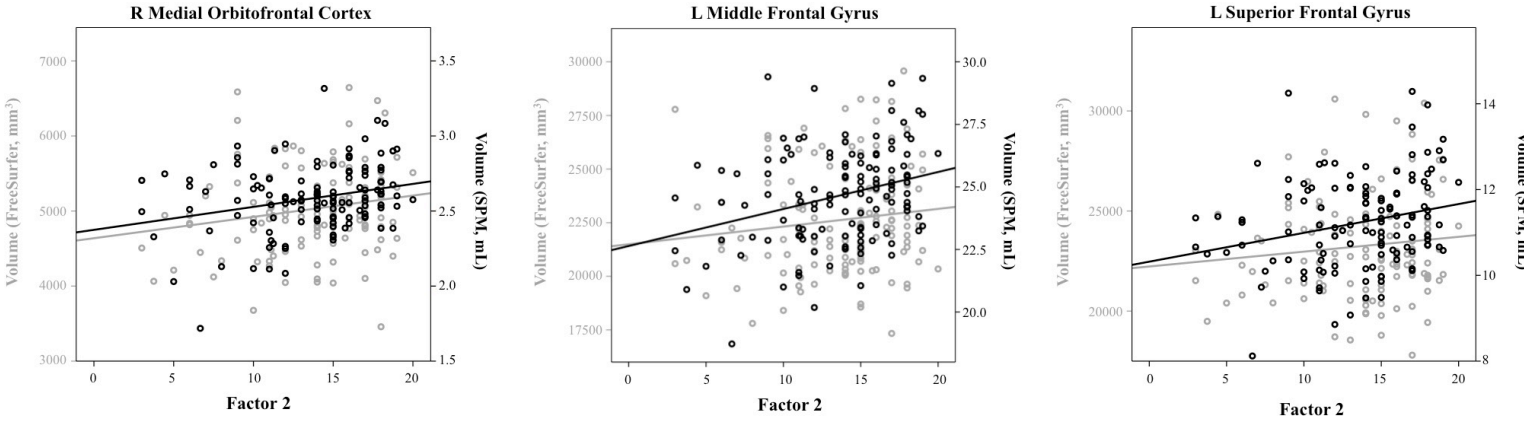

Voxel-Wise Volume Analysis

Voxel-wise regressions identified focal areas within the prefrontal cortex where volume was positively correlated with Factor 2 scores (all covariates included age, race, substance abuse severity, brain volume, and Factor 1 score) (**Figure 6).**

Mirroring the ROI results, these relationships were found in the right medial orbitofrontal cortex, left middle frontal gyrus, and left superior frontal gyrus, as well as in the right middle frontal gyrus, left medial orbitofrontal cortex, right superior frontal gyrus, and right anterior cingulate cortex. There were no significant relationships between PCL-R

Figure 6: *Results of voxel-wise analysis for the relationship between Factor 2 scores and volume in the prefrontal cortex.*

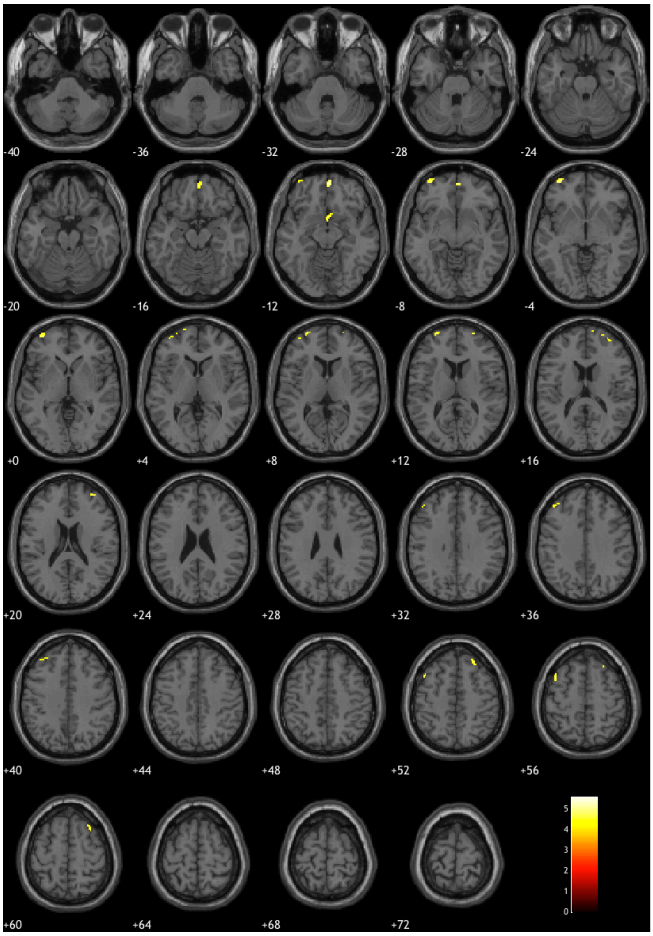

Positive relationships are shown in yellow.

total scores or Factor 1 scores and prefrontal cortex focal volumes. There were also no negative relationships between any psychopathy score-type and prefrontal focal volumes. See **Table 6** for complete results. In addition to the voxel-wise regressions restricted to the prefrontal cortex mask, we also performed whole-brain voxel-wise regressions to assess the specificity of psychopathy severity relations to volumes in the prefrontal cortex. These results show that while relationships between psychopathy severity and volume are not isolated to the prefrontal cortex, consistent with both the main analyses of this study and of a previous study of this sample [59], the prefrontal cortex and striatum are brain regions where volume is strongly positively correlated with Factor 2 severity.

Table 6. *Factor 2 (covarying for Factor 1) focal volume voxel-wise regressions in SPM*

Region	$p_{FWE\text{-}corr}$	Cluster Size	MNI Peak Coordinates	Relationship
Middle Frontal Gyrus (L)	0.003	184	(-34, 60, -3)	Positive
	0.013	92	(-42, 38, 34)	Positive
	0.005	84	(-26, 63, 10)	Positive
	0.008	55	(-42, 15, 54)	Positive
Middle Frontal Gyrus (R)	0.005	43	(34, 52, 20)	Positive
	0.012	27	(26, 62, 12)	Positive
Medial Orbitofrontal Cortex (R)	<0.001	162	(3, 56, -10)	Positive
Superior Frontal Gyrus (R)	0.006	83	(27, 26, 57)	Positive
	0.036	4	(10, 66, 16)	Positive
Superior Frontal Gyrus (L)	0.015	13	(-26, 15, 63)	Positive
	0.038	4	(-18, 68, 6)	Positive
Anterior Cingulate Cortex (R)	0.020	11	(3, 56, 3)	Positive
Medial Orbitofrontal Cortex (L)	0.004	69	(2, 8, -10)	Positive

Resting-State Functional Connectivity Analysis

Increased functional connectivity was observed between multiple regions of the prefrontal cortex in relation to Factor 2 scores (all covariates included age, race, substance abuse severity, and Factor 1 scores) (**Figure 7**).

Figure 7: RSFC results.

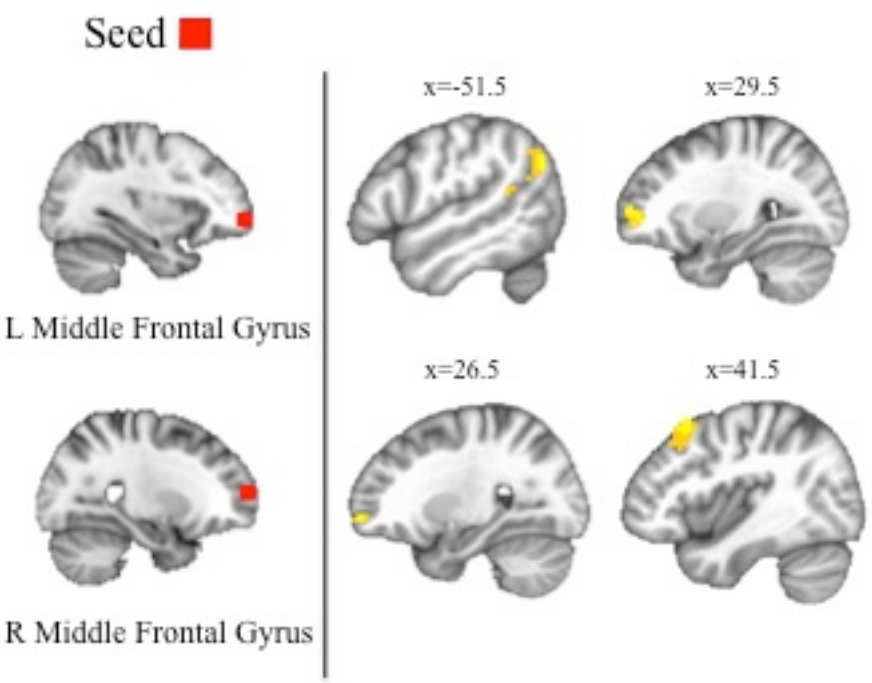

Positive relationships between RSFC and Factor 2 scores are shown in yellow.

In particular, Factor 2 scores were positively correlated with functional connectivity between left middle frontal gyrus and right anterolateral prefrontal cortex and between right middle frontal gyrus and right frontal polar cortex. See **Table 7** for complete results. RSFC was not evaluated for PCL-R Total scores or Factor 1 scores because there were no focal volumes significantly related to these score-types.

Table 7. *Factor 2 (covarying for Factor 1) RSFC regressions*

Focal Seed	Seed Origin Coordinates	RSFC Relationship with:	MNI Peak Coordinates	Cluster Size	t-value[a]
Middle Frontal Gyrus (L)	(-34, 60, -3)	Angular Gyrus (L)	(-51.5, -65.5, 33.5)	59	4.49
		Anterolateral Prefrontal Cortex (R)	(29.5, 51.5, 3.5)	57	3.71
Middle Frontal Gyrus (R)	(26, 62, 12)	Middle Frontal Gyrus (R)	(41.5, 18.5, 54.5)	90	5.16
		Frontal Polar Cortex (R)	(26.5, 60.5, -5.5)	63	4.48

[a] Positive t-value indicates positive relationship.

3.4 Discussion

This study used a multimodal neuroimaging approach to examine the relationship between psychopathic traits and structural and functional features of the prefrontal cortex. First, we investigated how volumes of frontal lobe subregions relate to psychopathy severity as measured by PCL-R Total, Factor 1, and Factor 2 scores. We found that across both FreeSurfer and SPM, PCL-R Total scores and Factor 2 scores were exclusively linked to larger prefrontal cortex subregion volumes. The most robust relationships were observed between Factor 2 scores and the volume of right medial orbitofrontal cortex and left dorsolateral prefrontal cortex (middle and superior frontal gyri). Next, we performed complementary voxel-wise analyses within the prefrontal cortex, which had the potential to reveal volumetric relationships within or across ROIs. This analysis also revealed exclusively positive relationships between Factor 2 severity and volume in specific regions of prefrontal cortex, including medial orbitofrontal cortex and dorsolateral prefrontal cortex. Finally, we assessed resting-state functional connectivity in areas where volume was related to psychopathy severity. We found that

Factor 2 scores were positively correlated with functional connectivity between prefrontal subregions, including between left middle frontal gyrus and right inferior frontal gyrus and between right middle frontal gyrus and right lateral orbitofrontal cortex.

Although prior studies using group-level designs have almost exclusively found decreased prefrontal gray matter in psychopathic individuals compared to non-psychopathic individuals[56,97,141-143], our results are consistent with a number of prior studies that have shown positive relationships between Factor 2 scores and regions of PFC, including medial dorsal and lateral frontal cortex[56], mOFC and ACC[57], and medial, middle, and superior frontal gyri[58]. It is interesting to note that most studies analyzing prefrontal gray matter and Factor 1 scores find a negative relationship[56,57,141], while most studies analyzing prefrontal gray matter and Factor 2 scores find a positive relationship[56-58]. These findings suggest that Factor 1 and Factor 2 traits are dissociable at the neural level despite being highly correlated in terms of PCL-R score. Thus, it is possible that measures of prefrontal gray matter structure in a given sample of psychopathic individuals depends on the relative severity of Factor 1 and Factor 2 traits in that sample. It is also worth noting that Factor 1 traits are more uniquely associated with psychopathy, whereas Factor 2 traits are shared more broadly as features of a number of disorders (e.g. antisocial personality disorder, impulse control disorders, etc.). Thus, the present results may speak more broadly to the neural correlates of impulsive-antisocial traits rather than of psychopathy specifically.

A positive association between prefrontal gray matter volume and Factor 2 trait severity could potentially be the result of aberrant neurodevelopment. Gray matter volume decreases throughout adolescence and early adulthood in several distinct clusters

of prefrontal cortex, including the medial and dorsolateral prefrontal subregions[152,153]. One possibility is that the observed positive associations between Factor 2 scores and PFC subregion volumes reflects deficient synaptic and neuronal pruning in these areas, resulting in ineffective and/or dysfunctional processing. Our data do not address this level of analysis directly, but they do suggest an interesting avenue for future research.

Factor 2's relevance to prefrontal cortex neurobiology can be understood conceptually by considering the types of experimental tasks on which psychopathic individuals perform poorly and the consequences that these deficits are likely to yield outside the laboratory. For instance, psychopathic individuals have been shown to perform poorly on tasks that require learning from punishment[154]; this function has been shown to involve OFC[155], a region found here to be enlarged in psychopathic individuals. A deficit in this function may increase the likelihood that psychopathic individuals engage in poor decision-making that results in impulsive and criminal behavior—traits that are indexed by Factor 2 score. Consistent with this interpretation, in a previous study with this same inmate sample we found that Factor 2 scores were specifically associated with volume of the nucleus accumbens subnucleus of the striatum[59]. The medial OFC region identified in this study is known to be densely interconnected with the nucleus accumbens[156,157], and both regions are central components of the brain circuitry involved in processing value and reward[158].

Though the literature on frontal lobe RSFC in psychopathy is more limited, the finding in this sample of a positive association between Factor 2 severity and intra-frontal RSFC is consistent with Contreras-Rodriguez and colleagues' group-level finding that psychopathic individuals had elevated intra-frontal RSFC compared to non-psychopathic

individuals. This study found that the RSFC difference was accompanied by decreased prefrontal gray matter concentration in psychopathic individuals compared to non-psychopathic individuals, but also by a positive relationship between prefrontal gray matter concentation and Factor 2 scores. These findings are also consistent with evidence of increased intra-frontal anatomical connectivity in psychopathy[159]. This converging evidence of heightened intra-frontal structural and functional connectivity in psychopathy is interesting to consider in the context of studies finding increased BOLD activity in prefrontal areas in psychopathic individuals during social decision-making[160], emotion processing[161,162] and moral judgment tasks[163] (but see also[164-166]). Psychopathic individuals' heightened recruitment of prefrontal areas that subserve abstract reasoning on these tasks—particularly dlPFC—has been interpreted as a compensatory mechanism used to maintain socially appropriate behavior in the absence of properly functioning limbic structures that subserve emotion processing[161]. It is possible that the enlarged volume of MFG and SFG (parts of the dlPFC) and associated increases in MFG RSFC to other prefrontal areas observed here and in other studies, along with the increased intra-frontal anatomical connectivity observed in relation to psychopathy[159], may either facilitate or reflect the enhanced recruitment of dlPFC in psychopathic individuals during these tasks.

One potential issue of this study that warrants consideration is the substantial rate of substance use disorder in this sample. Multiple studies have linked substance use disorder to structural and functional abnormalities in the frontal lobe. We included a continuous substance use severity variable in our regression models to account for this feature of the study population. Hence, the findings we report here do not appear to be

due to individual differences in substance abuse histories. Other substance use metrics such as the substance use disorder (SUD) measure on the Structured Clinical Interview for DSM-IV Axis I disorders (SCID-IV)[96] quantify abuse severity in a categorical manner, though it is not well-established which substance abuse measure is best suited for capturing meaningful differences in brain data. In supplementary analyses we conducted the regional volume analyses using the SCID-IV's categorical metric for presence of substance use disorder (None, Abuse, or Dependence) instead of the ASI's continuous measure, and findings remained essentially the same. In a future study, we will more fully examine the relationships between substance use characteristics and frontal lobe neurobiology in this sample. A related issue is that this study did not include a non-incarcerated comparison group, which makes it difficult to discern whether the observed findings represent "deficits" or "abnormalities". It is possible that increased prefrontal gray matter and intra-frontal functional connectivity facilitate enhanced function in certain domains and deficits in others. We may only conclude based on the present findings that these neurobiological features are associated with increased impulsive and antisocial traits. Another issue worth addressing in future studies is the relationship between volumetric and RSFC findings. While our approach allowed us to directly assess whether structural and functional abnormalities were co-localized, this method may be considered liable to statistical non-independence[131], in that the volume and RSFC of frontal lobe regions may be inherently linked. Future studies, in both clinical and non-clinical samples, could establish whether this is indeed consistently the case. Lastly, it should be noted that another study from our group used subjects from the present sample to examine RSFC in psychopathy within and between the default mode

network, frontoparietal network and cingulo-opercular network[149] and some evidence of a positive correlation between Factor 2 scores and intra-frontal RSFC was found. However, as prefrontal RSFC per se was not a primary focus of this previous study, only four frontal lobe seeds (mPFC, left and right dlPFC, and dACC) were assessed, seeds were not chosen in relation to volumetric data, and only clusters falling within masks of the specific brain networks of interest to the study were examined. The present study thus reports on new and more comprehensive data in relation to prefrontal RSFC in psychopathy.

In sum, we have analyzed a unique set of multimodal neuroimaging data from a large sample of incarcerated criminal offenders to help clarify the structural and functional characteristics of prefrontal cortex in psychopathy. Our findings provide evidence of co-localized prefrontal cortex enlargement and heightened intra-frontal RSFC related predominantly to the impulsive and antisocial traits of psychopathy. Having established the neurobiological correlates of impulsive-antisocial traits in psychopathic inmates, **Chapter 4** will investigate the neurobiological correlates of impulsive traits in a healthy adult sample.

Chapter 4: Neurobiological correlates of impulsivity in healthy adults: Lower prefrontal gray matter volume and spontaneous eye-blink rate but greater resting-state functional connectivity in basal ganglia-thalamo-cortical circuitry

Published as: Korponay, C., Dentico, D., Kral, T., Ly, M.M., Kruis, A., Goldman, R., Lutz, A. and Davidson, R.J., (in press). Neurobiological correlates of impulsivity in healthy adults: lower prefrontal gray matter volume and spontaneous eye-blink rate but greater resting-state functional connectivity in basal ganglia-thalamo-cortical circuitry. *NeuroImage*.

4.1 Introduction

The current study aims to advance the literature by providing an account of impulsivity's relationship to multiple neurobiological metrics in the brain's reward-processing and decision-making networks in healthy adults. We present the first multi-model dataset to simultaneously examine gray matter volume and resting-state functional connectivity in relation to impulsivity in a healthy sample. We also examine the relationship between impulsivity and spontaneous eye-blink rate to glean possible relationships with dopaminergic activity. Furthermore, we examine each of these neurobiological metrics with respect to both trait-based and task-based measures of impulsivity. The prior literature in healthy adults led us to hypothesize a negative relationship between impulsivity and prefrontal gray matter, though hypothesizes for the RSFC and sEBR relationships were non-directional due to a lack of consistent findings on these metrics in prior literature.

Overview

This study of n=105 healthy adults examines relationships between impulsivity and gray matter volume, resting-state functional connectivity, and spontaneous eye-blink

rate (sEBR), a peripheral measure of central dopaminergic activity. Impulsivity was measured both by self-rating of impulsivity using the Barratt Impulsiveness Scale (BIS-11) and by performance on a go/no-task. Since impulsivity is a multi-dimensional construct encapsulating a number of distinct cognitive processes, we evaluated the neurobiological metrics with respect to multiple metrics from the BIS-11 and go/no-go task that captured this range of impulsivity subdomains. On the BIS-11, we measured attentional, motor and non-planning impulsivity subscale scores in addition to total score; on the task, we measured accuracy on no-go trials to gauge the capacity to withhold prepotent responses, and post-error slowdown to measure the tendency to proceed more deliberately after negative feedback.

First, whole-brain voxel-wise analyses were used to examine relationships between GMV and the impulsivity metrics. Next, we examined the relationship between RSFC and the impulsivity metrics using seed-to-whole-brain analyses; in order to assess RSFC in different networks in the basal-ganglia-thalamo-cortical circuitry, we used six a priori basal ganglia seeds[9] that have been shown to participate in functionally distinct networks, in addition to a substantia nigra seed[167] and ventral tegmental area seed[167] to assess RSFC in distinct dopaminergic pathways. Lastly, we examined correlations between sEBR and the impulsivity metrics. Age and sex were used as covariates in all analyses. Additionally, all volumetric analyses also included intracranial volume as a covariate.

4.2 Methods

Participants

127 healthy adults were recruited from the community for a study on health and well-being through internet and local newspaper advertisements. Participants provided written informed consent for study procedures that were approved by the UW-Madison Health Sciences Internal Review Board. Criteria for exclusion included use of psychotropic or steroid drugs, night-shift work, diabetes, peripheral vascular disease or other diseases affecting circulation, pregnancy, and current smoking habit or alcohol or drug dependency; exclusion criteria were assessed via self-report. Structural magnetic resonance imaging (MRI) scans were obtained for 106 subjects; one subject's scan was excluded due to poor image registration. Thus, data from a total of 105 subjects [age, 48.6 ± 10.9 years (mean ± SD); 65 women, 40 men] were included in the gray matter volume analyses. 27 of these 105 subjects were excluded from RSFC analyses due to excessive motion during the functional MRI scan, and so data from 78 subjects were used in the RSFC analyses [age, 48.9 ± 11.0 (mean ± SD); 50 women, 28 men]. Spontaneous eye blink rate (sEBR) data was obtained for 98 of these 105 subjects, and so analyses involving sEBR included data from 98 subjects [age, 48.9 ± 10.8 years (mean ± SD); 58 women, 40 men].

Barratt Impulsiveness Scale (BIS-11)

The BIS-1[168] is a self-report questionnaire containing 30 questions, each of which requires the subject to choose between ‘Rarely/Never’, ‘Occasionally’, ‘Often’ and ‘Almost Always’. Items are scored from 1 to 4. Scoring yields a total score and three subscale scores derived by factor analysis: attentional impulsivity (e.g. "I am restless at the theatre or lectures"), motor impulsivity (e.g. "I do things without thinking"), and non-planning impulsivity (e.g. "I am more interested in the present than the future")[169]. Higher

scores indicate higher levels of impulsivity. The BIS-11 has good internal consistency (Cronbach's α= 0.83) and test–retest reliability (Spearman's rho= 0.83)[170].

Go/No-Go Task

Subjects completed an auditory go/no-go task based on the paradigm described in Shalgi et al (2009)[171]. Subjects were instructed to push the spacebar on a keyboard upon the presentation of an auditory syllable stimulus, except when the same syllable was repeated (no-go repeat trials) or when the syllable was "ke/" or "pa/" (no-go syllable trials). Subjects completed four blocks of 252 trials, of which 196 trials were go trials, 16 were no-go repeat trials, and 40 were no-go syllable trials. Accuracy was calculated as the percentage of correct button-pushes for go-trials and the percentage of correct withholds for no-go trials. Post-error slowdown was calculated as the difference between average reaction time on go-trials following incorrect no-go trials and average reaction time on go-trials following correct no-go trials.

Previous studies have shown that inhibitory capacity on no-go trials is sensitive to task demands, and that different task demands recruit distinct sets of brain regions and cognitive functions. For instance, Shalgi and colleagues find that subjects perform better on no-go syllable trials than no-go repeat trials[171]. This is consistent with a meta-analysis that classifies go/no-go tasks in which the no-go stimuli are constant (as in the no-go syllable trials) as "simple", and classifies go/no-go tasks in which the no-go stimuli change depending on context (as in the no-go repeat trials) as "complex"[172]; this study also found that complex no-go trials recruit prefrontal regions to a greater extent than simple no-go trials, likely due to the increased attentional and working memory loads

required for these trials. Given these performance and neurobiological differences, we analyzed accuracy on each type of no-go trial separately.

Image Acquisition

Images were acquired on a GE X750 3.0 Tesla MRI scanner device with an eight-channel head coil. Anatomical scans consisted of a high-resolution 3D T1-weighted inversion recovery fast gradient echo image (inversion time = 450 ms, 256 x 256 in-plane resolution, 256 mm FOV, 124 x 1.0 mm axial slices). Resting-state functional images were acquired in a single scan run using a gradient echo EPI sequence (64x64 in-plane resolution, 240mm FOV, TR/TE/Flip = 2000ms/25ms/60°, 40x4mm interleaved sagittal slices, and 210 3D volumes).

Structural MRI Preprocessing and Analysis

Preprocessing and analyses of structural MRI data were conducted in Statistical Parametric Mapping software (SPM12; http://www.fil.ion.ucl.ac.uk/spm). For preprocessing, T1 images were manually realigned; segmented into gray matter, white matter, and cerebrospinal fluid; normalized to Montreal Neurological Institute (MNI)-152 space; modulated after normalization to preserve volume; and smoothed with an 8mm full-width at half-maximum (FWHM) Gaussian kernel[102]. Individual Brain Atlases using Statistical Parametric Mapping (IBASPM) (http://www.thomaskoenig.ch/Lester/ibaspm.htm) in the Wake Forest University (WFU) Pick Atlas Toolbox was used to create any region of interest masks for small volume correction (SVC) analyses.

A separate whole-brain voxel-wise regression was conducted for each impulsivity metric (i.e. each BIS-11 score and each go/no-go performance metric). Significance for

whole-brain voxel-wise analyses was evaluated using family wise error (FWE) cluster correction. The cluster extent threshold corresponded to the statistical probability (α=0.05, or 5% chance) of identifying a random noise cluster at a predefined voxel-wise (i.e., whole-brain) threshold of $p<0.001$ (uncorrected). We used 3dClustSim (updated December 2015) to determine that a cluster-corrected size of ≥236 voxels was significant at $p_{FWE}<0.05$.

Resting-State fMRI Preprocessing and Analysis

Resting-state data were processed using a combination of FEAT (FMRI Expert Analysis Tool) Version 6.00, part of FSL (FMRIB's Software Library, www.fmrib.ox.ac.uk/fsl) and AFNI[100]. We removed the first four volumes from each subject's data, then used FSL's FEAT tool for motion correction with MCFLIRT[173], and non-brain removal using BET[174]. Transformation matrices for registration were computed and applied using FSL to register the subject's time series data to their anatomical template, and a 12DOF affine transformation was used to register the subject's anatomical to Montreal Neurological Institute (MNI) space using FLIRT[173,175]. Registration from high resolution structural to standard space was then further refined using FNIRT nonlinear registration[176,177]. MNI-normalized structural images were segmented with FAST and these segmentations were used to create voxel-wise average signal and derivates from eroded CSF and 2X eroded white-matter masks. These and 6 motion regressors of no interest were included in a nuisance regression using AFNI's 3dDeconvolve. The results from this regression were smoothed using a 5mm FWHM Gaussian kernel.

Six functionally distinct basal ganglia seeds, each with a radius of 3.5 mm, were created in each hemisphere based on coordinates reported by Di Martino and colleagues (2008)[9]. The origin coordinates of these seeds were in the inferior ventral striatum (±9, 9, -8), superior ventral striatum (±10, 15, 0), dorsal caudate (±13, 15, 9), dorsal caudal putamen (±28, 1, 3), dorsal rostral putamen (±25, 8, 6), and ventral rostral putamen (±20, 12, −3). Furthermore, a substantia nigra seed (±12, -12, -12) and midline ventral tegmental area seed (0, -15, -12), each with a radius of 2 mm, were created based on coordinates reported by Tomasi and Volkow (2012)[167].

Average time-series were extracted for each seed from each participant's preprocessed data. These timeseries were regressed back onto each participant's data using 3dDeconvolve. To further address motion, high motion time points (a frame-wise displacement (FD) measure larger than 0.2 mm) were modeled out of the data with an individual regressor. Participants with more than 25% (52 TRs) of the data censored were omitted from analysis, leading to a total of 27 excluded participants. The resultant maps were Fisher-Z transformed to stabilize correlation variance. Average Fisher-Z correlations were extracted from the target ROIs. Whole-brain, voxel-wise regressions were conducted using FSL's Randomise[178] thresholded at $p<0.05$ with 5000 permutations. A separate regression analysis was conducted for each impulsivity metric (i.e. each BIS-11 score and each go/no-go performance metric) for each seed.

Spontaneous Eye-blink Recording

Spontaneous eye-blink rates are affected by the time of day[179], and so data were collected around 7 pm for all participants to ensure that differences in the time of data collection could not contribute to any observed difference in eye-blink activity. Baseline

sEBR was extracted from high- density, 256-channel EEG data that were collected during a 10-min baseline EEG recording. Participants were seated in front of a computer screen. During the first 2 min and last 2 min of the baseline recording, participants were instructed to keep their eyes closed. During the 6 min in between these periods, participants were instructed to keep their eyes open while looking at a cross in the middle of a fixation screen. No explicit instruction was given about blinking behavior to insure its spontaneity. Eye-blink data were extracted from the 6-min baseline recording with eyes open. Artifacts and bad channels (i.e., channels with high impedance/poor contact with the scalp) were removed from the raw EEG data using EEGLAB, and a low-pass filter of 100 Hz was applied before data analysis. After performing an independent component analysis (ICA) in MATLAB, maximally independent components were selected based on the presence of eye-blink activity, its temporal activity, and its frontal distribution. Based on the time points of the individual eye-blinks, sEBR per minute was computed. The vertical eye-blink power spectrum is concentrated in the range 0.5 to 3 Hz. There, the power of blinks is in the order of 10 times larger in amplitude than the average cortical signals, and lasts for approximately 300 ms[180]. These particular characteristics enable reliable statistical separation of eye-blink-related signals from brain-related or EMG-related signal from the EEG signals. The amplitude threshold for peak detection was verified manually for every participant and manually adapted if needed to assure correct quantification of eye-blink rates.

4.3 Results

Self-report and Task-based Impulsivity Measures

Participant data for key self-report and task-based measures of impulsivity are summarized in **Table 8**.

Table 8. *Self-report and task-based impulsivity measures*

Variable	Mean ± S.D. (min-max)	Correlation with Age (p-value)	Males - Females (p-value)
BIS-11 Total	59.2 ± 8.1 (43-81)	.01 (0.962)	1.73 (0.291)
BIS-11 Attentional Impulsivity	15.7 ± 3.1 (8-24)	-.01 (0.932)	0.79 (0.208)
BIS-11 Motor Impulsivity	21.3 ± 3.0 (14-28)	-.16 (0.115)	-0.20 (0.741)
BIS-11 Non-planning Impulsivity	22.1 ± 4.1 (13-31)	.13 (0.189)	1.14 (0.165)
Go Trial Accuracy (%)	91.6 ± 7.0 (67.7-98.8)	-.20 (**0.045**)	0.20 (0.887)
No-Go (repeat) Trial Accuracy (%)	68.6 ± 18.1 (15.9-96.2)	.01 (0.960)	-5.88 (0.107)
No-Go (syllable) Trial Accuracy (%)	73.7 ± 15.3 (12.6-92.9)	.16 (0.110)	-8.86 (**0.004**)
Post-error Slowdown (ms)	84.8 ± 64.3 (-57.4-277.9)	.24 (**0.014**)	1.21 (0.931)

Relationships with $p<0.10$ are italicized. Relationships with $p<0.05$ are bolded.

Bivariate Pearson correlations between and within BIS-11 scores and go/no-go task performance metrics are summarized in **Table 9**.

Table 9. *Bivariate correlations between self-report and task-based impulsivity measures*

	1. BIS-11 Total	**2.** BIS-11 Attentional Impulsivity	**3.** BIS-11 Motor Impulsivity	**4.** BIS-11 Non-planning Impulsivity	**5.** Go Trial Accuracy	**6.** No-Go (repeat) Trial Accuracy	**7.** No-Go (syllable) Trial Accuracy	**8.** Post-error Slowdown
1.	-	.779 (**<.001**†)	.728 (**<.001**†)	.859 (**<.001**†)	-.077 (.436)	-.162 (*.099*)	-.003 (.979)	-.043 (.665)
2.		-	.374 (**<.001**†)	.513 (**<.001**†)	-.029 (.770)	-.166 (*.090*)	-.039 (.694)	-.172 (*.078*)
3.			-	.428 (**<.001**†)	-.042 (.669)	-.166 (*.091*)	-.029 (.771)	-.004 (.968)
4.				-	-.099 (.313)	-.073 (.459)	.045 (.647)	.049 (.621)
5.					-	.076 (.444)	.160 (.102)	-.420 (**<.001**†)
6.						-	.493 (**<.001**†)	.178 (*.069*)
7.							-	.195 (**.046**)
8.								-

Relationships with $p<0.10$ are italicized. Relationships with $p<0.05$ are bolded.
†Relationship remained significant after controlling for age and gender.

Weak trending ($p<0.1$) negative relationships were observed between accuracy on no-go repeat syllable trials and BIS-11 total, BIS-11 attentional impulsivity, and BIS-11 motor impulsivity scores; BIS-11 attentional impulsivity score also had a trending negative relationship with post-error slowdown. Post-error slowdown was significantly ($p<0.05$) negatively correlated with accuracy on go trials, significantly positively correlated with accuracy on no-go syllable trials, and had a positive trending relationship with accuracy on no-go repeat syllable trials. Accuracy on both types of no-go trials was significantly positively correlated.

Gray Matter Volume (GMV) and Impulsivity Measures

BIS-11

Whole-brain analyses, controlling for age, gender and intracranial volume, revealed that, at the corrected level, GMV in the right medial orbitofrontal cortex was negatively correlated with BIS-11 total, BIS-11 motor impulsivity, and BIS-11 non-planning impulsivity scores; GMV in the right and left paracingulate gyrus was also negatively correlated with BIS-11 non-planning impulsivity score (**Table 10; Figure 8)**.

Table 10. *Relationships between gray matter volume and BIS-11 scores*

	Region	**Cluster Size**	**MNI Peak Coordinates**	**Relationship**
BIS-11 Total	Medial Orbitofrontal Cortex (R)	487	(6, 34, -20)	Negative
BIS-11 Motor Impulsivity	Medial Orbitofrontal Cortex (R)	336	(4, 30, -21)	Negative
BIS-11 Non-planning Impulsivity	Paracingulate Gyrus (R)	427	(10, 28, 32)	Negative
	Paracingulate Gyrus (L)	289	(-4, 52, 9)	Negative
	Medial Orbitofrontal Cortex (R)	411	(6, 33, -21)	Negative

A cluster size of ≥236 voxels was significant at $p_{FWE}<0.05$

Figure 8: *Gray Matter Volume and BIS-11 scores*

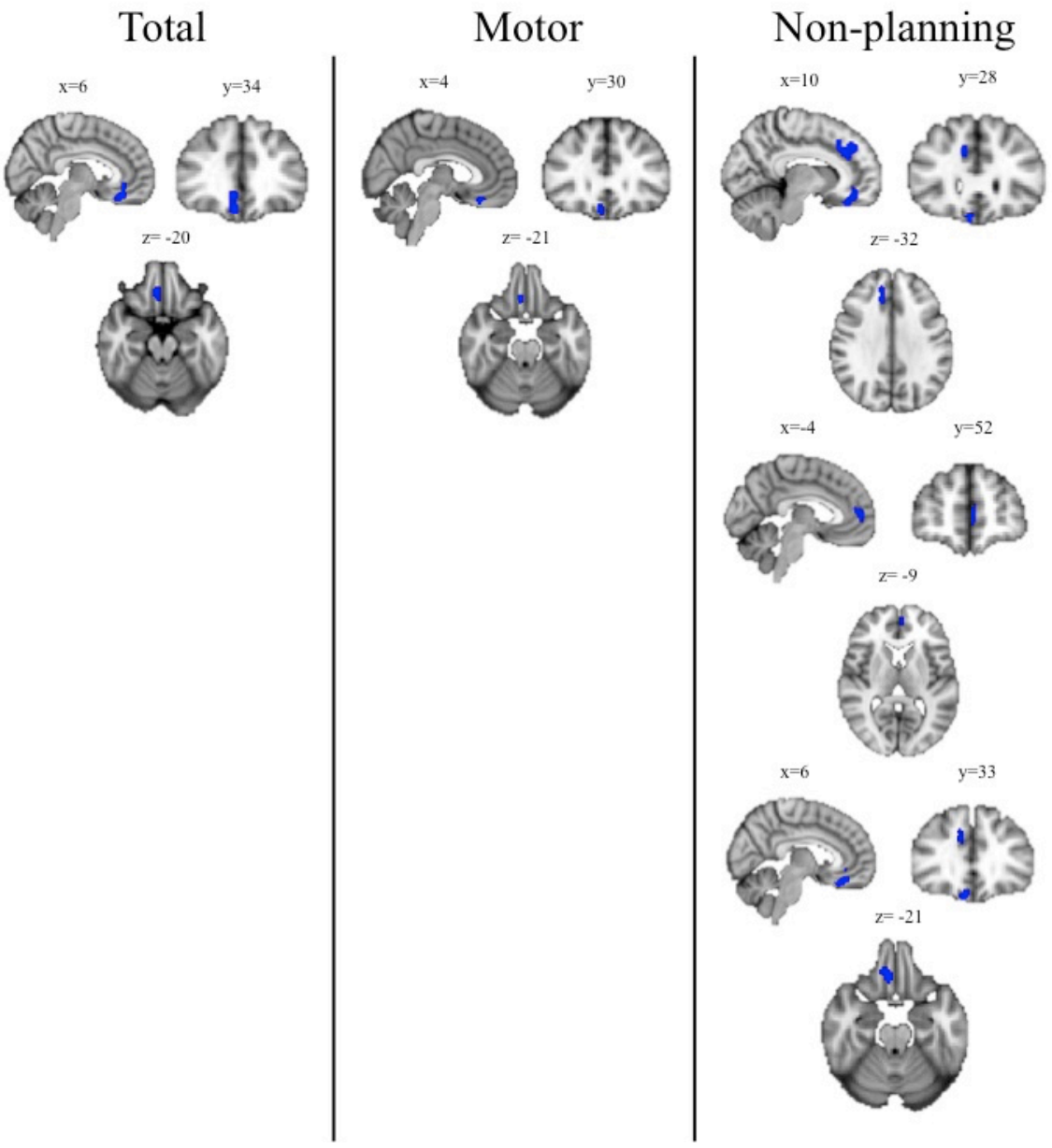

Blue clusters indicate areas where volume is significantly ($k > 236$; $p < .05$ corrected) negatively correlated with score. “Total” = BIS-11 total score; “Motor” = BIS-11 motor impulsivity score; "Nonplanning" = BIS-11 non-planning impulsivity score. There were no significant clusters related to BIS-11 attentional impulsivity score.

Go/No-Go

Whole-brain analyses, controlling for age, gender and intracranial volume, did not reveal any significant relationships between GMV and accuracy on either go or no-go trials or post-error slowdown at the corrected level.

Resting-State Functional Connectivity (RSFC) and Impulsivity Measures

BIS-11

Seed-to-whole-brain analyses, controlling for age and gender, revealed a significant relationship between BIS-11 motor impulsivity score and RSFC between the right dorsal caudate and clusters in the parietal and occipital lobes that included the precentral gyrus and precuneus (**Table 11**). Increased correlated coupling between these regions was associated with higher BIS-11 motor impulsivity score. In addition, a significant relationship was observed between BIS-11 non-planning impulsivity score and RSFC between the left substantia nigra and bilateral thalamus (**Table 12**). Decreased correlated coupling between these regions was associated with increased BIS-11 non-planning impulsivity score. There were no relationships observed between RSFC and BIS-11 total score or BIS-11 attentional impulsivity score.

Table 11. *Relationships between RSFC and BIS-11 motor impulsivity score*

Focal Seed	**RSFC Relationship with:**	**MNI Peak Coordinates**	**Cluster Size**	**t-value**
R Dorsal Caudate	L Superior Lateral Occipital Cortex	(-16, -62, 66)	2153	4.80
	L Cuneal Cortex	(-18, -74, 26)	573	4.15
	R Superior Parietal Lobule	(34, -44, 58)	292	4.45

Table 12. Relationships between RSFC and BIS-11non-planning impulsivity score

Focal Seed	**RSFC Relationship with:**	**MNI Peak Coordinates**	**Cluster Size**	**t-value**
L Substantia Nigra	R Thalamus	(0, -18, 10)	179	4.52

Go/No-Go

Seed-to-whole-brain analyses, controlling for age and gender, revealed significant relationships between no-go repeat trial accuracy and RSFC strength between a number of basal ganglia and ventral midbrain seeds and other nodes of the basal ganglia-thalamo-cortical network including the thalamus, motor cortex, temporal lobe, prefrontal cortex and neighboring areas of the basal ganglia (**Table 13**; **Figure 9**). Stronger correlated coupling in this circuitry was associated with worse accuracy, while decreased correlated coupling was associated with better accuracy. No relationships were found between RSFC and go trial accuracy, no-go syllable trial accuracy, or post-error slowdown.

Figure 9: *Resting-state functional connectivity and go/no-go performance*

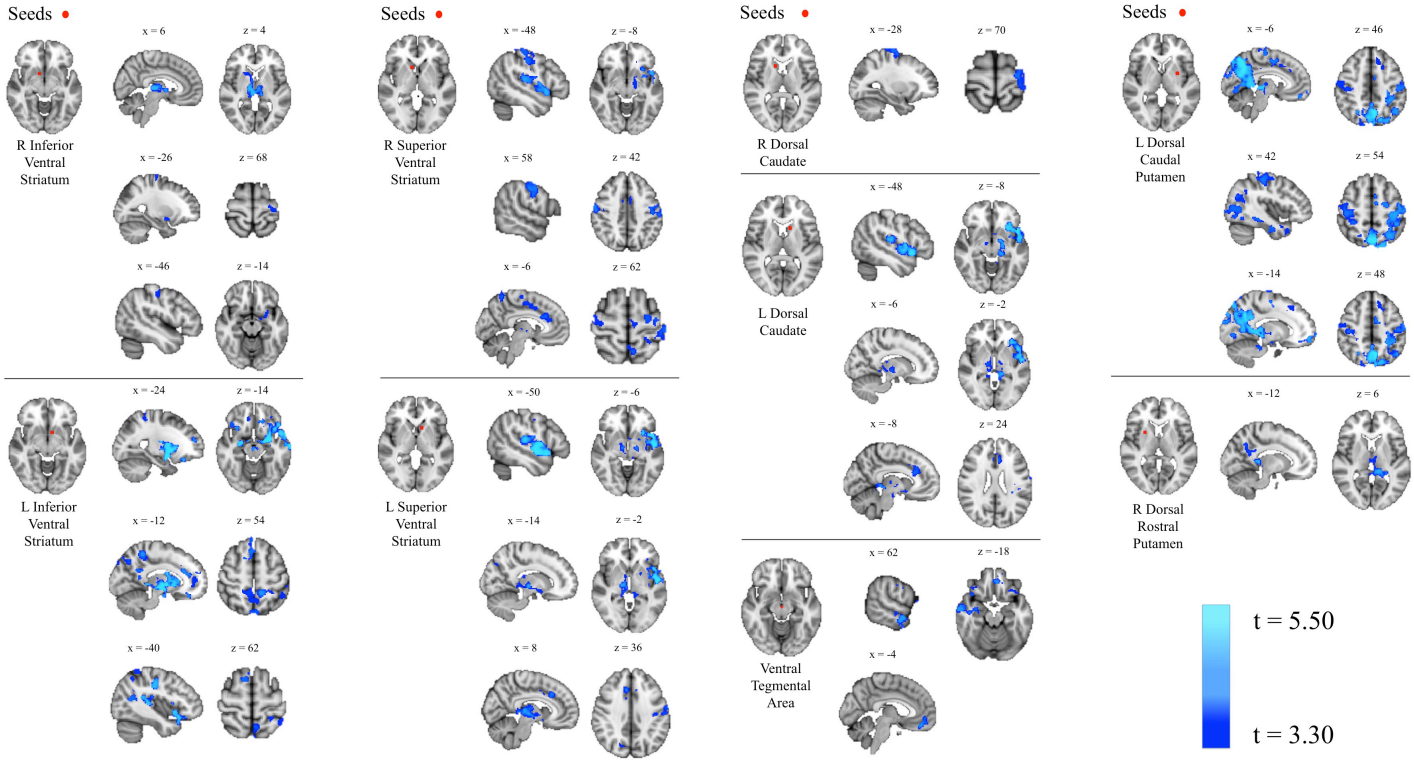

Table 13. *Relationships between RSFC and no-go (repeat) trial accuracy*

Focal Seed	RSFC Relationship with:	MNI Peak Coordinates	Cluster Size	t-value
R Inferior Ventral Striatum	R Thalamus	(6, -24, 4)	1106	4.76
	L Precentral Gyrus	(-26, -18, 68)	68	3.74
	L Postcenttral Gyrus	(-46, -18, 48)	61	3.78
	L Orbitofrontal Cortex	(-28, 8, -14)	56	3.56
L Inferior Ventral Striatum	L Amygdala	(-24, -2, -14)	15954	4.56
	L Precuneus	(-12, -46, 54)	1139	4.65
	L Superior Parietal Lobule	(-42, -50, 62)	178	3.37
R Superior Ventral Striatum	L Temporal Pole	(-48, 12, -8)	4068	5.02
	R Postcentral Gyrus	(58, -14, 42)	749	3.97
	L Precuneus	(-6, -56, 62)	648	3.76
	L Anterior Cingulate Cortex	(-8, 22, 24)	399	4.03
	L Supplementary Motor Cortex	(-4, -10, 52)	267	3.57
	R Thalamus	(6, -20, 2)	134	3.47
L Superior Ventral Striatum	L Planum Polare	(-50, -6, -6)	4441	5.38
	R Thalamus	(14, -16, -2)	771	4.75
	R Paracingulate Gyrus	(8, 24, 36)	308	4.97
R Dorsal Rostral Putamen	L Thalamus	(-12, -36, 6)	1264	5.23
R Dorsal Caudate	L Precentral Gyrus	(-28, -18, 70)	497	4.48
L Dorsal Caudate	L Temporal Pole	(-48, 12, -8)	3793	5.37
	R Thalamus	(14, -16, -2)	512	3.94
	L Anterior Cingulate Cortex	(-8, 26, 24)	318	4.78
Ventral Tegmental Area	R Middle Temporal Gyrus	(62, -8, -18)	1268	4.54
	L Medial Orbitofrontal Cortex	(-4, 42, -18)	839	5.00
L Dorsal Caudal Putamen	L Precuneus Cortex	(-6, -64, 46)	28178	4.57
	R Postcentral Gyrus	(42, -24, 54)	1579	3.89
	L Superior Frontal Gyrus	(-14, 24, 48)	251	3.63

Spontaneous Eye Blink Rate (sEBR) and Impulsivity Measures

Subjects had sEBRs ranging from 1.69 to 39.94 per minute (mean = 16.84, SD = 9.04). Relationships between sEBR and self-report and task-based impulsivity measures are summarized in **Table 14**. As sEBR can be affected by age[181,182] and gender[181-183],

these variables were regressed out of the analyses. sEBR was significantly positively correlated with accuracy on go trials and both types of no-go trials, and was significantly negatively correlated with BIS-11 motor impulsivity score (**Figure 10**).

Table 14. *Relationships between sEBR and self-report and task based impulsivity measures*

	Partial Correlation with sEBR (p-value)
BIS-11 Total	-.034 (.746)
BIS-11 Attentional Impulsivity	.035 (.738)
BIS-11 Motor Impulsivity	-.202 **(.048)**
BIS-11 Non-planning Impulsivity	.056 (.587)
Go Trial Accuracy (%)	.204 **(.047)**
No-Go (repeat syllable) Trial Accuracy (%)	.239 **(.019)**
No-Go (no-go syllable) Trial Accuracy (%)	.268 **(.008)**
Post-error Slowdown (ms)	-.122 (.238)

Relationships with $p<0.05$ are bolded.

Figure 10: *Spontaneous Eye Blink Rate and Impulsivity*

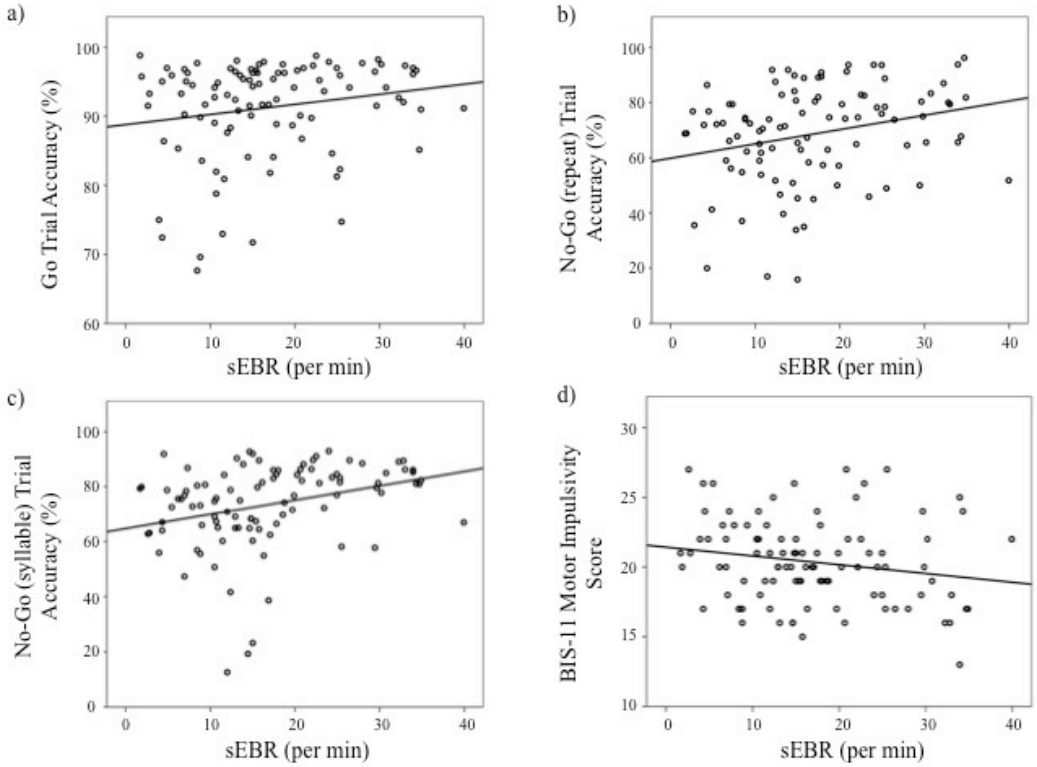

Plots of relationships between sEBR and go/no-go trial accuracy (a-c) and BIS-11 motor impulsivity score (d).

Relation of sEBR to GMV and RSFC

A whole-brain analysis, controlling for age, gender and intracranial volume, identified a cluster of size k=42 with peak coordinates at (-21, 8, -15) in the left putamen and extending into the left medial orbitofrontal cortex where volume was significantly positively correlated with sEBR at the uncorrected (p<0.001) level. This finding did not survive FWE cluster correction. Regression analyses controlling for age and gender did not find significant relationships between sEBR and RSFC between the seed regions and the rest of the brain.

4.4 Discussion

This study aimed to characterize how multiple neurobiological metrics relate to individual differences in impulsivity in the general population. Overall, we found that levels of gray matter volume, resting-state functional connectivity, and spontaneous eye-blink rate all predicted variability in self-reported and/or task-based measures of impulsivity. Specifically, greater levels of impulsivity were associated with lower gray matter volume in the orbital and medial prefrontal cortex and paracingulate gyrus, greater correlated functional connectivity throughout basal ganglia-thalamo-cortical circuitry, and lower spontaneous eye-blink rate, potentially indicative of reduced dopaminergic activity.

In terms of GMV, the present results align with prior studies finding a negative relationship between prefrontal gray matter and BIS-11 scores[19-21]. We found prefrontal GMV to be negatively correlated with the BIS-11 motor impulsivity subscale as well as the non-planning impulsivity subscale. The association of prefrontal regions with aspects of both rapid motor inhibitory control (motor impulsivity subscale) and deliberative decision-making (non-planning impulsivity subscale) is consistent with the fMRI

literature, which shows prefrontal activation during response inhibition on both go/no-go[184-187] and stop-signal tasks[30] as well as during delay discounting tasks when long-term options are chosen[188,189]. However, whereas the fMRI literature has generally implicated lateral prefrontal regions in these processes, our findings are in medial prefrontal regions. At the same time, we did not find GMV to be associated with any of the task-based measure of motor inhibition. This is at least the third study to report the absence of a relationship between GMV and performance on a rapid motor inhibition task in healthy subjects[190,191]. This suggests that the relationship between BOLD activation and gray matter volume in these regions may not be related in a linear or otherwise straightforward fashion. It is also worth noting here that, although worse performance on the go/no-go task was associated with higher BIS-11 scores, these correlations were not statistically significant, consistent with other studies that have found a lack of significant correlation between self-report and task-based measures of impulsivity[192].

Regarding RSFC, this is the first study to examine the relationship between RSFC and trait impulsivity and go/no-go task performance in a large healthy sample. We found that subjects with the greatest correlated coupling at rest between the basal ganglia and the thalamus, motor cortex, temporal lobe and prefrontal cortex had the poorest inhibitory capacity on the go/no-go task. Instances of elevated frontostriatal connectivity were primarily observed between nodes of the limbic processing stream - between medial regions of the prefrontal cortex and the ventromedial striatum - and nodes of the motor processing stream - between posterior dorsal regions of the prefrontal cortex and dorsal regions of the striatum. One interpretation of these findings is that more impulsive individuals have a basal ganglia-thalamo-cortical system that is more primed for action at

baseline; these individuals may thus have difficulty inhibiting this prepotent urge to act. These findings are consistent with a pharmacological challenge study that found that a decrease in RSFC between the ventral putamen and pregenual cingulate cortex was associated with a decrease in impulsivity on a delay-discounting task[27]. It is also interesting to note that this study found that the decrease in RSFC and impulsivity was induced by the up-regulation of dopamine levels via administration of tolcapone, which may be consistent with the present sEBR findings as both lower RSFC and higher sEBR (potentially indicative of elevated dopamine levels) were associated with less impulsivity.

The association of lower sEBR with greater self-reported motor impulsivity and worse motor inhibition on the go/no-go task found here is consistent with some lines of research on dopaminergic functioning, but at odds with others. First, these relationships align with findings from pharmacological studies showing that administration of drugs that increase extracellular levels of dopamine, such as methylphenidate and d-amphetamine, improves response inhibition in healthy subjects[29]. They also appear to be consistent with fMRI literature showing that striatal BOLD activation, which has been positively correlated with dopamine release[11,12], is present during motor inhibitory control[30,172,187,193-196]. However, the present results conflict with a prior study examining the relationship between sEBR and stop-signal task performance in healthy adults, which found that higher sEBR was associated with diminished inhibitory capacity[48]. Consistency with PET studies is more challenging to ascertain. PET imaging quantifies the availability of receptors for radiotracer binding, and this metric is difficult to interpret because it likely reflects the confluence of a variety of factors, including levels of the endogenous ligand that competes for receptor binding with the radiotracer and the density

of receptors themselves[33]. In healthy adults, several studies have found that decreased dopamine receptor availability in the dorsal striatum is associated with better rapid motor response inhibition[30,31]. These findings are consistent with the interpretation that the reduced receptor availability is in part due to increased competition from elevated levels of endogenous dopamine in individuals with better response inhibition capacities. However, in apparent contrast, another PET study found that decreased striatal dopamine receptor availability was associated with increased levels of trait impulsivity as measured by the BIS-11[32]. Other PET studies are more difficult to interpret within this framework: a study in healthy adults found that trait impulsivity measured with the BIS-11 was negatively correlated with availability of presynaptic D2 autoreceptors in the substantia nigra/ventral tegmental area, which have an inhibitory drive on striatal dopamine release[197]. Further research is needed in this area to elucidate the mechanisms determining how exactly dopamine affects motor response inhibition.

In addition to contextualizing these results within prior findings in healthy samples, it is also interesting to view them in the context of relationships found in clinical populations with very high levels of impulsivity. Regarding GMV, the inverse relationship found here between prefrontal GMV and impulsivity resembles findings from the ADHD literature, in that adults with ADHD have been found to have lower prefrontal GMV compared to healthy adults[198,199]. On the other hand, a number of studies have found that impulsive-antisocial traits in psychopathy are associated with greater prefrontal GMV[18,54] (but see[55]). Contextualizing the RSFC findings is more difficult, as RSFC studies in ADHD patients have found both greater and lower RSFC across different networks[200,201]; impulsive-antisocial traits in psychopathy have previously been

associated with greater strength of RSFC in this circuitry[59]. Collectively, these observations suggest that the neurobiological underpinnings of impulsivity in the general population may differ in degree, rather than in kind, from those responsible for excessive impulsivity in certain disorders such as ADHD, but may differ in kind from neural correlates of impulsivity in other disorders such as psychopathy. **Chapter 5** will examine the potential to predict the severity of an individual's level of impulsivity from their neural data using machine learning

Chapter 5: Using machine learning to predict levels of impulsive-antisocial psychopathic traits from voxel-level variation in gray matter volume

5.1 Introduction

One of the lofty goals of modern neuroscience is to be able to supplement more traditional assessments of an individual's risk for developing problematic behaviors or psychiatric disorders – which primarily draw on a combination of self-reported and clinician-evaluated behavioral criteria – with neural data. This so-called concept of "neuroprediction" or "neuroclassification" would allow mental health experts to essentially read-out an individual's current and future behavioral, neurocognitive, and psychiatric profile from a quantitative dataset detailing the structure and function of different parts of the individual's brain. Proof of concept of neuroprediction has already been demonstrated in several hundred academic studies over the past two decades, in which neural data has been used– with high levels of accuracy – to discriminate healthy individuals from individuals with or at risk for developing Alzheimer's disease, schizophrenia, ADHD, and many other disorders[202].

The key to this kind of data-driven neuroprediction is the use of computational models that are fed a large number of neural datasets and the known behavioral or psychiatric profile corresponding to each dataset. The computational model can then "learn" what type of behavioral or psychiatric profiles the neural datasets with particular characteristics tend to correspond to. Thus, when the model is given a new neural dataset for which the behavioral or psychiatric profile is not yet known, it can draw on its

previous learning to provide an answer. This computational process is often referred to as "machine learning".

The majority of prior studies applying machine learning to do neuroprediction have done what is known as "classification", in which the computational model classifies each neural dataset as belonging to one of two classes – usually a healthy group and a disordered group. Fewer studies have done what is know as "regression", in which the computational models predicts the level of some continuous measure corresponding to each neural dataset, such as age. Regression with machine learning could be more useful than classification in some contexts because it can provide finer grained details about the magnitude or severity of certain traits, such as anxiety, depression, or impulsivity. However, to the best of my knowledge, no study has yet reported on a model to ascertain an individual's level of impulsivity from his or her neural data. This type of application could potentially be of use in the legal system, as part of risk-for-reoffending evaluations. For instance, juries skeptical of a defendant's psychiatric evaluation or behavioral demeanor in the courtroom might find more confidence in an objective, quantitative read-out based on the defendant's neurobiological makeup.

As such, this study attempts to build a machine learning model to predict levels of impulsive-antisocial traits in criminal inmates based on their voxel-level variations in gray matter volume.

5.2 Methods

Participants

Participants (*N*=110) from a medium-security Wisconsin correctional facility were selected based on the following inclusion criteria: (1) less than 55 years old; (2) IQ

greater than 70; (3) no history of psychosis or bipolar disorder; (4) no history of significant head injury or post-concussion symptoms; (5) no current use of psychotropic medications; and (6) completed interview assessments for psychopathy

MRI Acquisition and Preprocessing

MRI data were acquired using the Mind Research Network's Siemens 1.5T Avanto Mobile MRI System equipped with a 32-element head coil. All participants underwent scanning on correctional facility grounds. A high-resolution T1-weighted structural image was acquired for each subject using a four-echo magnetization-prepared rapid gradient-echo sequence (TR=2530 ms; TE=1.64, 3.5, 5.36 and 7.22 ms; flip angle=7°; FOV=256x256 mm^2; matrix=128x128; slice thickness=1.33 mm; no gap; voxel size=1x1x1.33 mm^3; 128 interleaved sagittal slices). All four echoes were averaged into a single high-resolution image [97].

Preprocessing of structural MRI data was conducted in Statistical Parametric Mapping software (SPM12; http://www.fil.ion.ucl.ac.uk/spm). For preprocessing, T1 images were manually realigned; segmented into gray matter, white matter, and cerebrospinal fluid; normalized to Montreal Neurological Institute (MNI)-152 space; modulated after normalization to preserve volume; and smoothed with an 8mm full-width at half-maximum (FWHM) Gaussian kernel[102].

Machine Learning Model

While machine learning models run autonomously once built and executed, constructing these models requires design decisions at multiple points. The first decision point involves deciding what inputs, or "features", will be used to predict the outputs (level of impulsive-antisocial psychopathic traits on a scale from 0 to 20). Here, we chose

to use the quantities of gray matter volume present in each voxel of the brain as features for the model. To identify the voxels of interest, we applied a mask to isolate only voxels containing gray matter (as opposed to white matter or cerebrospinal fluid). The resulting mask contained 560,308 voxels; as such, the machine learning model had 560,308 features – or inputs/pieces of data – with which to predict an output. The information contained in each feature is the quantity of gray matter volume present in the voxel. Therefore, given the 110 subjects, a 110 x 560,308 matrix of data is extracted from the subject T1 scans, where each row lists the amount of gray matter volume present in each of the 560,308 voxels in that particular subject's brain.

However, 560,308 features is a vast amount of features; many will likely contain more noise than signal, and vice versa. Furthermore, the large number of features compared to the small sample size results in an issue known as the "curse of dimensionality" or "small-n-large-p", in which the model is at risk of "overfitting" and not being able to generalize to new cases. Therefore, the machine learning algorithm's accuracy can be aided by limiting the number of features to those that are most important or discriminative in predicting the output. Herein lies the second design decision point – choosing what is known as a "feature selection" method to winnow the number of features down to those with the most discriminative signal. Here, tried two different methods of feature selection. First, we tried a data-driven method called "recursive feature selection". In recursive feature selection, the machine learning model starts off with all of the original features (in this case 560,308), determines the discriminative weight of each feature, and then eliminates a user-determined percentage of the least discriminative features (here we use 10%). The model then goes through another iteration

and removes the 10% least discriminative features of the remaining voxels from the first iteration. The model continues to perform these iterations and remove features until a user-determined percentage of the most discriminative voxels are left at the end (here we use 10%). As such, after recursive feature selection, the machine learning model is left with only the 56,031 most discriminative voxels. As a second feature selection alternative, we also tried implementing a more restrictive brain mask that consisted of a priori regions that previous studies have implicated in impulsivity. This mask consisted of the whole prefrontal cortex and corpus striatum, and restricted the number of features to 181,745 voxels.

A final design decision point is the selection of the kind of machine learning algorithm to use. Here, we used a support vector machine (SVM) model with a linear kernel, and used leave-one-out (LOO) cross-validation for the training and testing of the model. LOO cross-validation allows for the maximization of training data while still ensuring that the model does not learn based upon the data of the subject to be tested.

5.3 Results

Using the SVM model without the use of any feature selection, the model's predicted Factor 2 score significantly correlated with the actual Factor 2 score across all subjects ($p=0.008$) but only to a low-moderate degree of accuracy ($R= .25$). The SVM model using recursive feature selection did slightly better; predicted Factor 2 scores significantly predicted actual Factor 2 scores ($p=0.004$) with an accuracy of $R=.27$. The SVM model using the a priori impulsivity brain mask performed the best, though still only slightly better than the others and at a low-moderate degree of accuracy ($p=0.003$,

R=.28). **Figure 11** displays a scatterplot of the predictions of the SVM model using the a priori impulsivity brain mask against subjects' actual Factor 2 scores.

Figure 11. *Correlation between actual and predicted Factor 2 scores*

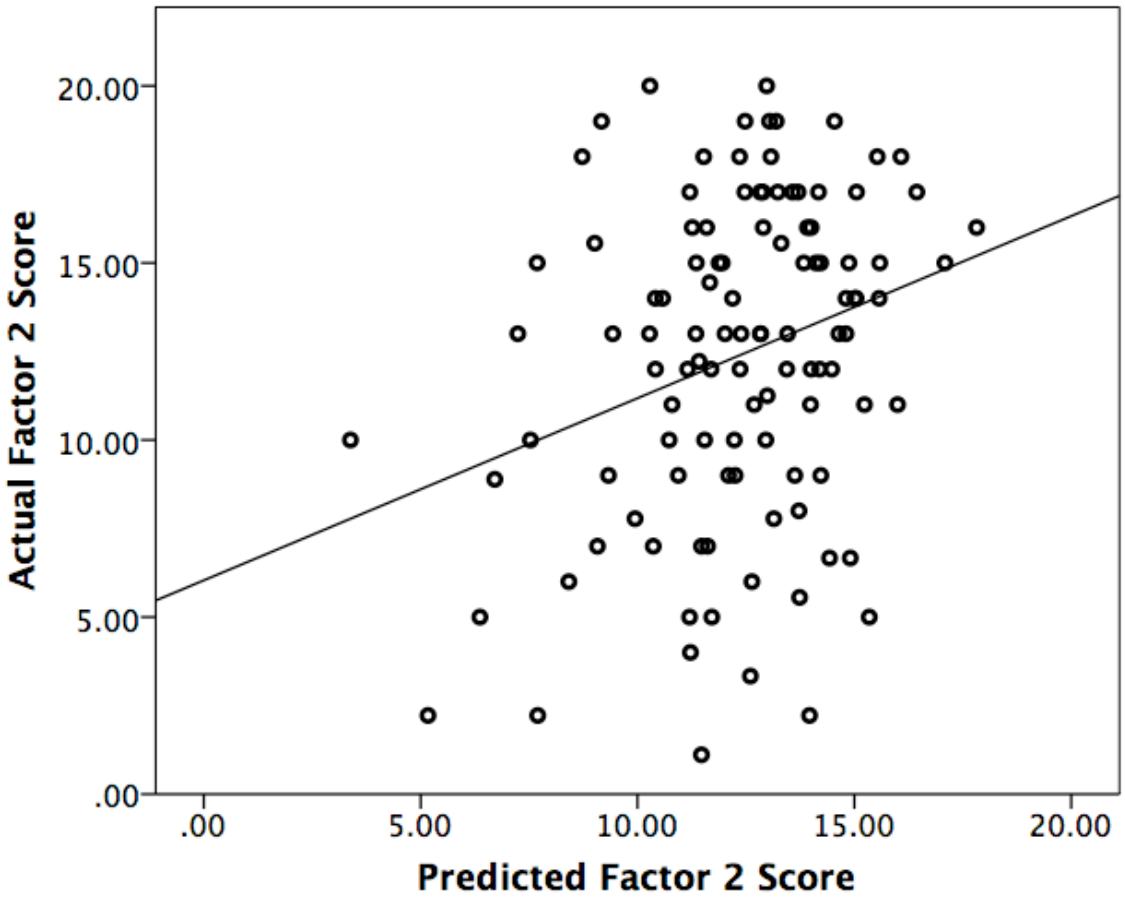

5.4 Discussion

While the low-moderate accuracy achieved by our model precludes its use for practical application just yet, it does provide proof of concept that this type of neuroprediction can be done. Specifically, it shows that machine learning models can identify variance in whole-brain gray matter volume that relates to the continuous magnitude of a personality trait – in this case, impulsive-antisocial psychopathic traits.

We can also find solace in the fact that some the model's most discriminative voxels were in areas like DLPFC whose structural properties have previously been associated with variance in impulsive traits.

Moving forward, the important questions are how to tweak the model to optimize accuracy. As discussed, changes can be made at three primary decision points – the choice of features to be used in the model, the choice of feature selection method to narrow the feature space to only the most discriminative ones, and the choice of machine learning algorithm to use. Beginning with the first decision point, here we used the quantity of gray matter volume within each voxel of the brain as the feature. Another option would be to instead use regional gray matter volumes, in which the total volume within gross anatomical regions (e.g. hippocampus, medial orbitofrontal cortex, etc.) would be used as features. This would dramatically lower the initial feature space (from 560, 308 to less than 100) but also potentially reduce detectable variance between subjects. At the second decision point, there are a host of other types of feature selection methods that can be tried in addition to recursive feature selection and a priori ROI masking. These include univariate filtering techniques (e.g. univariate t-test filtering) and embedded feature selection techniques such as least absolute shrinkage and selection operator **(**LASSO)[203]. Finally, the choice of machine learning algorithm can be changed. Within support vector machines (SVM), different types of kernels can be used; here we used a linear kernel, but there are also options such as the Gaussian kernel. More broadly, SVM can be substituted for different classes of machine learning models, such as relevance vector regression (RVR), which is based on a sparse Bayesian learning method.

Overall, this study demonstrated the potential to use neural data to ascertain levels of impulsive-antisocial traits in incarcerated adults. Future work can build off of this model to improve accuracy via the steps outlined above. Having examined the neural correlates of impulsivity in **Chapters 2-4,** and having demonstrated the potential to predict levels of impulsive traits from neural data in **Chapter 5**, **Chapter 6** will examine the potential of mindfulness meditation to reduce impulsivity and alter its neural correlates.

Chapter 6: The effect of mindfulness meditation on impulsivity and its neurobiological correlates in healthy adults

In Prep as: Korponay, C., Dentico, D., Kral, T., Ly, M.M., Kruis, A., Goldman, R., Lutz, A. and Davidson, R.J., The Effect of Mindfulness Meditation on Impulsivity and its Neurobiological Correlates in Healthy Adults

6.1 Introduction

The past few decades have seen a surge of interest in the effects of mindfulness meditation on the brain and cognitive functioning. A common aim of various styles of mindfulness meditation is the adoption of a nonreactive and observant stance toward one's emotions, thoughts and body states, as well as the self-regulation of attention[204]. Thus, on a conceptual basis, mindfulness meditation may be thought to confer benefits for, among other things, improving behavioral control and reducing impulsivity. Impulsivity is a multidimensional construct that may arise from any number of related but distinct cognitive deficits, such as an inability to sustain attention, inhibit prepotent urges, or wait and plan behavior[2]. A number of studies have found that levels of self-reported trait mindfulness are inversely correlated with levels of self-reported trait impulsivity[205-207].

In light of this conceptual appeal, interest has grown in the prospect of using mindfulness meditation to help treat conditions that feature high levels of impulsivity and deficits in behavioral control, such as attention-deficit/hyperactivity disorder (ADHD)[208] and substance use disorder (SUD)[209]. While disorders such as ADHD and SUD are multifaceted and likely stem from dysfunction of multiple neurobiological and cognitive domains, treatments that target the impulsive symptoms present in these disorders offer

one approach for improving outcomes. In addition, mindfulness meditation may offer a potential strategy for otherwise healthy individuals with high levels of impulsivity to improve their functioning, as high levels of impulsivity in the general population have been linked to poorer life outcomes such as lower levels of academic success[1] and increased propensity for substance abuse[210].

However, evidence that mindfulness meditation is effective in reducing impulsivity is sparse. While a number of studies in both healthy individuals[211,212] and individuals with ADHD[208] have found evidence that mindfulness meditation can improve attention and reduce attentional impulsivity, it is unclear whether mindfulness meditation is effective in helping to reduce other dimensions of impulsivity, such as difficulty inhibiting urges or difficulty planning long-term behavior. These other dimensions of impulsivity may play a larger role in disorders like SUD[2], and findings from a recent meta-analysis of 25 studies that found inconclusive data for mindfulness meditation as a treatment for SUD further prompt a more thorough examination of the effect of mindfulness meditation on impulsivity[209]. Only a handful of studies have directly examined the impact of mindfulness meditation interventions on non-attentional measures of impulsivity in healthy adults. One study in healthy adults found that three months of intensive mindfulness meditation training increased subjects' capacity to inhibit prepotent motor responses on a response inhibition task[213]. Another study found that while mindfulness-based cognitive therapy was effective in improving the ability to inhibit cognitive prepotent responses on the Hayling task, it did not improve the ability to inhibit motor behavior on a GoStop task[214].

A further issue that has yet to be comprehensively investigated is whether mindfulness meditation has an effect on the neurobiological correlates of impulsivity. Human neuroimaging studies have identified links between impulsivity and gray matter volume in the prefrontal cortex and basal ganglia, resting-state functional connectivity between the midbrain, basal ganglia, thalamus and prefrontal cortex, and the functioning of neurotransmitter systems that innervate this circuitry such as dopamine. Previous neuroimaging investigations of the effect of mindfulness meditation on the brain have tended to focus on regions and networks implicated in theory of mind, emotion regulation and attention, with less focus given to effects on the reward and decision-making circuitry detailed above that is relevant to impulsivity.

In order to address these important gaps in the literature, this study first examined the effect of an 8-week mindfulness intervention on impulsivity and its neurobiological correlates in healthy adults, and compared changes over time to both an active control group and a waitlist control group. We then examined whether impulsivity and its neurobiological correlates differed in long-term meditators (LTMs; n=28) compared to meditation-naïve participants (MNPs; n=105). Specifically, we examined impulsivity with performance on a task of behavioral inhibition (go/no-go task) and with self-ratings of attentional, motor, and non-planning impulsivity using the Barratt Impulsiveness Scale (BIS-11). The neurobiological correlates of interest were derived from a previous study of the MNPs in this sample[215], in which less gray matter volume in prefrontal regions, heightened resting-state functional connectivity in basal ganglia-thalamo-cortical circuitry, and lower spontaneous eye-blink rate (indicative of lower central dopamine levels) were predictive of higher levels of impulsivity at baseline.

6.2 Methods

Participants

Participants provided written informed consent for study procedures that were approved by the UW-Madison Health Sciences Internal Review Board. Meditation-naive participants were recruited for a study on health and well-being through advertisements in Madison, WI, area newspapers, e-mails, and through postings and discussions with meditation teachers and groups. LTMs were recruited in the United States at meditation centers and through related mailing lists, in addition to flyers and advertisements in newspapers. Criteria for exclusion for all participants included use of psychotropic or steroid drugs, night-shift work, diabetes, peripheral vascular disease or other diseases affecting circulation, needle phobia, pregnancy, current smoking habit, alcohol or drug dependency, and inability to attend weekly class and full-day group sessions. Additional exclusion criteria for MNPs included significant previous experience with meditation or other mind–body techniques (e.g., tai-chi, Qigong), remarkable exercise habits (engagement in moderate sport or recreational activities > 5 h per week; engagement in vigorous sport or recreational activities > 4 h per week), and inability to walk. Meditation recruitment criteria for LTMs included at least 3 years of daily meditation practice (at least 30 min per day), and at least three intensive retreats lasting 5 days or more. In total, after exclusion 158 healthy human subjects were recruited, which comprised 127 meditation-naive participants and 31 long-term meditators.

LTMs had an average of 9,154 lifetime hours of meditation practice, ranging from 1,439 to 29,046 total hours. Lifetime hours of practice were calculated based on subjects' reports of their average hours of formal (sitting and walking) meditation practice per

week and the total years of practice, including time spent in meditation retreats. All LTM participants were proficient in meditation practices as taught within the framework of either Theravada or Tibetan Buddhism. These practices included two attention-based meditations, which we referred to as open monitoring (OM) and focused attention (FA) meditations, as well as one compassion/loving-kindness meditation referred to as Metta meditation. Briefly, FA meditation involves directing and sustaining attention on a selected object (e.g., breathing), detecting mind wandering and distractors (e.g., thoughts) as well as disengagement of attention from distractors, and shifting of the focus of attention back to the selected object. By contrast, OM meditation has no explicit focus of attention, but rather requires nonreactive meta cognitive monitoring of anything that is experienced, thus replacing the "effortful" selection of an object as primary focus with an "effortless" sustained awareness of the rich features of each experience[216]. The practice of compassion/loving-kindness meditation is a form of concentration practice where the practitioner focuses his/her mind on the suffering of oneself or others and then on the wish that the individual(s) in question may be happy and free from suffering.

Structural and functional magnetic resonance imaging (MRI) scans were obtained for 106 MNPs and for 28 LTMs, and so all analyses were conducted within this set of subjects. One MNP's scan was excluded due to poor image registration. Thus, data from a total of 105 MNPs [age, 48.6 ± 10.9 years (mean ± SD); 65 women, 40 men] and 28 LTMs [age, 49.8 ± 10.1 years (mean ± SD); 15 women, 13 men] were available for gray matter volume analyses. 27 of the 105 MNPs and six of the 28 LTMs were excluded from RSFC analyses due to excessive motion during the functional MRI scan, and so data from 78 MNPs [age, 48.9 ± 11.0 (mean ± SD); 50 women, 28 men] and 22 LTMs [age,

48.8 ± 11.5 (mean ± SD); 11 women, 11 men] were available for RSFC analyses. Spontaneous eye blink rate (sEBR) data was obtained for 98 of the 105 MNPs [age, 48.9 ± 10.8 years (mean ± SD); 58 women, 40 men] and for 28 of the 28 LTMs. BIS-11 data obtained for 105 of the 105 MNPs and 28 of the 28 LTMs. Go/no-go data was obtained for 105 of the 105 MNPs and 26 of the 28 LTMs [age, 48.8 ± 9.9 years (mean ± SD); 13 women, 13 men].

Study Design and Interventions

BIS-11 scores, go/no-go task performance, gray matter volume, resting-state functional connectivity, and spontaneous eye-blink rate were measured at Time 1 (before the intervention period) in LTMs and MNPs. All LTM versus MNP group comparisons use the Time 1 data.

MNPs were then randomized into three groups by a logistical staff member through a random-number generator: an 8-week mindfulness-based stress reduction (MBSR; *n*=34) class, an 8-week Health Enhancement Program (HEP; *n*=36) as an active control group, or a no-intervention waiting list control group (WL; *n*=35). All of the impulsivity and neurobiological metrics were then measured again in MNPs at Time 2 (after the intervention period).

MBSR training consists of continuous focused attention on the breath, bodily sensations, and mental content while in seated postures, walking, and yoga[217]. This program can be conceptualized as incorporating OM-related meditations with FA- related meditations. In order to isolate the effects of mindfulness, we designed an active comparison intervention to control for the aspects of MBSR that are known to promote positive outcomes but are not specific to mindfulness, such as a supportive group

atmosphere, expert instruction, and engaging in activities that are believed to provide benefit. Our active comparison condition—HEP— matched MBSR in structure, instructor expertise, and content (see MacCoon et al. (2012)[218] for more detailed information). Like MBSR, HEP consisted of four components: (1) physical activity (e.g., walking); (2) balance, agility, and core strength; (3) nutritional education; and (4) music therapy. Each of these components was chosen to match the collateral benefits that MBSR may produce that are not unique to mindfulness. For example, physical activity with a focus on walking was selected to control for the physical benefits of walking meditation. Each component was delivered by an expert in the respective practice, over eight weekly 2.5-h sessions and one full-day session. Like those participating in MBSR training, HEP participants were assigned 45 to 60 min of daily at-home practice.

Barratt Impulsiveness Scale (BIS-11)

The BIS-11[168] is a self-report questionnaire containing 30 questions, each of which requires the subject to choose between 'Rarely/Never', 'Occasionally', 'Often' and 'Almost Always'. Items are scored from 1 to 4. Scoring yields a total score and three subscale scores derived by factor analysis: attentional impulsivity (e.g. "I am restless at the theatre or lectures"), motor impulsivity (e.g. "I do things without thinking"), and non-planning impulsivity (e.g. "I am more interested in the present than the future") [169]. Higher scores indicate higher levels of impulsivity. The BIS-11 has good internal consistency (Cronbach's $\alpha = 0.83$) and test–retest reliability (Spearman's rho= 0.83) [170].

Go/No-Go Task

Subjects completed an auditory go/no-go task based on the paradigm described in Shalgi et al (2009) [171]. Subjects were instructed to push the spacebar on a keyboard upon

the presentation of an auditory syllable stimulus, except when the same syllable was repeated (no-go repeat trials) or when the syllable was "ke/" or "pa/" (no-go syllable trials). Subjects completed four blocks of 252 trials, of which 196 trials were go trials, 16 were no-go repeat trials, and 40 were no-go syllable trials. Accuracy was calculated as the percentage of correct button-pushes for go-trials and the percentage of correct withholds for no-go trials. Post-error slowdown was calculated as the difference between average reaction time on go-trials following incorrect no-go trials and average reaction time on go-trials following correct no-go trials.

Previous studies have shown that inhibitory capacity on no-go trials is sensitive to task demands, and that different task demands recruit distinct sets of brain regions and cognitive functions. For instance, Shalgi and colleagues find that subjects perform better on no-go syllable trials than no-go repeat trials [171]. This is consistent with a meta-analysis that classifies go/no-go tasks in which the no-go stimuli are constant (as in the no-go syllable trials) as "simple", and classifies go/no-go tasks in which the no-go stimuli change depending on context (as in the no-go repeat trials) as "complex" [172]; this study also found that complex no-go trials recruit prefrontal regions to a greater extent than simple no-go trials, likely due to the increased attentional and working memory loads required for these trials. Given these performance and neurobiological differences, we analyzed accuracy on each type of no-go trial separately.

Image Acquisition

Images were acquired on a GE X750 3.0 Tesla MRI scanner device with an eight-channel head coil. Anatomical scans consisted of a high-resolution 3D T1-weighted inversion recovery fast gradient echo image (inversion time = 450 ms, 256 x 256 in-plane

resolution, 256 mm FOV, 124 x 1.0 mm axial slices). Resting-state functional images were acquired in a single scan run using a gradient echo EPI sequence (64x64 in-plane resolution, 240mm FOV, TR/TE/Flip = 2000ms/25ms/60°, 40x4mm interleaved sagittal slices, and 210 3D volumes).

Structural MRI Preprocessing and Analysis

Preprocessing and analyses of structural MRI data were conducted in Statistical Parametric Mapping software (SPM12; http://www.fil.ion.ucl.ac.uk/spm). For preprocessing, T1 images were manually realigned; segmented into gray matter, white matter, and cerebrospinal fluid; normalized to Montreal Neurological Institute (MNI)-152 space; modulated after normalization to preserve volume; and smoothed with an 8mm full-width at half-maximum (FWHM) Gaussian kernel[102]. Individual Brain Atlases using Statistical Parametric Mapping (IBASPM) (http://www.thomaskoenig.ch/Lester/ibaspm.htm) in the Wake Forest University (WFU) Pick Atlas Toolbox was used to create any region of interest masks for small volume correction (SVC) analyses.

Significance for whole-brain voxel-wise analyses was evaluated using family wise error (FWE) cluster correction. The cluster extent threshold corresponded to the statistical probability (α=0.05, or 5% chance) of identifying a random noise cluster at a predefined voxel-wise (i.e., whole-brain) threshold of $p<0.001$ (uncorrected). We used 3dClustSim (updated December 2015) to determine that a cluster-corrected size of ≥236 voxels was significant at $p_{FWE}<0.05$.

Resting-State fMRI Preprocessing and Analysis

Resting-state data were processed using a combination of FEAT (FMRI Expert Analysis Tool) Version 6.00, part of FSL (FMRIB's Software Library, www.fmrib.ox.ac.uk/fsl) and AFNI [100]. We removed the first four volumes from each subject's data, then used FSL's FEAT tool for motion correction with MCFLIRT [173], and non-brain removal using BET [174]. Transformation matrices for registration were computed and applied using FSL to register the subject's time series data to their anatomical template, and a 12DOF affine transformation was used to register the subject's anatomical to Montreal Neurological Institute (MNI) space using FLIRT [173,175]. Registration from high resolution structural to standard space was then further refined using FNIRT nonlinear registration [176,177]. MNI-normalized structural images were segmented with FAST and these segmentations were used to create voxel-wise average signal and derivates from eroded CSF and 2X eroded white-matter masks. These and 6 motion regressors of no interest were included in a nuisance regression using AFNI's 3dDeconvolve. The results from this regression were smoothed using a 5mm FWHM Gaussian kernel.

Six functionally distinct basal ganglia seeds, each with a radius of 3.5 mm, were created in each hemisphere based on coordinates reported by Di Martino and colleagues (2008) [9]. The origin coordinates of these seeds were in the inferior ventral striatum (±9, 9, -8), superior ventral striatum (±10, 15, 0), dorsal caudate (±13, 15, 9), dorsal caudal putamen (±28, 1, 3), dorsal rostral putamen (±25, 8, 6), and ventral rostral putamen (±20, 12, −3). Furthermore, a substantia nigra seed (±12, -12, -12) and midline ventral tegmental area seed (0, -15, -12), each with a radius of 2 mm, were created based on coordinates reported by Tomasi and Volkow (2012) [167].

Average time-series were extracted for each seed from each participant's preprocessed data. These timeseries were regressed back onto each participant's data using 3dDeconvolve. To further address motion, high motion time points (a frame-wise displacement (FD) measure larger than 0.2 mm) were removed. Participants with more than 25% (52 TRs) of the data censored were omitted from analysis, leading to a total of 27 excluded participants. The resultant maps were Fisher-Z transformed to stabilize correlation variance. Average Fisher-Z correlations were extracted from the target ROIs. Whole-brain, voxel-wise group level analysis was conducted using FSL's Randomize [178] thresholded at $p<0.05$ with 5000 permutations.

Spontaneous Eye-blink Recording

Since spontaneous eye-blink rates are affected by the time of day [179], data were collected around 7 pm for all participants to ensure that differences in the time of data collection could not contribute to any observed difference in eye-blink activity. Baseline sEBR was extracted from high- density, 256-channel EEG data that were collected during a 10-min baseline EEG recording. Participants were seated in front of a computer screen. During the first 2 min and last 2 min of the baseline recording, participants were instructed to keep their eyes closed. During the 6 min in between these periods, participants were instructed to keep their eyes open while looking at a cross in the middle of a fixation screen. No explicit instruction was given about blinking behavior to insure its spontaneity. Eye-blink data were extracted from the 6-min baseline recording with eyes open. Artifacts and bad channels (i.e., channels with high impedance/poor contact with the scalp) were removed from the raw EEG data using EEGLAB, and a low-pass filter of 100 Hz was applied before data analysis. After performing an independent

component analysis (ICA) in MATLAB, maximally independent components were selected based on the presence of eye-blink activity, its temporal activity, and its frontal distribution. Based on the time points of the individual eye-blinks, sEBR per minute was computed. The vertical eye-blink power spectrum is concentrated in the range 0.5 to 3 Hz. There, the power of blinks is in the order of 10 times larger in amplitude than the average cortical signals, and lasts for approximately 300 ms [180]. These particular characteristics enable reliable statistical separation of eye-blink-related signals from brain-related or EMG-related signal from the EEG signals. The amplitude threshold for peak detection was verified manually for every participant and manually adapted if needed to assure correct quantification of eye-blink rates.

6.3 Results

All analyses controlled for age and gender. Volumetric analyses additionally controlled for total intracranial volume.

Intervention

In order to assess whether MBSR training had an effect on impulsivity measures, a two-way repeated measures ANOVA was performed for each measure, with time as within-subject factor (pre-intervention Time 1 vs. post-intervention Time2) and group as between-subjects factor (WL, HEP, MBSR).

BIS-11 Self-Report

The overall group-by-time interaction was found to be non-significant for attentional impulsivity score (Wilks' lambda=0.988, p=0.563), motor impulsivity score (Wilks' lamda=0.999, p=0.952), and total impulsivity score (Wilks' lambda=0.964, p=0.166), but was significant for non-planning impulsivity score (Wilks' lambda=0.941,

p=0.050). Post-hoc analysis showed that this interaction was driven by non-significant decreases in non-planning impulsivity score from Time 1 to Time 2 in WL and HEP subjects but a non-significant increase in score from Time 1 to Time 2 in MBSR subjects. Within the MBSR group, none of the BIS-11 score-types significantly decreased from Time 1 to Time 2, whereas within the HEP group, total impulsivity score (Wilks' lambda=0.701, *p*<0.001), attentional impulsivity score (Wilks' lambda=0.749, *p*=0.002), and motor impulsivity score (Wilks' lambda=0.841, *p*=0.014) significantly decreased from Time 1 to Time 2. None of the BIS-11 score-types significantly decreased in WL subjects from Time 1 to Time 2. See **Figure 12**.

Figure 12. *BIS-11 Scores at Time 1 and Time 2*

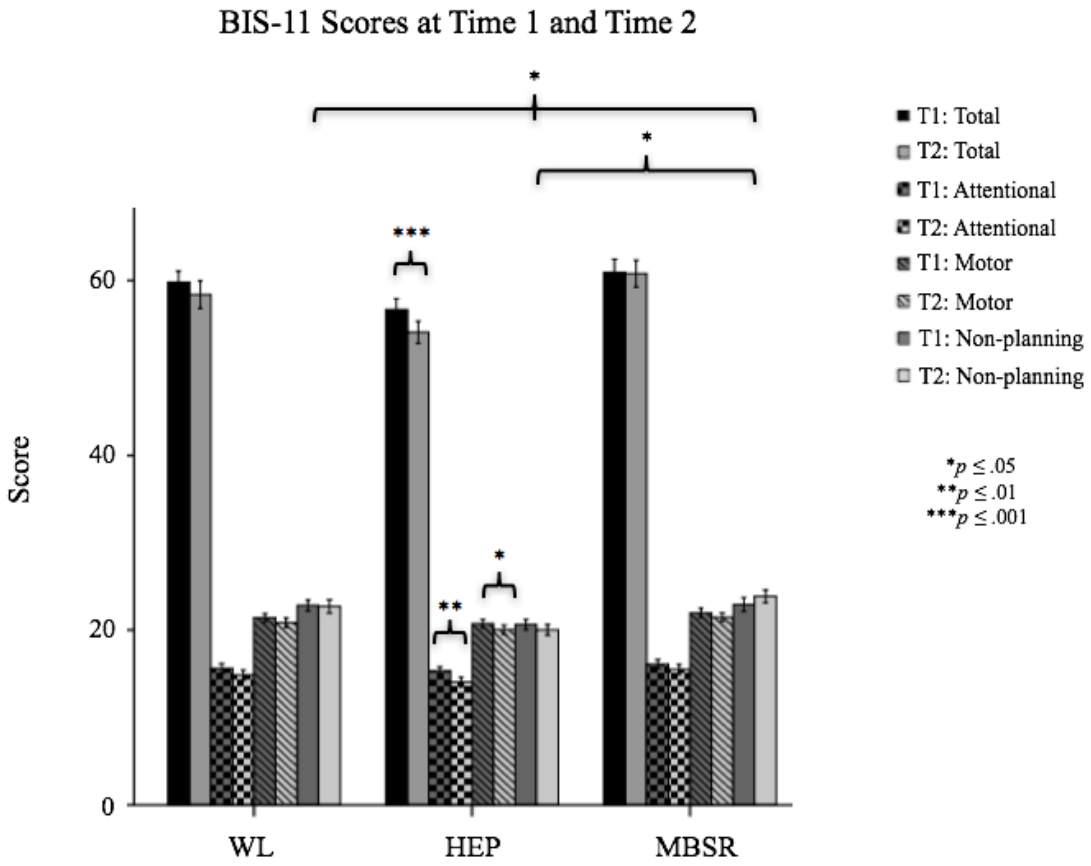

Go/No-Go Task

The overall group-by-time interaction was found to be non-significant for go trial accuracy (Wilks' lambda=0.989, p=0.580), no-go repeat trial accuracy (Wilks' lambda=0.978, p=0.333), no-go syllable trial accuracy (Wilks' lamda=0.985, p=0.482), and post-error slowdown (Wilks' lambda=0.979, p=0.343). Post-hoc analyses showed that accuracy on all three trial-types significantly increased from Time 1 to Time 2 in all three groups. Post-error slowdown decreased from Time 1 to Time 2 in all three groups, but this decrease was only significant for the HEP group (Wilks' lambda=0.814, p=0.008). See **Figures 13-14**.

Figure 13. *Go/No-Go Accuracy at Time 1 and Time 2*

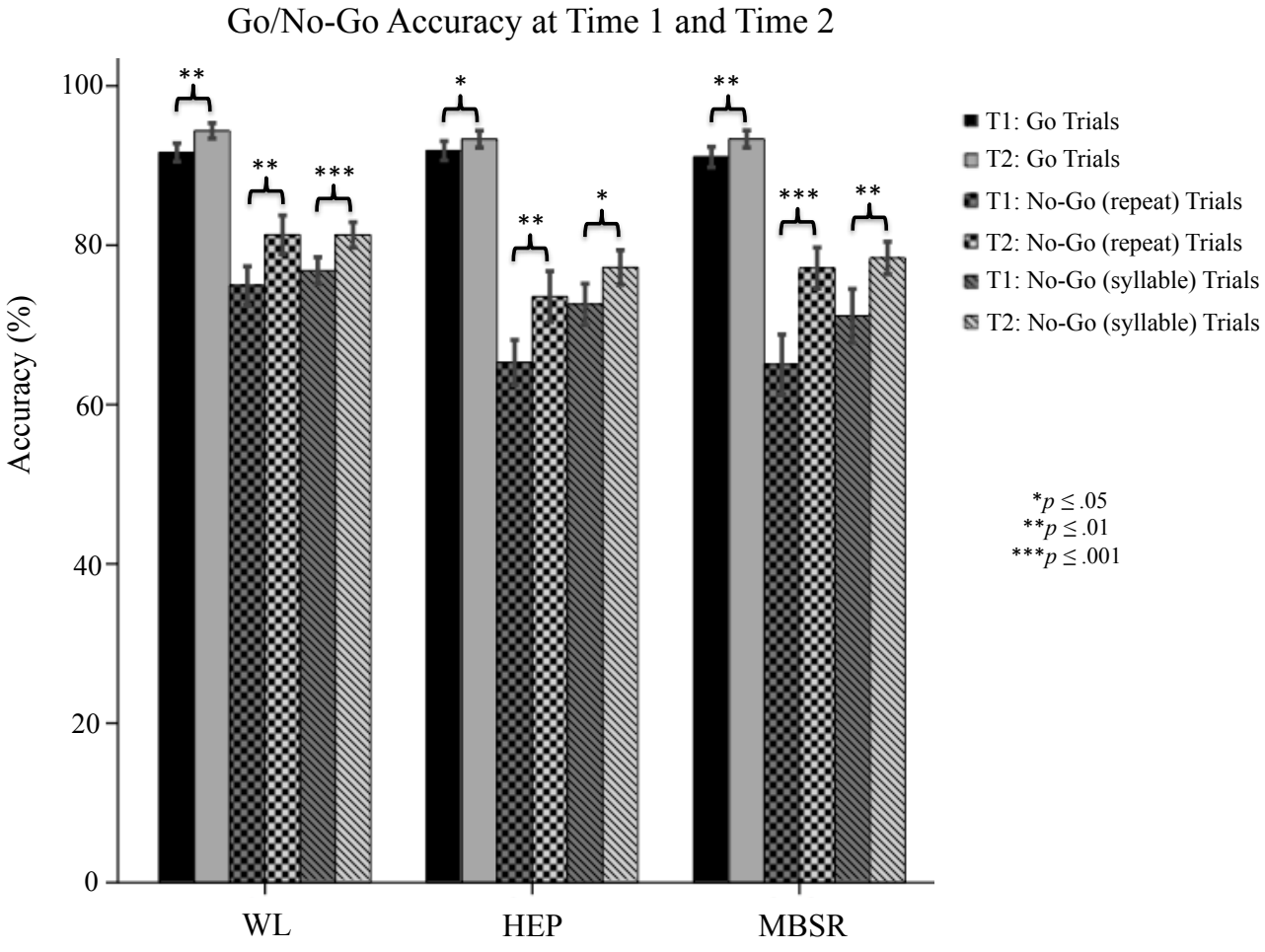

Figure 14. *Go/No-Go Post-Error Slowdown at Time 1 and Time 2*

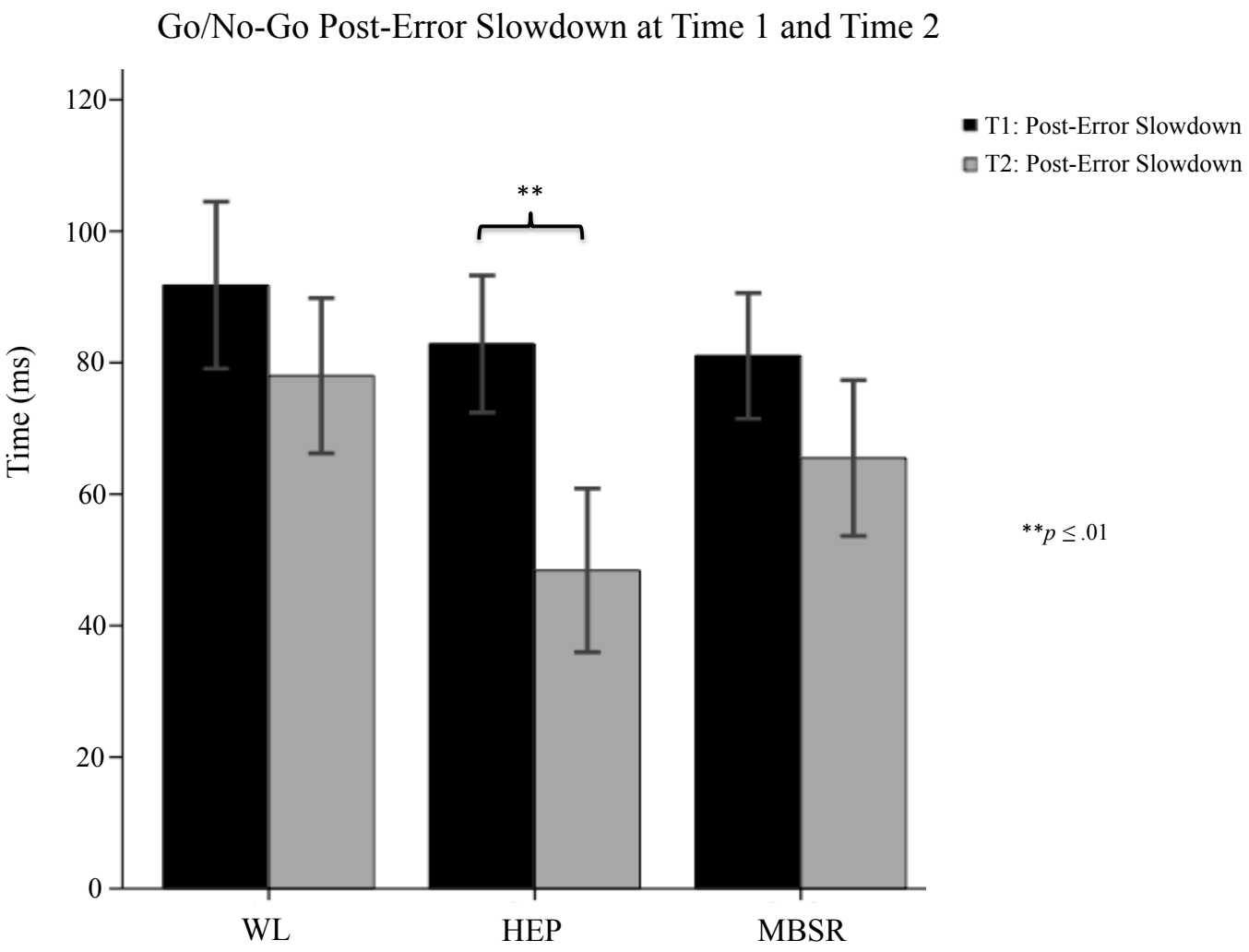

Gray Matter Volume

Whole-brain analyses revealed no significant differences between groups in the change in gray matter volume from Time 1 to Time 2.

Resting-State Functional Connectivity

No significant differences were found between groups in the change in RSFC from Time 1 to Time 2 between any of the seed regions and the rest of the brain.

Spontaneous Eye-blink Rate

Findings from a group-by-time interaction in relation to sEBR have previously been reported in a superset of this sample by Kruis and colleagues, in which no significant interaction was found. As this sample differs slightly from the one previously reported on, we repeated the analysis here in order to ensure that the relationship holds in the present sample. Indeed, we found that the interaction was non-significant (Wilks' lambda=0.997, p=0.872), and post-hoc analyses found that sEBR did not change significantly from Time 1 to Time 2 in any of the three groups. See **Figure 15**.

Figure 15. *Spontaneous eye-blink rate at Time 1 and Time 2*

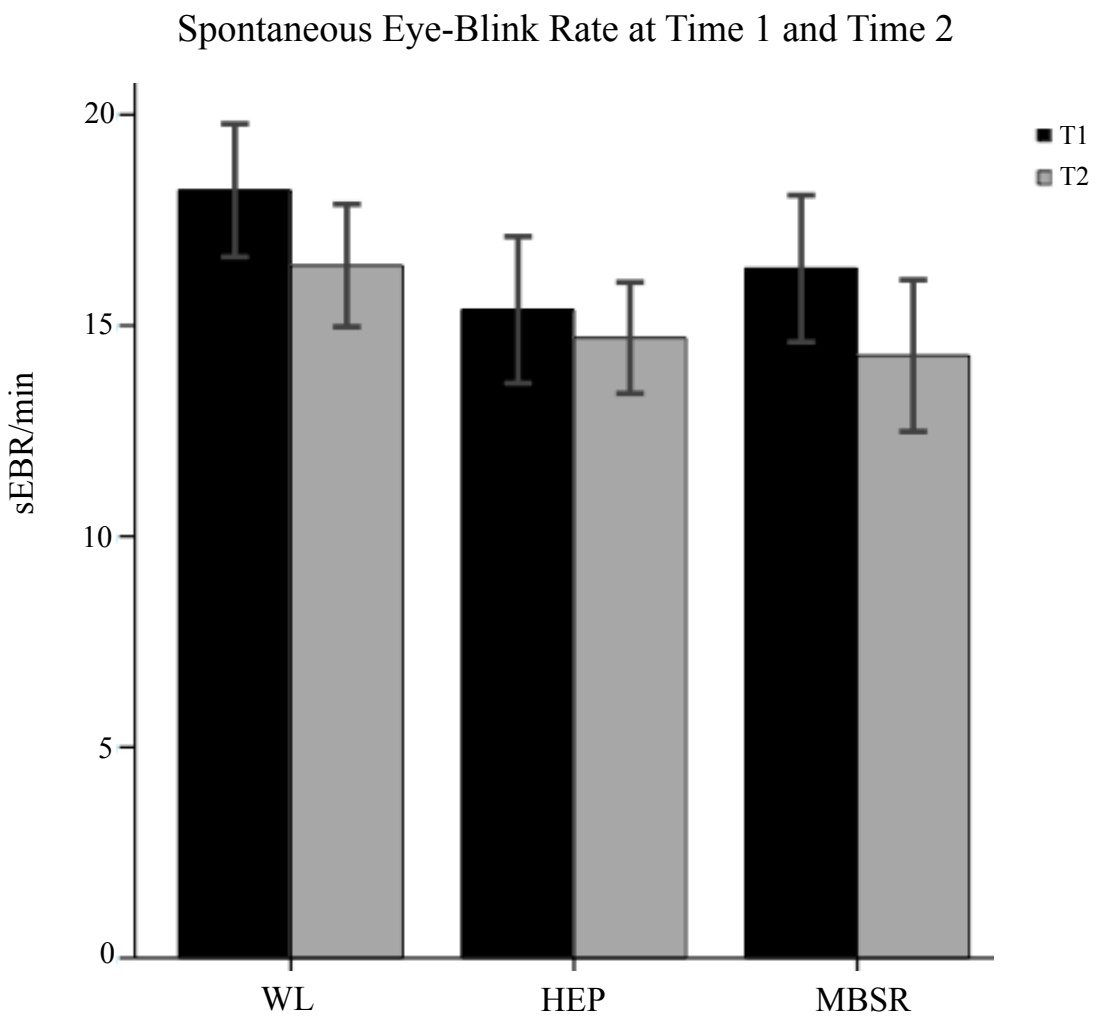

LTMs vs. MNPs

BIS-11 Self-Report

Compared to MNPs, LTMs scored lower (less impulsive) on the attentional impulsivity subscale (B=-1.51, *p*=0.027), but higher (more impulsive) on the motor impulsivity subscale (B=1.31, *p*=0.049), and non-planning impulsivity subscale (B=2.36, *p*=0.009). Groups did not differ significantly on overall score (B=2.15, *p*=0.219). See **Figure 16**.

Figure 16. *BIS-11 Scores: LTMs vs. MNPs at Time 1*

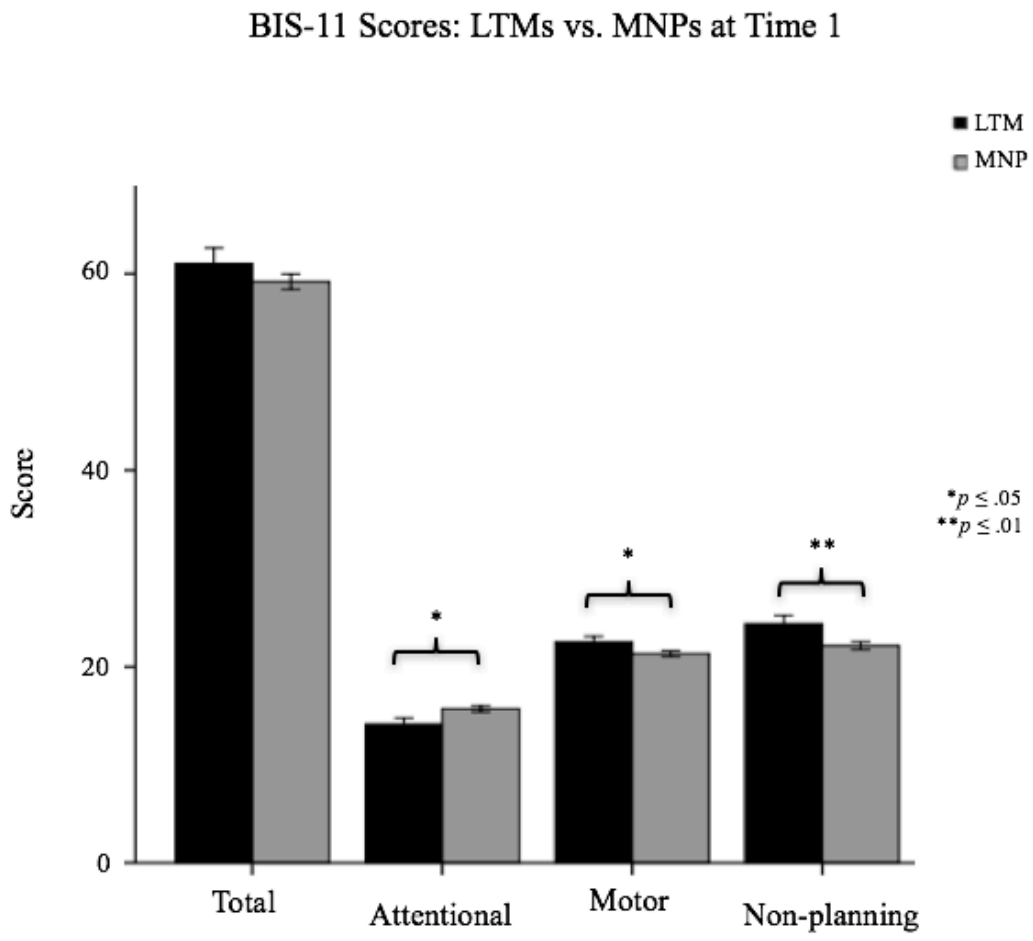

Go/No-Go Task

LTMs did not differ significantly from MNPs on go trial accuracy (B=-3.13, p=0.060), no-go (repeat) trial accuracy (B=1.57, p=0.685), no-go (syllable) trial accuracy (B=1.61, p=0.617), or post-error slowdown (B=23.1, p=0.132). **See Figures 17-18**.

Figure 17. *Go/No-Go Accuracy: LTMs vs. MNPs at Time 1*

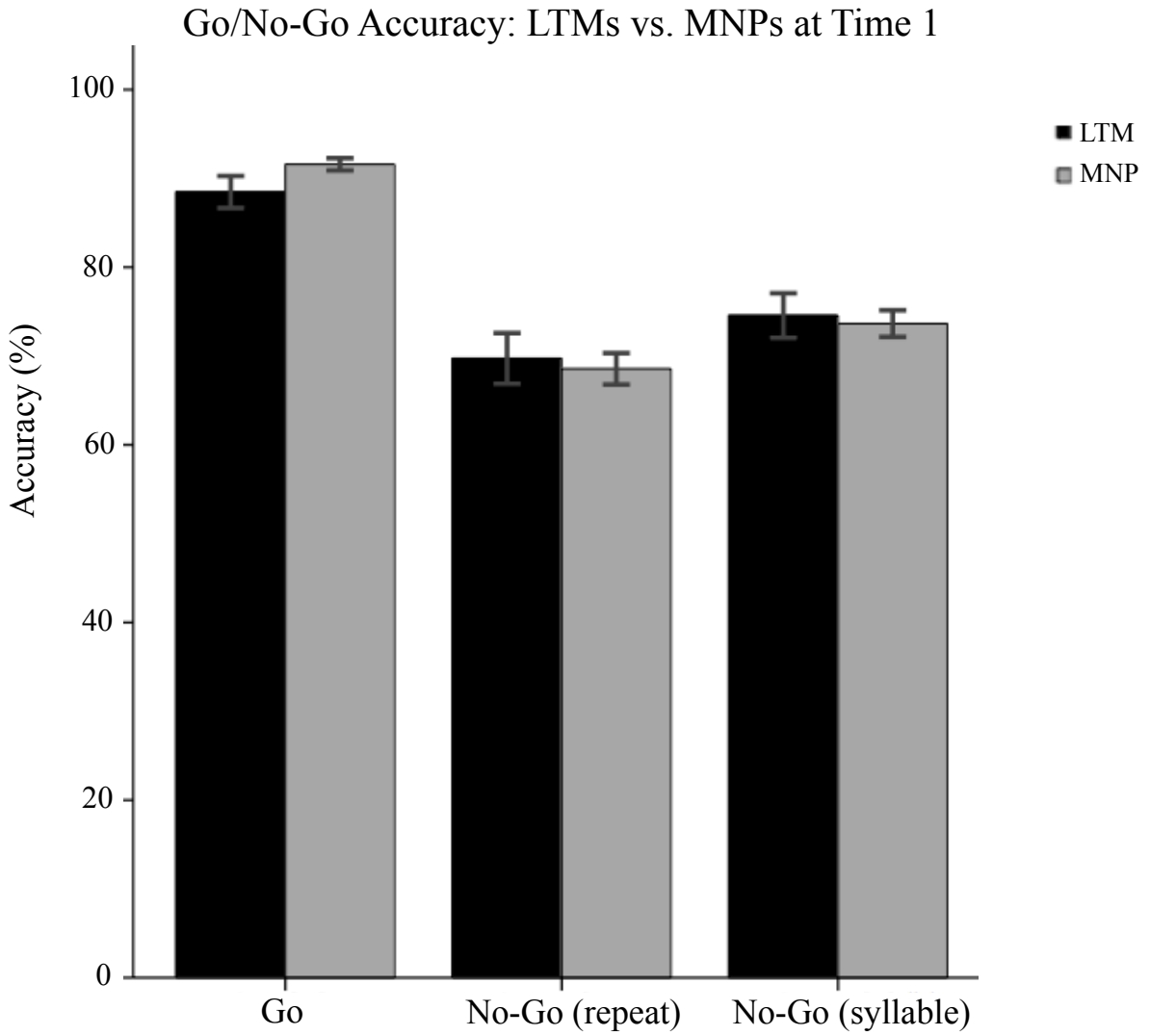

Figure 18. *Go/No-Go Post-Error Slowdown: LTMs vs. MNPs at Time 1*

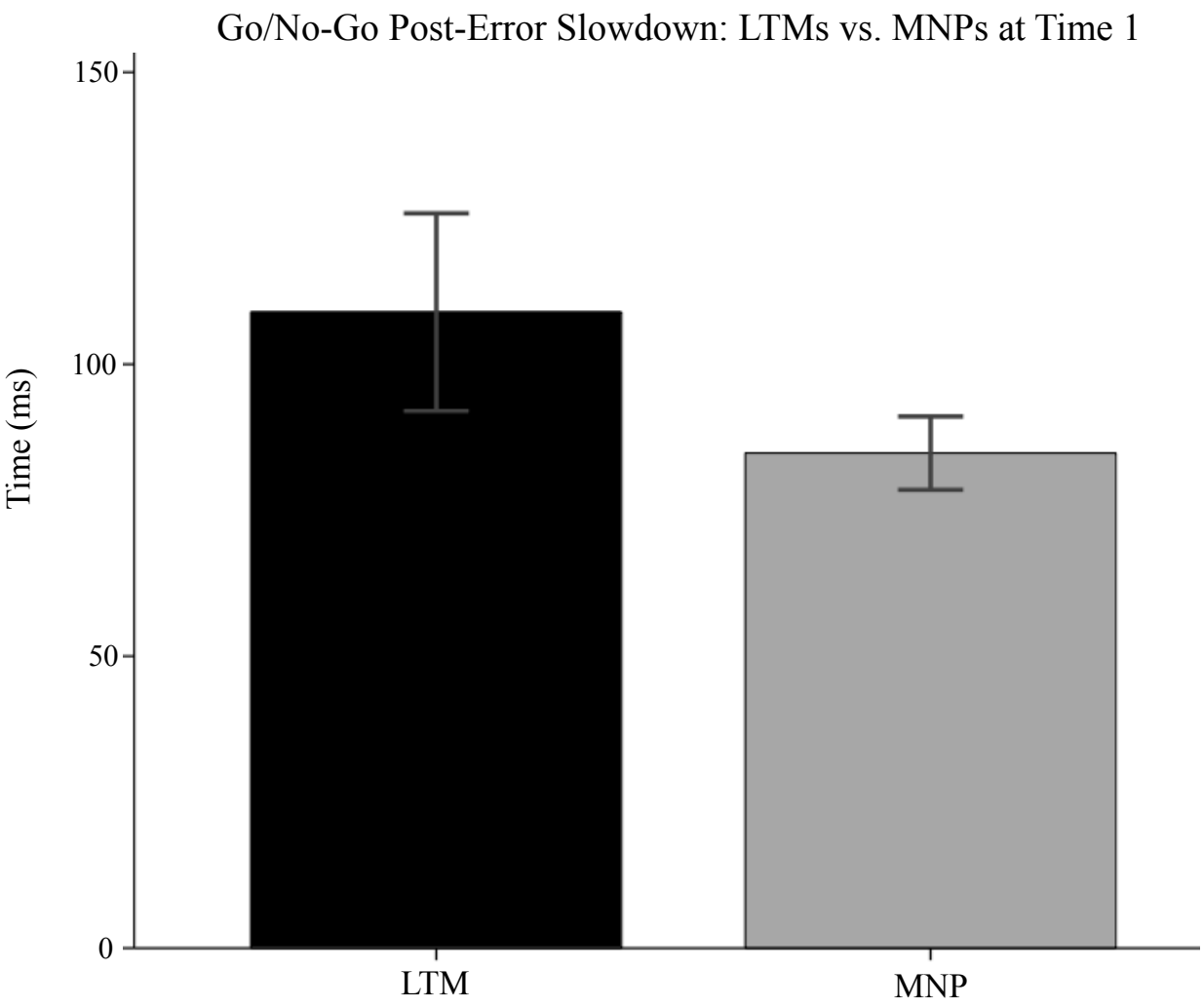

Gray Matter Volume

Whole-brain analyses showed that LTMs had less gray matter volume than MNPs in significant clusters encompassing parts of bilateral medial orbitofrontal cortex, inferior frontal gyrus, paracingulate gyrus, parahipocampal gryus, temporal pole, striatum, amygdala and cerebellum, as well as left dorsolateral prefrontal cortex and precentral gyrus. On the other hand, LTMs were found to have more gray matter volume than MNPs in significant clusters encompassing parts of the precuneus, posterior cingulate

cortex, precentral gyrus, fusiform gyrus, angular gyrus and middle temporal gyrus. See **Tables 15a-b** and **Figure 19** for full results.

Table 15a. *Regions with less volume in LTMs compared to MNPs*

Region	Other Regions in Cluster	Cluster Size	MNI Peak Coordinates
R Frontal Operculum Cortex	R Inferior Frontal Gyrus, R Medial Orbitofrontal Cortex, R Lateral Orbitofrontal Cortex, R Putamen	4972	(48, 24, 2)
L Cerebellum	R Cerebellum	17477	(-34, -54, -33)
L Middle Frontal Gyrus	L Superior Frontal Gyrus	997	(-28, 2, 57)
L Medial Orbitofrontal Cortex	L Paracingulate Gyrus, R Paracingulate Gyrus, R Subcallosal Cortex, R Frontal Pole, R Inferior Frontal Gyrus, R Frontal Operculum Cortex, R Nucleus Accumbens, L Nucleus Accumbens, R Caudate, L Caudate, R Putamen, L Putamen, R Insula, L Insula	7137	(-10, 32, -30)
L Middle Frontal Gyrus	L Precentral Gyrus	534	(-39, 9, 32)
R Amygdala	R Parahippocampal Gyrus, R Temporal Pole	995	(24, -2, -20)
R Inferior Temporal Gyrus		443	(45, -9, -46)
L Middle Frontal Gyrus		440	(-30, 0, 57)
L Temporal Pole	L Parahippocampal Gyrus, L Amygdala	527	(-26, 3, -46)

Table 15b. *Regions with more volume in LTMs compared to MNPs*

Region	Other Regions in Cluster	Cluster Size	MNI Peak Coordinates
L Precuneus	L Posterior Cingulate Gyrus	2366	(-15, -56, 45)
L Precentral Gyrus		339	(-16, -15, 56)
L Middle Temporal Gyrus	L Fusiform Gyrus, L Lingual Gyrus	2418	(-48, -50, -4)
L Lingual Gyrus	L Occipital Pole	906	(-14, -80, -4)
L Cerebellum		342	(-16, -60, -44)
R Lingual Gyrus	R Fusiform Gyrus	392	(21, -69, -4)

Figure 19. *Gray Matter Volume: LTMs vs. MNPs at Time 1*

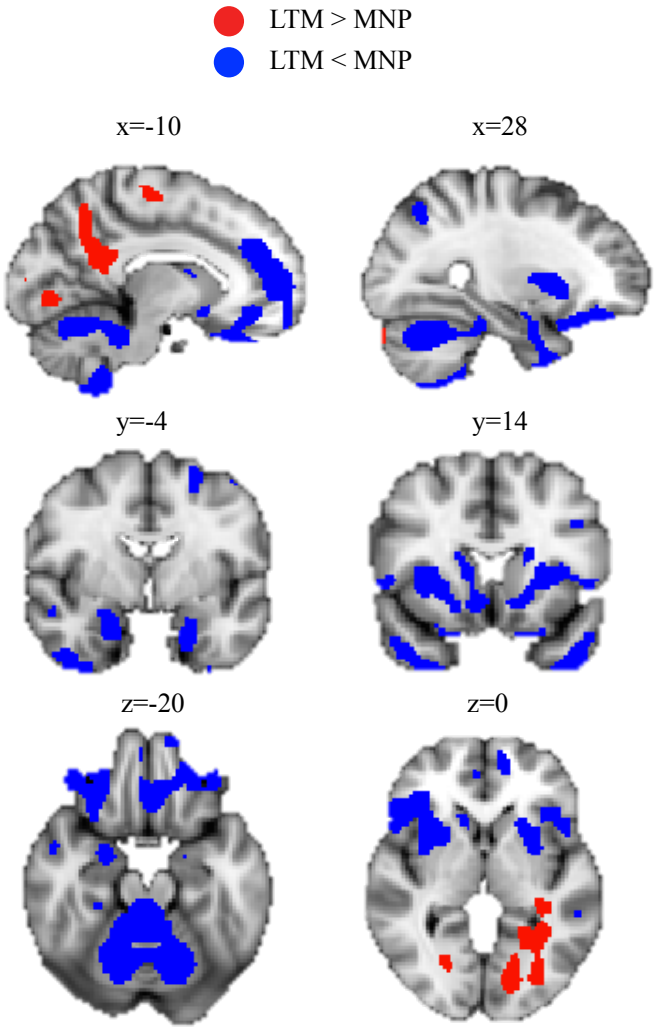

Resting-State Functional Connectivity

Compared to MNPs, LTMs had increased positively correlated RSFC between the ventral tegmental area and areas within the inferior and superior frontal gyri, between the substantia nigra and globus pallidus, thalamus, and default mode network nodes such as

the precuneus and angular gyrii, and between the inferior ventral striatum and default mode network nodes. See **Table 16** and **Figure 20** for full results.

Table 16. *Greater RSFC in LTMs compared to MNPs*

Focal Seed	RSFC Relationship with:	Other Regions in Cluster	MNI Peak Coordinates	Cluster Size	t-value
R Substantia Nigra	R Precuneus	L Globus Pallidus, R Thalamus, L Thalamus, L Precuneus, L Posterior Cingulate Gyrus, R Posterior Cingulate Gyrus	(6, -76, 52)	3053	4.48
	L Cerebellum	L Midbrain	(-30, -44, -44)	1761	4.26
	L Temporal Pole		(-36, 20, -32)	901	3.86
	R Middle Temporal Gyrus	R Angular Gyrus	(66, -50, 12)	748	4.69
	L Lateral Occipital Cortex	L Angular Gyrus	(-46, -62, 22)	551	4.50
	R Inferior Temporal Gyrus	R Inferior Lateral Occipital Cortex	(52, -56, -16)	333	4.19
L Substantia Nigra	R Angular Gyrus	R Supramarginal Gyrus, R Superior Temporal Gyrus, R Middle Temporal Gyrus, R Inferior Temporal Gyrus	(54, -46, 34)	2220	4.09
R Ventral Rostral Putamen	L Inferior Temporal Gyrus		(-52, -54, -14)	94	3.68
L Ventral Rostral Putamen	L Occipital Fusiform Gyrus		(-28, -86, -16)	13	4.18
R Inferior Ventral Striatum	L Precuneus	R Precuneus, L Posterior Cingulate Gyrus. R Posterior Cingulate Gyrus	(-6, -54, 48)	1275	4.26
Ventral Tegmental Area	L Inferior Temporal Gyrus	L Inferior Frontal Gyrus, L Middle Temporal Gyrus, L Angular Gyrus, L Insula,	(-50, -56, -10)	5050	4.51
	R Inferior Lateral Occipital Cortex		(58, -66, -4)	501	5.05
	L Superior Frontal Gyrus		(-16, 14, 50)	448	5.37
	L Cerebellum		(-18, -50, -52)	241	4.49
	L Supramarginal Gyrus		(-46, -44, 40)	199	3.50
	R Superior Frontal Gyrus		(6, 30, 62)	129	4.45
	L Heschl's Gyrus		(-36, -28, 10)	89	3.90

Figure 20. *Resting-State Functional Connectivity: LTMs vs. MNPs at Time 1*

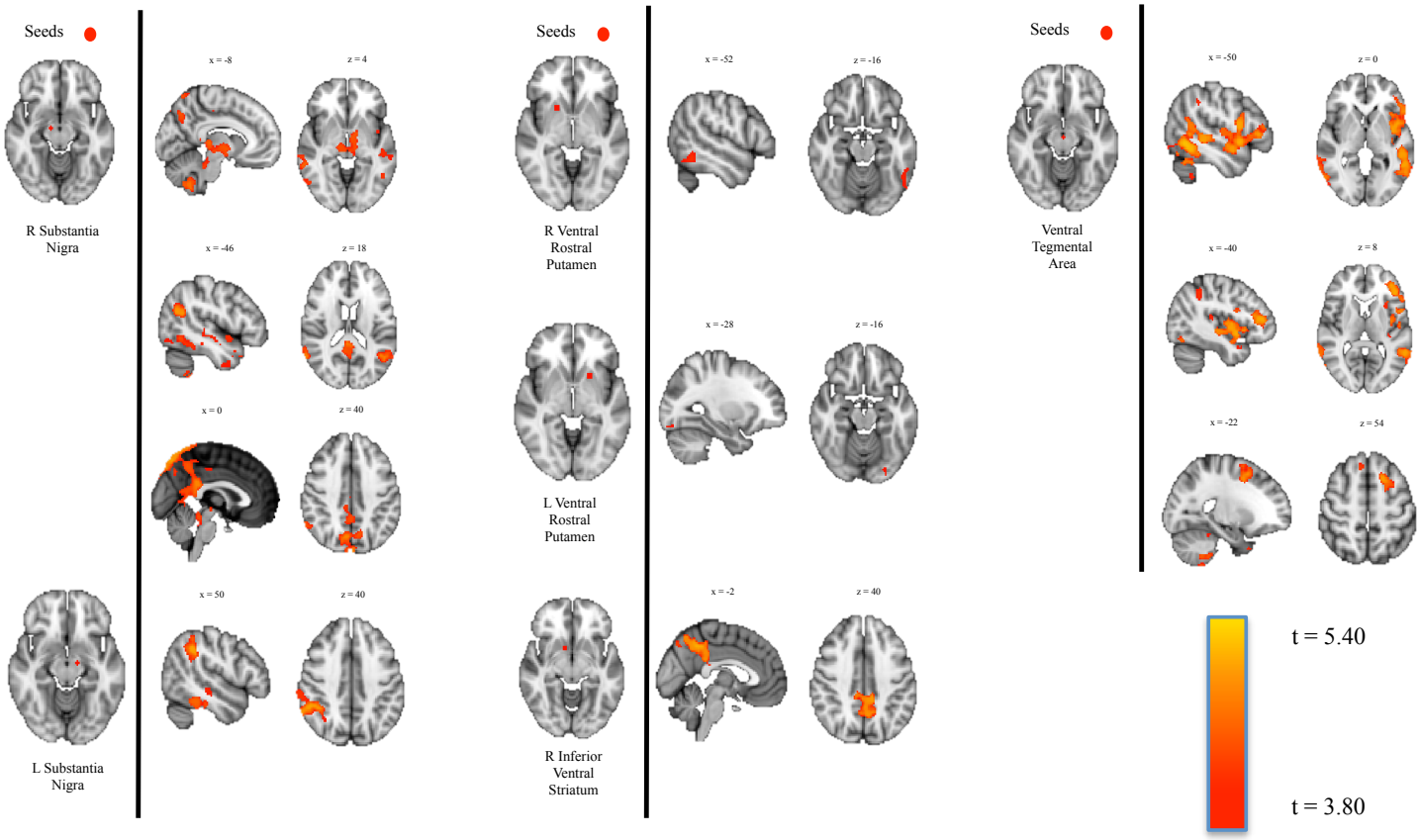

Spontaneous Eye-blink Rate

Findings of a group difference in sEBR have previously been reported in a superset of this sample by Kruis and colleagues[219], with LTMs having been found to have significantly lower sEBR than MNPs. As this sample differs slightly from the one previously reported on, we repeated the analysis here in order to ensure that the relationship holds in the present sample. Indeed, LTMs had significantly lower sEBR than MNPs (B=-4.73, p=0.015). See **Figure 21**.

Figure 21. *Spontaneous eye-blink rate: LTMs vs. MNPs at Time 1*

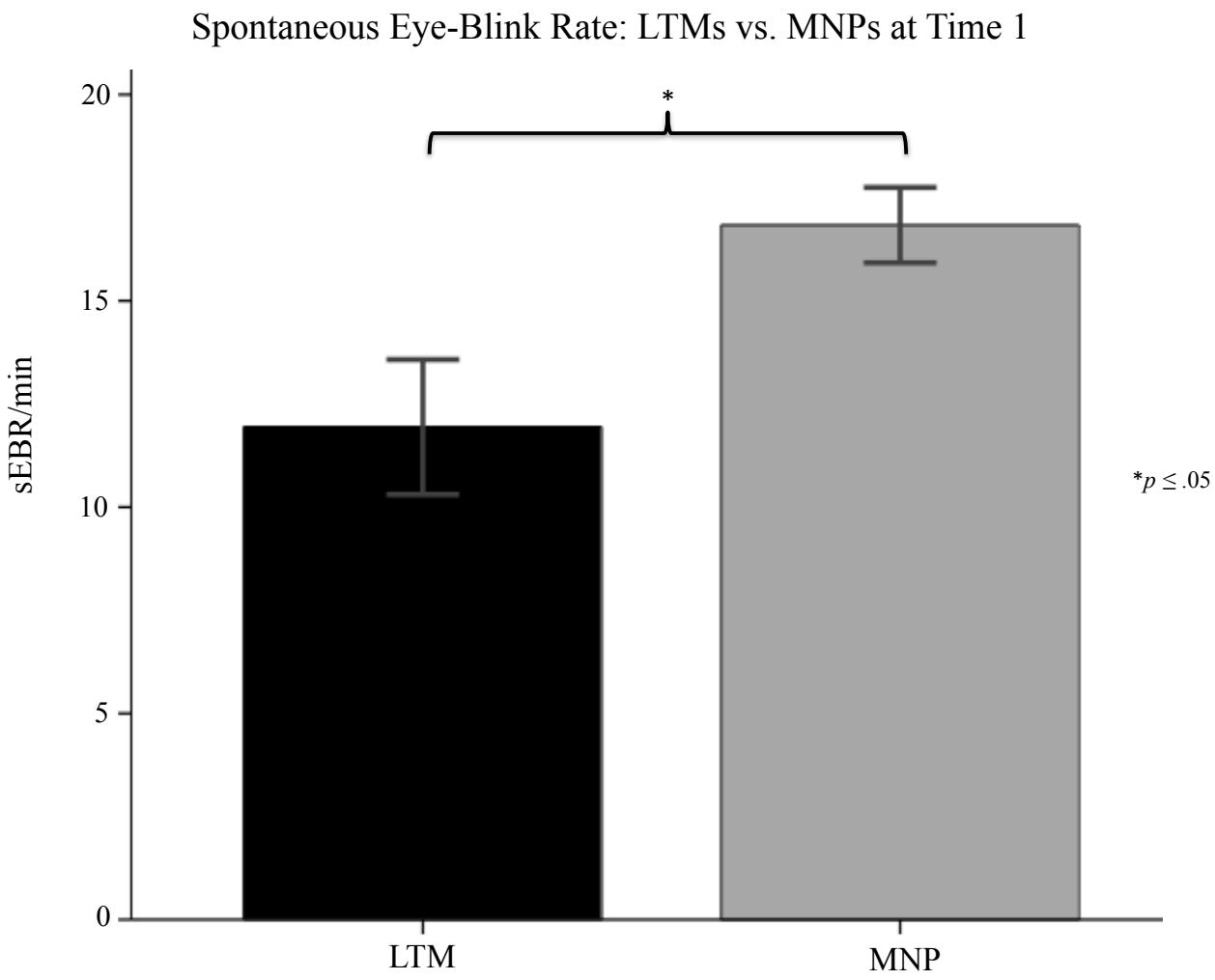

Total Lifetime Practice Hours in LTMs

Total lifetime practice hours (TLPH) were log-transformed in order to normalize the data (logTLPH).

BIS-11 Self-Report

logTLPH had a trending association with attentional impulsivity score (B=-1.78, p=0.065) and non-significant relationships with motor impulsivity score (B=0.823,

p=0.412), non-planning impulsivity score (B=0.427, *p*=0.745), and total impulsivity score (B=-0.532, *p*=0.829).

Go/No-Go Task

logTLPH was not significantly related to go trial accuracy (B=-3.11, *p*=0.255), no-go repeat trial accuracy (B=6.39, *p*=0.130), no-go syllable trial accuracy (B=4.26, *p*=0.262), or post-error slowdown (B=30.90, *p*=0.196).

Gray Matter Volume

A whole-brain analysis did not reveal any significant clusters where logTLPH was related to gray matter volume.

Resting-State Functional Connectivity

logTLPH was not significantly related to RSFC between any of the seed regions and the rest of the brain.

Spontaneous Eye-blink Rate

logTLPH was not significantly related to sEBR in this sample (B=-2.68, *p*=0.297), consistent with the findings from the superset reported by Kruis and colleagues[219].

6.4 Discussion

Recent interest has grown in using mindfulness meditation to help treat conditions featuring high levels of impulsivity such as substance abuse and ADHD. However, impulsivity is a multidimensional trait that can arise from deficits in one of several cognitive faculties, such as maintaining attention, inhibiting urges, and/or prospectively planning behavior. While a number of studies find that mindfulness can improve attention, it remains unclear whether mindfulness is effective in improving other

cognitive faculties whose deficiency can contribute to impulsive behavior. As such, This study first examined the effect of an eight-week mindfulness intervention on dimensions of impulsivity – gauged by performance on a go/no-go task and self-ratings of attentional, motor, and non-planning impulsivity on the Barratt Impulsiveness Scale (BIS-11) – and on gray matter volume and resting-state functional connectivity in the brain's decision-making circuitry, as well as on spontaneous eye blink-rate (a physiological indicator of dopaminergic functioning). We also examined cross-sectional differences in these metrics between long-term meditators (LTMs; *n*=28) and meditation-naïve participants (MNPs; *n*=105). We found that the eight-week mindfulness intervention did not result in any behavioral or neurobiological changes compared to either an active or wait-list control group. LTMs self-reported heightened capacity to maintain attention compared to MNPs, and within LTMs there was a trending negative association between lifetime practice hours and attentional impulsivity. However, LTMs did not display heightened capacity to withhold prepotent motor responses on the go/no-go task, and self-reported marginally higher scores on the motor and non-planning subscales of the BIS-11. LTMs were also found to have lower frontostriatal gray matter volume, heightened resting-state functional connectivity between the basal ganglia, midbrain, thalamus and cortex (in particular, elevated RSFC was observed between nodes of the mesolimbic dopamine pathway (i.e. VTA and PFC) and between nodes of the "direct" cortico-basal ganglia pathway (i.e. substantia nigra and thalamus) and lower spontaneous eye-blink rate compared to MNPs. Collectively, these findings suggest that, first, neither short-term nor long-term mindfulness meditation practice may be effective for improving inhibitory motor control or prospective planning capacity in otherwise healthy adults, but that, consistent with

other literature, long-term meditative practice may provide benefits for attentional control. As such, the ability of mindfulness meditation to reduce impulsive behavior may depend on which deficient cognitive faculty or faculties an individual's impulsivity is derived from. Second, the findings suggest that there are meaningful neurobiological differences in dopaminergic circuitry between LTMs and the general population, and that these differences may be relevant to LTMs heightened attentional control capacities.

Several methodological issues should be considered in interpreting these findings. Due to the cross-sectional design of the LTM vs. MNP comparisons, it is not possible to determine the extent to which group differences in impulsivity and neurobiology reflect effects of long-term meditation practice separate from effects of self-selection and pre-existing differences. Indeed, the absence of a general pattern of significant correlations between lifetime practice hours and the impulsivity or neurobiological metrics suggests that these findings might be primarily attributable to pre-existing differences. Individuals who self-select to spend substantial time meditating may be a unique group. Furthermore, it is possible that this unique group of individuals comprising the LTMs may interpret the BIS-11 self-report differently than the general population (MNPs) or may hold themselves to different standards. For instance, endorsing the item "I am more interested in the present than the future" would increase a subject's non-planning impulsivity BIS score, yet this concept is at the core of mindfulness practice – being mindful of and attentive to the present moment. Mindfulness and impulsiveness both share a focus on the present[220]. However, whereas impulsivity arises from hasty and heedless reactions to present circumstances, mindfulness is defined by a heightened awareness of the present that is nonreactive and observant in nature. The BIS-11 may not be optimally designed to

pick up on this subtle yet crucial distinction, and so scores for LTMs may be incorrectly inflated.

In interpreting the findings from the intervention, it is first important to note that the particular mindfulness meditation intervention used here, MBSR, is just one of a number of kinds of mindfulness meditation interventions. While MBSR may not be effective in reducing impulsivity in healthy adults, other studies may wish to examine the effects of alternative forms of mindfulness meditation on impulsivity. Furthermore, the results from this healthy sample do not necessarily suggest that use of this intervention in clinical populations with abnormally high levels of impulsivity would be ineffective.

Nonetheless, the findings from this study suggest that the use of mindfulness meditation to help treat impulsivity may be most effective for individuals whose impulsivity arises from attention deficits, rather than from deficits in motor inhibition capacity or prospective planning capacity. The next chapter presents a summary and integration of the research findings from **Chapters 2-6**.

Chapter 7: General Discussion

7.1 Discussion

This objective of this dissertation was three-fold:

1) Determine whether the neurobiological underpinnings of impulsivity in psychopathy are distinct from or an extreme manifestation of the neurobiological underpinnings of high levels of impulsivity in the general population,
2) Assess whether individual levels of impulsive-antisocial psychopathic traits can be ascertained from neural data – specifically voxel-level variation in gray matter volume– using machine learning, and
3) Examine the efficacy mindfulness meditation as an intervention to reduce impulsive behavior and alter its neurobiological underpinnings.

In **Chapters 2-3**, I found that impulsive-antisocial psychopathic traits in adult male inmates were associated with increased gray matter volume in the right medial orbitfrontal cortex, bilateral dorsolateral prefrontal cortex, bilateral nucleus accumbens, and bilateral putalem, as well as with increased intra-prefrontal and intra-striatal resting-state functional connectivity. In **Chapter 4**, I found that impulsivity in a sample of healthy adults from the general population was associated with decreased gray matter volume in the right medial orbitofrontal cortex and bilateral paracingulate gyrus, and with increased resting-state functional connectivity between nodes of the basal ganglia-thalamo-cortical loop, including between left medial orbitofrontal cortex and right inferior ventral striatum, between left superior frontal gyrus and left dorsal caudal

putamen, and between left anterior cingulate cortex and right superior ventral striatum. Together, these findings indicate that, first, while variance in medial prefrontal gray matter volume is associated with variability in impulsivity in both populations, the nature of aberrance in this region in the individuals with the highest impulsivity in each population is different. Specifically, the relationship is opposite in the subregion of right medial orbitofrontal cortex. Second, while impulsivity in both populations was associated with increased resting-state functional connectivity between nodes of the reward and decision-making network, the particular connections implicated in each sample were different. In the inmate sample, impulsivity was associated with elevated RSFC primarily in local circuits of the reward and decision-making network (i.e. intra-prefrontal and intra-striatal), whereas in the healthy sample, impulsivity was associated with RSFC largely in more global circuits (i.e. frontostriatal and striatothalamic). Overall, these results suggest that the neurobiological underpinnings of impulsivity in psychopathy are not simply an extreme manifestation of the neurobiological underpinnings of high levels of impulsivity in the general population, but are distinct. For instance, impulsivity in psychopathy and high levels of impulsivity in the general population both appear to be related to structural abnormality of the right medial orbitfrontal cortex, an area that is important for learning, prediction, and decision-making involving reward and emotion related information[221]. However, the different nature of structural aberrence in this region in each sample suggests that the clinical levels of impulsivity that characterize psychopathy arise from a unique etiological mechanism that is separate from those that lead to impulsivity in the general population. For instance, the increased levels of gray matter volume in individuals with psychopathy may point to abnormal development and

insufficient synaptic pruning. This more nuanced understanding that impulsivity in psychopathy may arise from a distinct etiological mechanism may be valuable for guiding more disorder-specific treatments for impulsivity in psychopathy.

More generally, these findings lend support to the notion suggested by studies of dopaminergic functioning that there are multiple neurobiological paths to impulsivity. Just as findings suggest that extreme levels of dopaminergic functioning at either end of the spectrum – hypoactive or hyperactive – are associated with impulsivity, the present findings suggest that very low or very high levels of medial prefrontal gray matter are associated with impulsivity. Furthermore, this would be consistent with the idea that neurobiological metrics in this circuitry are interrelated with one another. In fact, in **Chapter 4** I provide, to the best of my knowledge, the first evidence of a relationship between gray matter volume and dopaminergic functioning (as indexed by spontaneous eyeblink rate), in which volume in a cluster spanning the left putamen and medial orbitofrontal cortex was positively associated with spontaneous eyeblink rate. This relationship was further supported by the fact that both decreased medial orbitofrontal cortex volume and decreased spontaneous eyeblink rate were associated with increased impulsivity. If this relationship is valid, then we might expect the increased medial orbitofrontal cortex volume observed in relation to impulsivity in psychopathy to be accompanied by excessively elevated dopaminergic functioning – opposite the case in the healthy population. Indeed, as discussed earlier, there is some evidence for this. Two studies of cerebrospinal fluid, from which levels of the dopamine metabolite homovanillic acid (HVA) can be measured, have found a positive correlation between HVA levels and severity of psychopathic traits in criminal offenders[60,61]. In addition, a

PET study found that increasing severity of impulsive-antisocial psychopathic traits in a community sample was associated with greater dopamine release in the nucleus accumbens in response to reward[12]. And a study of spontaneous eyeblink rate (sEBR) in criminal inmates (of which individuals with psychopathy comprise a disproportionate percentage of in general[4]) found that higher sEBR – indicative of higher levels of dopaminergic functioning – was associated with greater impulsivity[62].

The findings in **Chapter 5** provided proof of concept that levels of impulsivity can be ascertained for single individuals based on their neural data. Although the accuracy achieved by the present model was only low/moderate, tweaks to the model (i.e. the use of additional neuroimaging modalities such as RSFC as features, or the use of more complex machine learning algorithms like relevance vector regression) and advances in both machine learning methodology and neuroimaging technology may eventually help improve accuracy to the point of being viable for practical use.

The type of machine learning model used here may help to circumvent a major criticism of neuroscience's application in the courtroom (e.g., for risk assessment). In academic research, data is usually compared between two sizable groups of subjects, and in traditional univariate analyses, an *average* value of the metric of interest for each group, rather than individual values, are used as the basis for statistical comparison. This kind of design is strategic because averages taken from many individuals are more representative of true population values than values taken from single individuals. This is because a population as a whole typically has a considerable degree of variability within it, and while most people in a population will have a value close to the average, plenty will have slightly more extreme values. Thus, when comparing two groups, it is possible

for some individuals from one population to have values that overlap with the values of some individuals from the other population. In academic research, the ability to use two large groups mitigates this issue because it enables the comparison of averages, which may not overlap between the two populations even if some segment of the individuals do. However, in the courtroom, the values of single individuals need to be assessed, and with traditional methods, this introduces statistical ambiguity. The machine learning approach avoids this issue by making single subject computations rather than calculating group averages. In other words, it directly assigns values or group membership to the individuals.

7.2 Limitations, Discrepancies, and Future Directions

Different instruments were used to measure impulsivity in the incarcerated sample (i.e. Factor 2 score from the PCL-R) than in the healthy, non-incarcerated sample (i.e. BIS-11), preventing the ability to make completely direct comparisons between findings from the two samples. Furthermore, Factor 2 score on the PCL-R is not a "pure" measure of impulsivity. The items that comprise the Factor 2 dimension of the PCL-R were distilled out by factor analysis of the PCL-R items[222], and index a broad array of antisocial traits and behaviors that include some more explicitly related to impulsivity (e.g. "impulsivity", "poor behavioral control", "need for stimulation"), some more complex behaviors and life events that may indirectly index impulsivity (e.g. "sexual promiscuity", "juvenile delinquincy", "revocation of conditional release", "criminal versaility"), and some where the relevancy of impulsivity is more vague (e.g. "lack of realistic long-term goals", "irresponsibility", "many short-term marital relationships"). Nonetheless, studies have shown correlations between BIS-11 scores the impulsivity

subscale score of psychopathy severity measures in both non-incarcerated samples (using the Psychopathic Personality Inventory-Revised)[223] and incarcerated samples (using the PCL-R)[224]. The study in an incarcerated sample found that Factor 2 score was significantly positively correlated with BIS-11 total score (R=0.26), BIS-11 motor impulsivity subscale score (R=0.28), and BIS-11 non-planning impulsivity subscale score (R=0.31), but not with BIS-11 attentional impulsivity subscale score (R=0.05). In our sample, we were able to corroborate the correlation between Factor 2 PCL-R score and BIS-11 scores by administering the BIS-11 to a subset of the incarcerated sample (n=49). Correlation analyses confirmed a direct and significant relationship between a subject's Factor 2 score and his BIS-11 total score of modest effect size (see **Table 17** and **Figure 22** below). In line with the study cited above, Factor 2 score was significantly correlated with BIS-11 total score, motor impulsivity subscale score, and non-planning impulsivity subscale score, but it did not significantly correlate with attentional impulsivity subscale score.

Table 17. *Correlation between Factor 2 score and BIS-11 scores*

	BIS-11 Total	**BIS-11 Motor**	**BIS-11 Non-Planning**	**BIS-11 Attentional**
Factor 2	R = .333 (p = 0.019)*	R = .296 (p= 0.039)*	R = .342 (p = 0.016)*	R = .147 (p= 0.315)

Figure 22. *Scatterplot of Factor 2 scores and BIS-11 total scores*

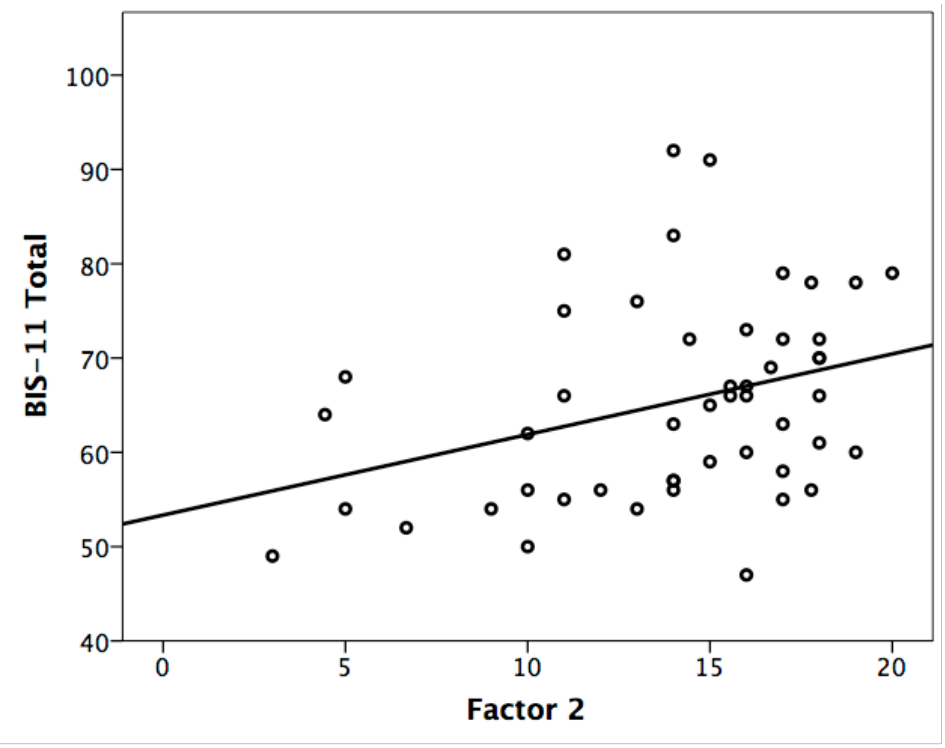

Overall, prior work and the current data suggest support for the ability to compare relationships between impulsivity and neurobiological metrics between the two samples studied here, though it also highlights that the instruments used in each population are undoubtedly distinct to some extent. Further limiting direct comparisons between the two samples is the fact that the brain scans for the two samples were taken with different scanners and different imaging parameters. Future research aiming to assess the validity of the comparisons drawn in this work should seek to measure impulsivity with the same instrument and acquire imaging data with the same scanner and imaging parameters in both population samples.

One technical methodological limitation to note is the use of subcortical ROI seed sizes (3.5mm and 1.5mm in radius) in the functional connectivity analyses that are

considerably smaller than the effective spatial resolution of the functional imaging data after smoothing (8mm). While seeds of this size are commonly used in the literature for subcortical structures in order to account for the small size of these structures, their small size relative to the effective spatial resolution of the data may nonetheless present issues for spatial localization and specificity.

Lastly, it should be noted that the initial aim of the machine learning analysis (Chapter 5) was to attempt to predict recidivism status (i.e. whether an inmate had reoffended within three years of release from their previous sentence) from voxel-level variation in gray matter volume. The classifier for this analysis performed at chance level, suggesting that gray matter volume alone may not be a sufficient neurobiological metric to aid in the prediction of this complex behavioral outcome. However, because of the small sample size of this analysis (n=43), it is insufficiently powered to definitively conclude this. Future research with larger sample sizes can help clarify the value of using neurobiological metrics to predict recidivism.

7.3 Conclusion

This dissertation first finds that some of the neural signatures of impulsivity are different in the general population than they are in a population with clinical levels of impulsivity – incarcerated offenders with psychopathic traits. Namely, individuals in the general population with the highest levels of impulsivity were found to have the lowest levels of gray matter volume in the right medial orbitofrontal cortex and bilateral paracingulate gyrus, whereas individuals in the incarcerated sample with the highest levels of impulsive-antisocial traits were found to have the highest levels of gray matter volume in the right medial orbitofrontal and dorsolateral prefrontal cortex, as well as in

the dorsal and ventral striatum. These findings suggest that structural abnormality of the right medial orbitofrontal cortex may be an important factor in predisposing both otherwise healthy individuals and individuals with psychopathy to impulsive behavior, but that this abnormality may take on more than one form and arise from different etiologies in each population. In addition, while impulsivity in both samples was found to be associated with elevated levels of resting-state functional connectivity in prefrontal and striatal circuits, elevated RSFC within the incarcerated sample was found mostly in local circuits within the basal ganglia-thalamo-cortical loop (i.e. intra-prefrontal and intra-striatal) whereas elevated RSFC within the healthy sample spanned more global circuits of the loop (i.e. nigrostriatal and striatothalamic). Overall, these findings suggest that impulsivity in psychopathy arises not simply from magnification in severity of the same neurobiological profile that predisposes individuals in the healthy population to high levels of impulsivity, but from a distinct pathophysiological mechanism.

Second, use of a machine learning model was demonstrated to predict incarcerated offenders' levels of impulsive-antisocial traits based on levels of gray matter volume throughout the brain, though the model achieved only low to moderate accuracy. Lastly, evidence was found that long-term, but not short-term, mindfulness meditation may be effective in reducing some, but not all, dimensions of impulsive behavior in the general population, and that long-term meditators have less gray matter volume throughout both the prefrontal cortex and striatum than non-meditators. Collectively, these studies help clarify the neural underpinnings of impulsive behavior, provide proof of concept of a method to identify impulsive individuals from neural data, and provide a

more nuanced understanding of the potential for mindfulness meditation to be used as a treatment for impulsive behavior.

References

1. Duckworth AL, Seligman ME. Self-discipline outdoes IQ in predicting academic performance of adolescents. *Psychol Sci.* 2005;16(12):939-944.
2. De Wit H. Impulsivity as a determinant and consequence of drug use: a review of underlying processes. *Addiction biology.* 2009;14(1):22-31.
3. Charnigo R, Noar SM, Garnett C, Crosby R, Palmgreen P, Zimmerman RS. Sensation seeking and impulsivity: combined associations with risky sexual behavior in a large sample of young adults. *J Sex Res.* 2013;50(5):480-488.
4. Kiehl KA, Hoffman MB. The Criminal Psychopath: History, Neuroscience, Treatment, and Economics. *Jurimetrics.* 2011;51:355-397.
5. Haber SN. The primate basal ganglia: parallel and integrative networks. *J Chem Neuroanat.* 2003;26(4):317-330.
6. Haber SN. Corticostriatal circuitry. *Dialogues Clin Neurosci.* 2016;18(1):7-21.
7. Averbeck BB, Lehman J, Jacobson M, Haber SN. Estimates of projection overlap and zones of convergence within frontal-striatal circuits. *Journal of Neuroscience.* 2014;34(29):9497-9505.
8. Lehericy S, Ducros M, De Moortele V, et al. Diffusion tensor fiber tracking shows distinct corticostriatal circuits in humans. *Annals of Neurology.* 2004;55(4):522-529.
9. Di Martino A, Scheres A, Margulies DS, et al. Functional connectivity of human striatum: a resting state FMRI study. *Cereb Cortex.* 2008;18(12):2735-2747.

10. Knutson B, Gibbs SE. Linking nucleus accumbens dopamine and blood oxygenation. *Psychopharmacology (Berl).* 2007;191(3):813-822.

11. Schott BH, Minuzzi L, Krebs RM, et al. Mesolimbic functional magnetic resonance imaging activations during reward anticipation correlate with reward-related ventral striatal dopamine release. *J Neurosci.* 2008;28(52):14311-14319.

12. Buckholtz JW, Treadway MT, Cowan RL, et al. Mesolimbic dopamine reward system hypersensitivity in individuals with psychopathic traits. *Nat Neurosci.* 2010;13(4):419-421.

13. Vollm BA, de Araujo IE, Cowen PJ, et al. Methamphetamine activates reward circuitry in drug naive human subjects. *Neuropsychopharmacology.* 2004;29(9):1715-1722.

14. Nagano-Saito A, Leyton M, Monchi O, Goldberg YK, He Y, Dagher A. Dopamine depletion impairs frontostriatal functional connectivity during a set-shifting task. *J Neurosci.* 2008;28(14):3697-3706.

15. Honey GD, Suckling J, Zelaya F, et al. Dopaminergic drug effects on physiological connectivity in a human cortico-striato-thalamic system. *Brain.* 2003;126(Pt 8):1767-1781.

16. Cole DM, Oei NY, Soeter RP, et al. Dopamine-dependent architecture of cortico-subcortical network connectivity. *Cereb Cortex.* 2013;23(7):1509-1516.

17. Kelly C, de Zubicaray G, Di Martino A, et al. L-dopa modulates functional connectivity in striatal cognitive and motor networks: a double-blind placebo-controlled study. *J Neurosci.* 2009;29(22):7364-7378.

18. Contreras-Rodriguez O, Pujol J, Batalla I, et al. Functional Connectivity Bias in the Prefrontal Cortex of Psychopaths. *Biol Psychiatry.* 2015;78(9):647-655.

19. Matsuo K, Nicoletti M, Nemoto K, et al. A voxel-based morphometry study of frontal gray matter correlates of impulsivity. *Hum Brain Mapp.* 2009;30(4):1188-1195.

20. Holmes AJ, Hollinshead MO, Roffman JL, Smoller JW, Buckner RL. Individual differences in cognitive control circuit anatomy link sensation seeking, impulsivity, and substance use. *Journal of Neuroscience* 2016;36(14):4038-4049.

21. Schilling C, Kuhn S, Romanowski A, Schubert F, Kathmann N, Gallinat J. Cortical thickness correlates with impulsiveness in healthy adults. *Neuroimage.* 2012;59(1):824-830.

22. Bjork JM, Momenan R, Hommer DW. Delay discounting correlates with proportional lateral frontal cortex volumes. *Biol Psychiatry.* 2009;65(8):710-713.

23. Cho SS, Pellecchia G, Aminian K, et al. Morphometric correlation of impulsivity in medial prefrontal cortex. *Brain Topogr.* 2013;26(3):479-487.

24. Dombrovski AY, Siegle GJ, Szanto K, Clark L, Reynolds CF, Aizenstein H. The temptation of suicide: striatal gray matter, discounting of delayed rewards, and suicide attempts in late-life depression. *Psychol Med.* 2012;42(6):1203-1215.

25. Angelides NH, Gupta J, Vickery TJ. Associating resting-state connectivity with trait impulsivity. *Soc Cogn Affect Neurosci.* 2017.

26. Li N, Ma N, Liu Y, et al. Resting-state functional connectivity predicts impulsivity in economic decision-making. *J Neurosci.* 2013;33(11):4886-4895.

27. Kayser AS, Allen DC, Navarro-Cebrian A, Mitchell JM, Fields HL. Dopamine, corticostriatal connectivity, and intertemporal choice. *J Neurosci.* 2012;32(27):9402-9409.

28. Daberkow DP, Brown HD, Bunner KD, et al. Amphetamine paradoxically augments exocytotic dopamine release and phasic dopamine signals. *J Neurosci.* 2013;33(2):452-463.

29. de Wit H, Enggasser JL, Richards JB. Acute administration of d-amphetamine decreases impulsivity in healthy volunteers. *Neuropsychopharmacology.* 2002;27(5):813-825.

30. Ghahremani DG, Lee B, Robertson CL, et al. Striatal Dopamine D-2/ D-3 Receptors Mediate Response Inhibition and Related Activity in Frontostriatal Neural Circuitry in Humans. *Journal of Neuroscience.* 2012;32(21):7316-7324.

31. Robertson CL, Ishibashi K, Mandelkern MA, et al. Striatal D1- and D2-type dopamine receptors are linked to motor response inhibition in human subjects. *J Neurosci.* 2015;35(15):5990-5997.

32. Lee B, London ED, Poldrack RA, et al. Striatal dopamine d2/d3 receptor availability is reduced in methamphetamine dependence and is linked to impulsivity. *J Neurosci.* 2009;29(47):14734-14740.

33. Groman SM, James AS, Seu E, et al. In the blink of an eye: relating positive-feedback sensitivity to striatal dopamine D2-like receptors through blink rate. *J Neurosci.* 2014;34(43):14443-14454.

34. Karson CN, Burns RS, LeWitt PA, Foster NL, Newman RP. Blink rates and disorders of movement. *Neurology.* 1984;34(5):677-678.

35. Cavanagh JF, Masters SE, Bath K, Frank MJ. Conflict acts as an implicit cost in reinforcement learning. *Nat Commun.* 2014;5.

36. Elsworth JD, Lawrence MS, Roth RH, et al. D(1) and D(2) Dopamine-Receptors Independently Regulate Spontaneous Blink Rate in the Vervet Monkey. *J Pharmacol Exp Ther.* 1991;259(2):595-606.

37. Jutkiewicz EM, Bergman J. Effects of dopamine D1 ligands on eye blinking in monkeys: Efficacy, antagonism, and D1/D2 interactions. *J Pharmacol Exp Ther.* 2004;311(3):1008-1015.

38. Kaminer J, Powers AS, Horn KG, Hui CN, Evinger C. Characterizing the Spontaneous Blink Generator: An Animal Model. *Journal of Neuroscience.* 2011;31(31):11256-11267.

39. Karson CN. Physiology of normal and abnormal blinking. *Adv Neurol.* 1988;49:25-37.

40. Kleven MS, Koek W. Differential effects of direct and indirect dopamine agonists on eye blink rate in cynomolgus monkeys. *J Pharmacol Exp Ther.* 1996;279(3):1211-1219.

41. Lawrence MS, Redmond DE. Mptp Lesions and Dopaminergic Drugs Alter Eye Blink Rate in African-Green Monkeys. *Pharmacol Biochem Be.* 1991;38(4):869-874.

42. Taylor JR, Elsworth JD, Lawrence MS, Sladek JR, Roth RH, Redmond DE. Spontaneous blink rates correlate with dopamine levels in the caudate nucleus of MPTP-treated monkeys. *Exp Neurol.* 1999;158(1):214-220.

43. Groman SM, James AS, Seu E, et al. In the Blink of an Eye: Relating Positive-Feedback Sensitivity to Striatal Dopamine D-2-Like Receptors through Blink Rate. *Journal of Neuroscience.* 2014;34(43):14443-14454.

44. Nakano T. The right angular gyrus controls spontaneous eyeblink rate: A combined structural MRI and TMS study. *Cortex.* 2017;88:186-191.

45. Basso MA, Powers AS, Evinger C. An explanation for reflex blink hyperexcitability in Parkinson's disease. I. Superior colliculus. *J Neurosci.* 1996;16(22):7308-7317.

46. Dang LC, Samanez-Larkin GR, Castrellon JJ, et al. Spontaneous eye blink rate (EBR) is uncorrelated with dopamine D2 receptor availability and unmodulated by dopamine agonism in healthy adults. *eNeuro.* 2017;4(5).

47. Karson CN, LeWitt PA, Calne DB, Wyatt RJ. Blink rates in parkinsonism. *Ann Neurol.* 1982;12(6):580-583.

48. Colzato LS, van den Wildenberg WP, van Wouwe NC, Pannebakker MM, Hommel B. Dopamine and inhibitory action control: evidence from spontaneous eye blink rates. *Exp Brain Res.* 2009;196(3):467-474.

49. Byrne KA, Norris DD, Worthy DA. Dopamine, depressive symptoms, and decision-making: the relationship between spontaneous eye blink rate and depressive symptoms predicts Iowa Gambling Task performance. *Cogn Affect Behav Neurosci.* 2016;16(1):23-36.

50. Smith SS, Newman JP. Alcohol and drug abuse-dependence disorders in psychopathic and nonpsychopathic criminal offenders. *J Abnorm Psychol.* 1990;99(4):430-439.

51. Hare RD. The Hare psychopathy checklist-revised (2nd ed.). *Toronto: Multi-Health Systems.* 2003.

52. Walters GD. Predicting institutional adjustment and recidivism with the psychopathy checklist factor scores: a meta-analysis. *Law Hum Behav.* 2003;27(5):541-558.

53. Edens JF, Poythress NG, Jr., Lilienfeld SO, Patrick CJ. A prospective comparison of two measures of psychopathy in the prediction of institutional misconduct. *Behav Sci Law.* 2008;26(5):529-541.

54. Cope LM, Shane MS, Segall JM, et al. Examining the effect of psychopathic traits on gray matter volume in a community substance abuse sample. *Psychiatry Res.* 2012;204(2-3):91-100.

55. Cope LM, Ermer E, Nyalakanti PK, Calhoun VD, Kiehl KA. Paralimbic gray matter reductions in incarcerated adolescent females with psychopathic traits. *J Abnorm Child Psychol.* 2014;42(4):659-668.

56. Contreras-Rodriguez O, Pujol J, Batalla I, et al. Functional Connectivity Bias in the Prefrontal Cortex of Psychopaths. *Biol Psychiat.* 2015;78(9):647-655.

57. Ermer E, Cope LM, Nyalakanti PK, Calhoun VD, Kiehl KA. Aberrant paralimbic gray matter in incarcerated male adolescents with psychopathic traits. *J Am Acad Child Adolesc Psychiatry.* 2013;52(1):94-103 e103.

58. Cope LM, Shane MS, Segall JM, et al. Examining the effect of psychopathic traits on gray matter volume in a community substance abuse sample. *Psychiat Res-Neuroim.* 2012;204(2-3):91-100.

59. Korponay C, Pujara M, Deming P, et al. Impulsive-antisocial dimension of psychopathy linked to enlargement and abnormal functional connectivity of the striatum. *Biol Psychiatry: CNNI.* in press.

60. Soderstrom H, Blennow K, Manhem A, Forsman A. CSF studies in violent offenders. I. 5-HIAA as a negative and HVA as a positive predictor of psychopathy. *J Neural Transm (Vienna).* 2001;108(7):869-878.

61. Soderstrom H, Blennow K, Sjodin AK, Forsman A. New evidence for an association between the CSF HVA:5-HIAA ratio and psychopathic traits. *J Neurol Neurosurg Psychiatry.* 2003;74(7):918-921.

62. Huang Z, Stanford SS, Barratt ES. Blink rate related to impulsiveness and task demands during performance of event-related potential tasks. *Personality and individual differences.* 1994;16(4):645-648.

63. Plichta MM, Scheres A. Ventral-striatal responsiveness during reward anticipation in ADHD and its relation to trait impulsivity in the healthy population: a meta-analytic review of the fMRI literature. *Neurosci Biobehav Rev.* 2014;38:125-134.

64. Cohen MX, Krohn-Grimberghe A, Elger CE, Weber B. Dopamine gene predicts the brain's response to dopaminergic drug. *Eur J Neurosci.* 2007;26(12):3652-3660.

65. Cools R, D'Esposito M. Inverted-U-shaped dopamine actions on human working memory and cognitive control. *Biol Psychiatry.* 2011;69(12):e113-125.

66. Arnsten AF. Catecholamine influences on dorsolateral prefrontal cortical networks. *Biol Psychiatry.* 2011;69(12):e89-99.

67. Eagle DM, Robbins TW. Inhibitory control in rats performing a stop-signal reaction-time task: effects of lesions of the medial striatum and d-amphetamine. *Behav Neurosci.* 2003;117(6):1302-1317.

68. Richards JB, Sabol KE, de Wit H. Effects of methamphetamine on the adjusting amount procedure, a model of impulsive behavior in rats. *Psychopharmacology (Berl).* 1999;146(4):432-439.

69. Berridge CW, Devilbiss DM, Andrzejewski ME, et al. Methylphenidate preferentially increases catecholamine neurotransmission within the prefrontal cortex at low doses that enhance cognitive function. *Biol Psychiatry.* 2006;60(10):1111-1120.

70. Eagle DM, Tufft MR, Goodchild HL, Robbins TW. Differential effects of modafinil and methylphenidate on stop-signal reaction time task performance in the rat, and interactions with the dopamine receptor antagonist cis-flupenthixol. *Psychopharmacology (Berl).* 2007;192(2):193-206.

71. Perry JL, Stairs DJ, Bardo MT. Impulsive choice and environmental enrichment: effects of d-amphetamine and methylphenidate. *Behav Brain Res.* 2008;193(1):48-54.

72. de Wit H, Crean J, Richards JB. Effects of d-amphetamine and ethanol on a measure of behavioral inhibition in humans. *Behav Neurosci.* 2000;114(4):830-837.

73. Voon V, Reynolds B, Brezing C, et al. Impulsive choice and response in dopamine agonist-related impulse control behaviors. *Psychopharmacology (Berl).* 2010;207(4):645-659.

74. Leroi I, Barraclough M, McKie S, et al. Dopaminergic influences on executive function and impulsive behaviour in impulse control disorders in Parkinson's disease. *J Neuropsychol.* 2013;7(2):306-325.

75. Villa C, Pascual-Sedano B, Pagonabarraga J, Kulisevsky J. Impulse control disorders and dopaminergic treatments in Parkinson's disease. *Rev Neurol (Paris).* 2011;167(11):827-832.

76. Weintraub D. Dopamine and impulse control disorders in Parkinson's disease. *Ann Neurol.* 2008;64 Suppl 2:S93-100.

77. Logue AW, Tobin H, Chelonis JJ, Wang RY, Geary N, Schachter S. Cocaine decreases self-control in rats: a preliminary report. *Psychopharmacology (Berl).* 1992;109(1-2):245-247.

78. Evenden JL, Ryan CN. The pharmacology of impulsive behaviour in rats: the effects of drugs on response choice with varying delays of reinforcement. *Psychopharmacology (Berl).* 1996;128(2):161-170.

79. Charrier D, Thiebot MH. Effects of psychotropic drugs on rat responding in an operant paradigm involving choice between delayed reinforcers. *Pharmacol Biochem Behav.* 1996;54(1):149-157.

80. Wade TR, de Wit H, Richards JB. Effects of dopaminergic drugs on delayed reward as a measure of impulsive behavior in rats. *Psychopharmacology (Berl).* 2000;150(1):90-101.

81. van Gaalen MM, van Koten R, Schoffelmeer AN, Vanderschuren LJ. Critical involvement of dopaminergic neurotransmission in impulsive decision making. *Biol Psychiatry.* 2006;60(1):66-73.

82. Shiels K, Hawk Jr LW, Reynolds B, et al. Effects of methylphenidate on discounting of delayed rewards in attention deficit/hyperactivity disorder. *Experimental and clinical psychopharmacology.* 2009;17(5).

83. Vollm B, Richardson P, McKie S, Elliott R, Dolan M, Deakin B. Neuronal correlates of reward and loss in Cluster B personality disorders: a functional magnetic resonance imaging study. *Psychiatry Res.* 2007;156(2):151-167.

84. Everitt BJ, Belin D, Economidou D, Pelloux Y, Dalley JW, Robbins TW. Review. Neural mechanisms underlying the vulnerability to develop compulsive drug-seeking habits and addiction. *Philos Trans R Soc Lond B Biol Sci.* 2008;363(1507):3125-3135.

85. Volkow ND, Tomasi D, Wang GJ, et al. Predominance of D2 receptors in mediating dopamine's effects in brain metabolism: effects of alcoholism. *J Neurosci.* 2013;33(10):4527-4535.

86. Nader MA, Czoty PW, Gould RW, Riddick NV. Review. Positron emission tomography imaging studies of dopamine receptors in primate models of addiction. *Philos Trans R Soc Lond B Biol Sci.* 2008;363(1507):3223-3232.

87. Glenn AL, Yang Y. The potential role of the striatum in antisocial behavior and psychopathy. *Biol Psychiatry.* 2012;72(10):817-822.

88. Bjork JM, Chen G, Hommer DW. Psychopathic tendencies and mesolimbic recruitment by cues for instrumental and passively obtained rewards. *Biol Psychol.* 2012;89(2):408-415.

89. Pujara M, Motzkin JC, Newman JP, Kiehl KA, Koenigs M. Neural correlates of reward and loss sensitivity in psychopathy. *Soc Cogn Affect Neurosci.* 2014;9(6):794-801.

90. Schiffer B, Muller BW, Scherbaum N, et al. Disentangling structural brain alterations associated with violent behavior from those associated with substance use disorders. *Arch Gen Psychiatry.* 2011;68(10):1039-1049.

91. Boccardi M, Bocchetta M, Aronen HJ, et al. Atypical nucleus accumbens morphology in psychopathy: another limbic piece in the puzzle. *Int J Law Psychiatry.* 2013;36(2):157-167.

92. Glenn AL, Raine A, Yaralian PS, Yang Y. Increased volume of the striatum in psychopathic individuals. *Biol Psychiatry.* 2010;67(1):52-58.

93. Vieira JB, Ferreira-Santos F, Almeida PR, Barbosa F, Marques-Teixeira J, Marsh AA. Psychopathic traits are associated with cortical and subcortical volume alterations in healthy individuals. *Soc Cogn Affect Neurosci.* 2015;10(12):1693-1704.

94. Ermer E, Cope LM, Nyalakanti PK, Calhoun VD, Kiehl KA. Aberrant paralimbic gray matter in criminal psychopathy. *J Abnorm Psychol.* 2012;121(3):649-658.

95. Harpur T, Hare R, Hakstian A. Two-factor conceptualization of psychopathy: Construct validity and assessment implications. *Psychological Assessment: A Journal of consulting and clinical Psychology.* 1989;1(1).

96. First M. Structured clinical interview for DSM-IV-TR axis I disorders, research version, non-patient edition (SCID-I/NP). New York: Biometrics Research: New York State Psychiatric Institute; 2002.

97. Ly M, Motzkin JC, Philippi CL, et al. Cortical thinning in psychopathy. *Am J Psychiatry.* 2012;169(7):743-749.

98. Philippi CL, Pujara MS, Motzkin JC, Newman J, Kiehl KA, Koenigs M. Altered resting-state functional connectivity in cortical networks in psychopathy. *J Neurosci.* 2015;35(15):6068-6078.

99. Fischl B. FreeSurfer. *Neuroimage.* 2012;62(2):774-781.

100. Cox RW. AFNI: software for analysis and visualization of functional magnetic resonance neuroimages. *Comput Biomed Res.* 1996;29(3):162-173.

101. Fischl B, Dale AM. Measuring the thickness of the human cerebral cortex from magnetic resonance images. *Proc Natl Acad Sci U S A.* 2000;97(20):11050-11055.

102. Ashburner J, Friston KJ. Voxel-based morphometry--the methods. *Neuroimage.* 2000;11(6 Pt 1):805-821.

103. Fox MD, Snyder AZ, Vincent JL, Corbetta M, Van Essen DC, Raichle ME. The human brain is intrinsically organized into dynamic, anticorrelated functional networks. *Proc Natl Acad Sci U S A.* 2005;102(27):9673-9678.

104. Avants B, Gee JC. Geodesic estimation for large deformation anatomical shape averaging and interpolation. *Neuroimage.* 2004;23 Suppl 1:S139-150.

105. Power JD, Barnes KA, Snyder AZ, Schlaggar BL, Petersen SE. Spurious but systematic correlations in functional connectivity MRI networks arise from subject motion. *Neuroimage.* 2012;59(3):2142-2154.

106. Satterthwaite TD, Elliott MA, Gerraty RT, et al. An improved framework for confound regression and filtering for control of motion artifact in the

preprocessing of resting-state functional connectivity data. *Neuroimage.* 2013;64:240-256.

107. Yan CG, Cheung B, Kelly C, et al. A comprehensive assessment of regional variation in the impact of head micromovements on functional connectomics. *Neuroimage.* 2013;76:183-201.

108. Rajagopalan V, Pioro EP. Disparate voxel based morphometry (VBM) results between SPM and FSL softwares in ALS patients with frontotemporal dementia: which VBM results to consider? *BMC Neurol.* 2015;15:32.

109. Forman SD, Cohen JD, Fitzgerald M, Eddy WF, Mintun MA, Noll DC. Improved assessment of significant activation in functional magnetic resonance imaging (fMRI): use of a cluster-size threshold. *Magn Reson Med.* 1995;33(5):636-647.

110. Carp J. The secret lives of experiments: methods reporting in the fMRI literature. *Neuroimage.* 2012;63(1):289-300.

111. Fein G, Landman B, Tran H, et al. Brain atrophy in long-term abstinent alcoholics who demonstrate impairment on a simulated gambling task. *Neuroimage.* 2006;32(3):1465-1471.

112. Franklin TR, Acton PD, Maldjian JA, et al. Decreased gray matter concentration in the insular, orbitofrontal, cingulate, and temporal cortices of cocaine patients. *Biol Psychiatry.* 2002;51(2):134-142.

113. Makris N, Oscar-Berman M, Jaffin SK, et al. Decreased volume of the brain reward system in alcoholism. *Biol Psychiatry.* 2008;64(3):192-202.

114. Tanabe J, Tregellas JR, Dalwani M, et al. Medial orbitofrontal cortex gray matter is reduced in abstinent substance-dependent individuals. *Biol Psychiatry.* 2009;65(2):160-164.

115. Yuan Y, Zhu Z, Shi J, et al. Gray matter density negatively correlates with duration of heroin use in young lifetime heroin-dependent individuals. *Brain Cogn.* 2009;71(3):223-228.

116. Walhovd KB, Fjell AM, Reinvang I, et al. Effects of age on volumes of cortex, white matter and subcortical structures. *Neurobiol Aging.* 2005;26(9):1261-1270; discussion 1275-1268.

117. Miller AK, Alston RL, Corsellis JA. Variation with age in the volumes of grey and white matter in the cerebral hemispheres of man: measurements with an image analyser. *Neuropathol Appl Neurobiol.* 1980;6(2):119-132.

118. Tiihonen J, Kuikka J, Bergstrom K, et al. Altered striatal dopamine re-uptake site densities in habitually violent and non-violent alcoholics. *Nat Med.* 1995;1(7):654-657.

119. Amen DG, Stubblefield M, Carmicheal B, Thisted R. Brain SPECT findings and aggressiveness. *Ann Clin Psychiatry.* 1996;8(3):129-137.

120. Soderstrom H, Hultin L, Tullberg M, Wikkelso C, Ekholm S, Forsman A. Reduced frontotemporal perfusion in psychopathic personality. *Psychiatry Res.* 2002;114(2):81-94.

121. Gatzke-Kopp LM, Beauchaine TP, Shannon KE, et al. Neurological correlates of reward responding in adolescents with and without externalizing behavior disorders. *J Abnorm Psychol.* 2009;118(1):203-213.

122. Avila C, Garbin G, Sanjuan A, et al. Frontostriatal response to set switching is moderated by reward sensitivity. *Soc Cogn Affect Neurosci.* 2012;7(4):423-430.

123. Cohen MX, Schoene-Bake JC, Elger CE, Weber B. Connectivity-based segregation of the human striatum predicts personality characteristics. *Nat Neurosci.* 2009;12(1):32-34.

124. O'Doherty JP. Reward representations and reward-related learning in the human brain: insights from neuroimaging. *Curr Opin Neurobiol.* 2004;14(6):769-776.

125. Haber SN, Knutson B. The reward circuit: linking primate anatomy and human imaging. *Neuropsychopharmacology.* 2010;35(1):4-26.

126. Blair KS, Newman C, Mitchell DG, et al. Differentiating among prefrontal substrates in psychopathy: neuropsychological test findings. *Neuropsychology.* 2006;20(2):153-165.

127. Narayan VM, Narr KL, Kumari V, et al. Regional cortical thinning in subjects with violent antisocial personality disorder or schizophrenia. *Am J Psychiatry.* 2007;164(9):1418-1427.

128. Wolf RC, Pujara MS, Motzkin JC, et al. Interpersonal traits of psychopathy linked to reduced integrity of the uncinate fasciculus. *Hum Brain Mapp.* 2015;36(10):4202-4209.

129. Chang L, Alicata D, Ernst T, Volkow N. Structural and metabolic brain changes in the striatum associated with methamphetamine abuse. *Addiction.* 2007;102 Suppl 1:16-32.

130. Gu H, Salmeron BJ, Ross TJ, et al. Mesocorticolimbic circuits are impaired in chronic cocaine users as demonstrated by resting-state functional connectivity. *Neuroimage.* 2010;53(2):593-601.

131. Kriegeskorte N, Simmons WK, Bellgowan PS, Baker CI. Circular analysis in systems neuroscience: the dangers of double dipping. *Nat Neurosci.* 2009;12(5):535-540.

132. Damasio AR. The somatic marker hypothesis and the possible functions of the prefrontal cortex. *Philos T R Soc B.* 1996;351(1346):1413-1420.

133. Grabenhorst F, Rolls ET. Value, pleasure and choice in the ventral prefrontal cortex. *Trends Cogn Sci.* 2011;15(2):56-67.

134. Miller EK, Cohen JD. An integrative theory of prefrontal cortex function. *Annu Rev Neurosci.* 2001;24:167-202.

135. Devinsky O, Morrell MJ, Vogt BA. Contributions of anterior cingulate cortex to behaviour. *Brain.* 1995;118 (Pt 1):279-306.

136. Shackman AJ, Salomons TV, Slagter HA, Fox AS, Winter JJ, Davidson RJ. The integration of negative affect, pain and cognitive control in the cingulate cortex. *Nat Rev Neurosci.* 2011;12(3):154-167.

137. Eslinger PJ, Damasio AR. Severe disturbance of higher cognition after bilateral frontal lobe ablation: patient EVR. *Neurology.* 1985;35(12):1731-1741.

138. Damasio AR. *Descartes ' Error* New York: Putnam; 1994.

139. Bechara A, Damasio H, Tranel D, Damasio AR. Deciding advantageously before knowing the advantageous strategy. *Science.* 1997;275(5304):1293-1295.

140. Barrash J, Tranel D, Anderson SW. Acquired personality disturbances associated with bilateral damage to the ventromedial prefrontal region. *Dev Neuropsychol.* 2000;18(3):355-381.

141. de Oliveira-Souza R, Hare RD, Bramati IE, et al. Psychopathy as a disorder of the moral brain: Fronto-temporo-limbic grey matter reductions demonstrated by voxel-based morphometry. *Neuroimage.* 2008;40(3):1202-1213.

142. Muller JL, Sommer M, Dohnel K, Weber T, Schmidt-Wilcke T, Hajak G. Disturbed prefrontal and temporal brain function during emotion and cognition interaction in criminal psychopathy. *Behav Sci Law.* 2008;26(1):131-150.

143. Yang YL, Raine A, Lencz T, Bihrle S, LaCasse L, Colletti P. Volume reduction in prefrontal gray matter in unsuccessful criminal psychopaths. *Biol Psychiat.* 2005;57(10):1103-1108.

144. Ermer E, Cope LM, Nyalakanti PK, Calhoun VD, Kiehl KA. Aberrant Paralimbic Gray Matter in Criminal Psychopathy. *Journal of Abnormal Psychology.* 2012;121(3):649-658.

145. Motzkin JC, Newman JP, Kiehl KA, Koenigs M. Reduced Prefrontal Connectivity in Psychopathy. *J Neurosci.* 2011;31(48):17348-17357.

146. Pujol J, Batalla I, Contreras-Rodriguez O, et al. Breakdown in the brain network subserving moral judgment in criminal psychopathy. *Soc Cogn Affect Neur.* 2012;7(8):917-923.

147. Juarez M, Kiehl KA, Calhoun VD. Intrinsic limbic and paralimbic networks are associated with criminal psychopathy. *Hum Brain Mapp.* 2013;34(8):1921-1930.

148. Shannon BJ, Raichle ME, Snyder AZ, et al. Premotor functional connectivity predicts impulsivity in juvenile offenders. *Proc Natl Acad Sci U S A.* 2011;108(27):11241-11245.

149. Philippi CL, Pujara MS, Motzkin JC, Newman J, Kiehl KA, Koenigs M. Altered Resting-State Functional Connectivity in Cortical Networks in Psychopathy. *J Neurosci.* 2015;35(15):6068-6078.

150. McLellan AT, Kushner H, Metzger D, et al. The Fifth Edition of the Addiction Severity Index. *J Subst Abuse Treat.* 1992;9(3):199-213.

151. Eklund A, Nichols TE, Knutsson H. Cluster failure: Why fMRI inferences for spatial extent have inflated false-positive rates. *Proc Natl Acad Sci U S A.* 2016;113(28):7900-7905.

152. Gogtay N, Giedd JN, Lusk L, et al. Dynamic mapping of human cortical development during childhood through early adulthood. *Proc Natl Acad Sci U S A.* 2004;101(21):8174-8179.

153. Giorgio A, Watkins KE, Chadwick M, et al. Longitudinal changes in grey and white matter during adolescence. *Neuroimage.* 2010;49(1):94-103.

154. Newman JP. Reaction to Punishment in Extroverts and Psychopaths - Implications for the Impulsive Behavior of Disinhibited Individuals. *J Res Pers.* 1987;21(4):464-480.

155. O'Doherty J, Kringelbach ML, Rolls ET, Hornak J, Andrews C. Abstract reward and punishment representations in the human orbitofrontal cortex. *Nat Neurosci.* 2001;4(1):95-102.

156. Gabbott PL, Warner TA, Jays PR, Salway P, Busby SJ. Prefrontal cortex in the rat: projections to subcortical autonomic, motor, and limbic centers. *J Comp Neurol.* 2005;492(2):145-177.

157. Sesack SR, Deutch AY, Roth RH, Bunney BS. Topographical organization of the efferent projections of the medial prefrontal cortex in the rat: an anterograde tract-tracing study with Phaseolus vulgaris leucoagglutinin. *J Comp Neurol.* 1989;290(2):213-242.

158. Pujara M, Koenigs M. Mechanisms of reward circuit dysfunction in psychiatric illness: prefrontal-striatal interactions. *Neuroscientist.* 2014;20(1):82-95.

159. Yang YL, Raine A, Joshi AA, et al. Frontal information flow and connectivity in psychopathy. *Brit J Psychiat.* 2012;201(5):408-409.

160. Rilling JK, Glenn AL, Jairam MR, et al. Neural correlates of social cooperation and non-cooperation as a function of psychopathy. *Biol Psychiatry.* 2007;61(11):1260-1271.

161. Kiehl KA, Smith AM, Hare RD, et al. Limbic abnormalities in affective processing by criminal psychopaths as revealed by functional magnetic resonance imaging. *Biol Psychiatry.* 2001;50(9):677-684.

162. Gordon HL, Baird AA, End A. Functional differences among those high and low on a trait measure of psychopathy. *Biol Psychiatry.* 2004;56(7):516-521.

163. Glenn AL, Raine, A., Schug, R. A., Young, L., & Hauser, M. Increased DLPFC activity during moral decision-making in psychopathy. *Molecular Psychiatry* 2009;14(10).

164. Harenski CL, Harenski KA, Shane MS, Kiehl KA. Aberrant neural processing of moral violations in criminal psychopaths. *J Abnorm Psychol.* 2010;119(4):863-874.

165. Decety J, Skelly LR, Kiehl KA. Brain response to empathy-eliciting scenarios involving pain in incarcerated individuals with psychopathy. *JAMA Psychiatry.* 2013;70(6):638-645.

166. Decety J, Skelly L, Yoder KJ, Kiehl KA. Neural processing of dynamic emotional facial expressions in psychopaths. *Soc Neurosci.* 2014;9(1):36-49.

167. Tomasi D, Volkow ND. Functional connectivity of substantia nigra and ventral tegmental area: maturation during adolescence and effects of ADHD. *Cereb Cortex.* 2012;24(4):935-944.

168. Patton J, Stanford M. Barratt impulsiveness scale, version 11 [BIS 11]. *Sourcebook of adult assessment.* 1995:361-364.

169. Patton JH, Stanford MS, Barratt ES. Factor structure of the Barratt impulsiveness scale. *J Clin Psychol.* 1995;51(6):768-774.

170. Stanford MS, Mathias CW, Dougherty DM, Lake SL, Anderson NE, Patton JH. Fifty years of the Barratt Impulsiveness Scale: An update and review. *Pers Indiv Differ.* 2009;47(5):385-395.

171. Shalgi S, Barkan I, Deouell LY. On the positive side of error processing: error-awareness positivity revisited. *Eur J Neurosci.* 2009;29(7):1522-1532.

172. Simmonds DJ, Pekar JJ, Mostofsky SH. Meta-analysis of Go/No-go tasks, demonstrating that fMRI activation associated with response inhibition is task-dependent. *Neuropsychologia.* 2008;46(1):224-232.

173. Jenkinson M, Bannister P, Brady M, Smith S. Improved optimization for the robust and accurate linear registration and motion correction of brain images. *Neuroimage.* 2002;17(2):825-841.

174. Smith SM. Fast robust automated brain extraction. *Hum Brain Mapp.* 2002;17(3):143-155.

175. Jenkinson M, Smith S. A global optimisation method for robust affine registration of brain images. *Med Image Anal.* 2001;5(2):143-156.

176. Andersson JLR, Jenkinson M, Smith SM. Non-linear optimisation. *FMRIB technical report TR07JA1*. 2007.

177. Andersson JLR, Jenkinson M, Smith SM. Non-linear registration, aka Spatial normalisation. *FMRIB technical report TR07JA2*. 2007.

178. Winkler AM, Ridgway GR, Webster MA, Smith SM, Nichols TE. Permutation inference for the general linear model. *Neuroimage.* 2014;92:381-397.

179. Barbato G, Ficca G, Muscettola G, Fichele M, Beatrice M, Rinaldi F. Diurnal variation in spontaneous eye-blink rate. *Psychiatry Res.* 2000;93(2):145-151.

180. Nazarpour K, Wongsawat Y, Sanei S, Chambers JA, Oraintara S. Removal of the eye-blink artifacts from EEGs via STF-TS modeling and robust minimum variance beamforming. *IEEE Trans Biomed Eng.* 2008;55(9):2221-2231.

181. Chen WH, Chiang TJ, Hsu MC, Liu JS. The validity of eye blink rate in Chinese adults for the diagnosis of Parkinson's disease. *Clin Neurol Neurosurg.* 2003;105(2):90-92.

182. Sforza C, Rango M, Galante D, Bresolin N, Ferrario VF. Spontaneous blinking in healthy persons: an optoelectronic study of eyelid motion. *Ophthalmic Physiol Opt.* 2008;28(4):345-353.

183. Bentivoglio AR, Bressman SB, Cassetta E, Carretta D, Tonali P, Albanese A. Analysis of blink rate patterns in normal subjects. *Mov Disord.* 1997;12(6):1028-1034.

184. Garavan H, Ross TJ, Stein EA. Right hemispheric dominance of inhibitory control: an event-related functional MRI study. *Proc Natl Acad Sci U S A.* 1999;96(14):8301-8306.

185. Horn NR, Dolan M, Elliott R, Deakin JF, Woodruff PW. Response inhibition and impulsivity: an fMRI study. *Neuropsychologia.* 2003;41(14):1959-1966.

186. Liddle PF, Kiehl KA, Smith AM. Event-related fMRI study of response inhibition. *Hum Brain Mapp.* 2001;12(2):100-109.

187. Brown SM, Manuck SB, Flory JD, Hariri AR. Neural basis of individual differences in impulsivity: contributions of corticolimbic circuits for behavioral arousal and control. *Emotion.* 2006;6(2):239-245.

188. McClure SM, Ericson KM, Laibson DI, Loewenstein G, Cohen JD. Time discounting for primary rewards. *J Neurosci.* 2007;27(21):5796-5804.

189. McClure SM, Laibson DI, Loewenstein G, Cohen JD. Separate neural systems value immediate and delayed monetary rewards. *Science.* 2004;306(5695):503-507.

190. Casey BJ, Castellanos FX, Giedd JN, et al. Implication of right frontostriatal circuitry in response inhibition and attention-deficit/hyperactivity disorder. *J Am Acad Child Adolesc Psychiatry.* 1997;36(3):374-383.

191. McAlonan GM, Cheung V, Chua SE, et al. Age-related grey matter volume correlates of response inhibition and shifting in attention-deficit hyperactivity disorder. *Br J Psychiatry.* 2009;194(2):123-129.

192. Reynolds B, Ortengren A, Richards JB, de Wit D. Dimensions of impulsive behavior: Personality and behavioral measures. *Pers Indiv Differ.* 2006;40(2):305-315.

193. Vink M, Kahn RS, Raemaekers M, van den Heuvel M, Boersma M, Ramsey NF. Function of striatum beyond inhibition and execution of motor responses. *Hum Brain Mapp.* 2005;25(3):336-344.

194. Kelly AMC, Hester R, Murphy K, Javitt DC, Foxe JJ, Garavan H. Prefrontal-subcortical dissociations underlying inhibitory control revealed by event-related fMRI. *Eur J Neurosci.* 2004;19(11):3105-3112.

195. Zandbelt BB, Vink M. On the Role of the Striatum in Response Inhibition. *Plos One.* 2010;5(11).

196. Li CS, Yan P, Sinha R, Lee TW. Subcortical processes of motor response inhibition during a stop signal task. *Neuroimage.* 2008;41(4):1352-1363.

197. Buckholtz JW, Treadway MT, Cowan RL, et al. Dopaminergic network differences in human impulsivity. *Science.* 2010;329(5991):532.

198. Seidman LJ, Valera EM, Makris N, et al. Dorsolateral prefrontal and anterior cingulate cortex volumetric abnormalities in adults with attention-

deficit/hyperactivity disorder identified by magnetic resonance imaging. *Biol Psychiatry.* 2006;60(10):1071-1080.

199. Hesslinger B, Tebartz van Elst L, Thiel T, Haegele K, Hennig J, Ebert D. Frontoorbital volume reductions in adult patients with attention deficit hyperactivity disorder. *Neurosci Lett.* 2002;328(3):319-321.

200. Tomasi D, Volkow ND. Abnormal functional connectivity in children with attention-deficit/hyperactivity disorder. *Biol Psychiatry.* 2012;71(5):443-450.

201. Konrad K, Eickhoff SB. Is the ADHD brain wired differently? A review on structural and functional connectivity in attention deficit hyperactivity disorder. *Hum Brain Mapp.* 2010;31(6):904-916.

202. Arbabshirani MR, Plis S, Sui J, Calhoun VD. Single subject prediction of brain disorders in neuroimaging: Promises and pitfalls. *Neuroimage.* 2017;145(Pt B):137-165.

203. Mwangi B, Tian TS, Soares JC. A review of feature reduction techniques in neuroimaging. *Neuroinformatics.* 2014;12(2):229-244.

204. Bishop S, Lau M, Shapiro S, et al. Mindfulness: A proposed operational definition. *Clinical psychology: Science and practice.* 2004;11(3):230-241.

205. Lattimore P, Fisher N, Malinowski P. A cross-sectional investigation of trait disinhibition and its association with mindfulness and impulsivity. *Appetite.* 2011;56(2):241-248.

206. Peters JR, Erisman SM, Upton BT, Baer RA, Roemer L. A preliminary investigation of the relationships between dispositional mindfulness and impulsivity. *Mindfulness.* 2011;2(4):228-235.

207. Murphy C, MacKillop J. Living in the here and now: interrelationships between impulsivity, mindfulness, and alcohol misuse. *Psychopharmacology.* 2012;219(2):527-536.

208. Zylowska L, Ackerman DL, Yang MH, et al. Mindfulness meditation training in adults and adolescents with ADHD: a feasibility study. *J Atten Disord.* 2008;11(6):737-746.

209. Zgierska A, Rabago D, Chawla N, Kushner K, Koehler R, Marlatt A. Mindfulness meditation for substance use disorders: A systematic review. *Substance Abuse.* 2009;30(4):266-294.

210. Kreek MJ, Nielsen DA, Butelman ER, LaForge KS. Genetic influences on impulsivity, risk taking, stress responsivity and vulnerability to drug abuse and addiction. *Nat Neurosci.* 2005;8(11):1450-1457.

211. Valentine E, Sweet P. Meditation and attention: a comparison of the effects of concentrative and mindfulness meditation on sustained attention. *Mental Health, Religion and Culture.* 1999;2:59-70.

212. Jha AP, Krompinger J, Baime MJ. Mindfulness training modifies subsystems of attention. *Cogn Affect Behav Neurosci.* 2007;7(2):109-119.

213. Sahdra BK, MacLean KA, Ferrer E, et al. Enhanced response inhibition during intensive meditation training predicts improvements in self-reported adaptive socioemotional functioning. *Emotion.* 2011;11(2):299-312.

214. Heeren A, Van Broeck N, Philippot P. The effects of mindfulness on executive processes and autobiographical memory specificity. *Behav Res Ther.* 2009;47(5):403-409.

215. Korponay C, Dentico D, Kral T, et al. Neurobiological correlates of impulsivity in healthy adults: lower prefrontal gray matter volume and spontaneous eye-blink rate but greater resting-state functional connectivity in basal ganglia-thalamo-cortical circuitry. under review.

216. Lutz A, Slagter HA, Dunne JD, Davidson RJ. Attention regulation and monitoring in meditation. *Trends Cogn Sci.* 2008;12(4):163-169.

217. Kabat-Zinn J. *Full catastrophe living: Using the wisdom of your body and mind to face stress, pain, and illness.* New York, NY: Delacorte; 1990.

218. MacCoon DG, Imel ZE, Rosenkranz MA, et al. The validation of an active control intervention for Mindfulness Based Stress Reduction (MBSR). *Behav Res Ther.* 2012;50(1):3-12.

219. Kruis A, Slagter HA, Bachhuber DR, Davidson RJ, Lutz A. Effects of meditation practice on spontaneous eyeblink rate. *Psychophysiology.* 2016;53(5):749-758.

220. Murphy C, MacKillop J. Living in the Here and Now: Interrelationships between Impulsivity, Mindfulness, and Alcohol Misuse. *Psychopharmacology* 2012;219(2):527-536.

221. Kringelbach ML. The human orbitofrontal cortex: linking reward to hedonic experience. *Nature Reviews Neuroscience* 2005;6(9):691-702.

222. Harpur TJ, Hare RD, Hakstian AR. Two-factor conceptualization of psychopathy: Construct validity and assessment implications. *Psychological Assessment: A Journal of Consulting and Clinical Psychology.* 1989;1(1):6-17.

223. Morgan JE, Gray NS, Snowden RJ. The relationship between psychopathy and impulsivity: A multi-impulsivity measurement approach. *Pers Indiv Differ.* 2011;51:429-434.

224. Snowden RJ, Gray NS. Impulsivity and psychopathy: associations between the barrett impulsivity scale and the psychopathy checklist revised. *Psychiatry Res.* 2011;187(3):414-417.